THERMODYNAMIC STUDY
OF
COUPLED CHEMICAL REACTIONS

Thesis by

Eugene Byrd Nebeker

In Partial Fulfillment of the Requirements

For the Degree of

Doctor of Philosophy

California Institute of Technology

Pasadena, California

1965

(Submitted May 11, 1965)

ACKNOWLEDGMENTS

The author wishes to express his gratitude to Professor C. J. Pings for the initiation and continuing support of this endeavor. His patience, interest, and encouragement are sincerely appreciated.

The helpful discussions, constructive criticism, and encouragement of many fellow graduate students has been valued. Notable among these contributors was Joe Woodward.

Many useful suggestions and assistance in the design and construction of the experimental apparatus were received from Seichi Nakawatse, Willard DeWitt, and George Griffith. Paul Holmen, Henry Smith, and Hollis Reamer were very accommodating and helpful regarding the use of subsidiary equipment.

During my graduate studies, scholarships and assistantships were received from the California Institute of Technology. A fellowship was also accepted from the Woodrow Wilson Foundation. The funds for this investigation were contributed by The Research Corporation and also by the Directorate of Chemical Sciences of the Air Force Office of Scientific Research. This financial support is gratefully acknowledged.

ABSTRACT

To investigate the principles of Non-Equilibrium Thermodynamics, an experimental and theoretical study of a chemical reacting system is made. Nitric oxide, iodine, chlorine, iodine monochloride, and nitrosyl chloride in the gas phase are the macroscopic chemical species which comprise this system.

The system displays a coupling behavior which is uncommon to chemical reacting systems. However, this behavior may be useful in explaining some biological phenomena. The observed coupling effect results in a phenomenological coefficient matrix which is not diagonal.

None of the macroscopic derivations of the Onsager reciprocity relations which are examined appear to be generally applicable. However, a limited derivation is proposed which not only identifies the phenomenological coefficients in the linear rate laws for chemical reacting systems but also indicates the validity of the Onsager relations. Linear transformations of the fluxes and forces which diagonalize or destroy the symmetry of the phenomenological coefficient matrix are not applicable to a chemical reacting system.

Photometric methods are used to experimentally determine the reaction velocities and chemical affinities of this system. The phenomenon of coupling is definitely exhibited by this system, as shown by the existence of the coupling coefficients, L_{12} and L_{21}, and by the presence of a negative AV product. The applicability of linear phenomenological rate laws and also rate laws which

include quadratic terms are investigated. The linear rate laws are better approximations as the system approaches equilibrium and may be useful at appreciable distances from equilibrium in certain cases. A conclusive test of the Onsager reciprocity relations could not be made.

TABLE OF CONTENTS

LIST OF TABLES

LIST OF FIGURES

NOMENCLATURE

English Symbols

a	chemical activity
A	chemical affinity
b	thermodynamic variable capable of measuring the deviation of the system from equilibrium
C	concentration
D_a	determinant of the stoichiometric equation transformation matrix
D_L	determinant of the phenomenological coefficient matrix
d_eS	infinitesimal increment of the entropy flowing into or out of the system
d_iS	infinitesimal increment of the entropy produced in the system
E	total internal energy
G	Gibbs free energy
i	multiplier phototube anode current
I	transmitted light intensity
I_o	incident light intensity
J	flux
k_f	forward reaction rate constant
k_r	reverse reaction rate constant
m	number of moles
M	molecular weight
ℓ	length of light path
L	phenomenological coefficient
P	total pressure

English Symbols

R	universal gas constant
R_i	electrical resistance of R_i resistor
s	overall sensitivity of the multiplier phototube
S	total entropy
$\dot{S}$	rate of entropy production in the system
t	time
t_o	time at which system is perturbed from equilibrium
T	absolute temperature
v	voltage proportional to the transmitted light intensity
v_o	voltage proportional to the incident light intensity
v_i	voltage drop across R_i resistor
$v_{osc.}$	voltage measured by oscilloscope
V	velocity of overall reaction rate
V_f	forward reaction rate
$\underline{V}$	total volume
W	element of skew symmetric matrix
X	thermodynamic driving force

Greek Symbols

α	element of the stoichiometric equation transformation matrix
α^*	cofactor divided by determinant of stoichiometric equation transformation matrix
ϵ	extinction coefficient
λ	wavelength

Greek Symbols

μ	chemical potential
ν	stoichiometric coefficient
ξ	degree of advancement of extent of reaction
σ	rate of entropy production in the system
σ^2	variance

Script Symbols

$\mathcal{A}$	affinity matrix
$\mathcal{I}$	identity matrix
$\mathcal{L}$	phenomenological coefficient matrix
$\mathcal{P}$	transformation matrix for the velocities or fluxes
$\mathcal{Q}$	transformation matrix for the affinities or forces
$\mathcal{V}$	velocity matrix
$\mathcal{W}$	skew symmetric matrix

Subscripts

eq.	at equilibrium conditions

Superscripts

$'$	quantity created by a linear transformation
$\sim$	transpose of a matrix
i	initial value at the start of a run

I. INTRODUCTION

Classical thermodynamics is seriously limited in describing physico-chemical processes because it is based on the concept of true equilibrium states[1]. Also, the treatment of irreversible[2] processes by classical thermodynamics is often inadequate. In most areas of science and engineering, equilibrium is only rarely attained, and irreversible processes are usually encountered.

Therefore, Non-Equilibrium Thermodynamics was developed as a study of systems which are not at equilibrium and in which irreversible transport processes are occurring. For this endeavor, classical thermodynamics is extended by supplementing the First and Second Laws and the basic definitions of thermodynamics with additional postulates.

The purpose of this investigation is to examine some of these postulates for the case of chemical reactions. Chemical reactions are chosen not only because the applicability of these postulates to a chemical reacting system has not been examined before, but also

---

[1] Equilibrium is the time invariant state of a system in which no spontaneous processes occur, and all macroscopic quantities remain unchanged.

[2] In defining reversible processes, Prigogine and Defay[(44)] consider a system which undergoes some transformation ABC. This change is reversible if an inverse change CBA exists such that: 1) the variables characterizing the state of the system return through the same values, but in the reverse order, and 2) exchanges of heat, matter, and work with the surroundings have the reverse sign and take place in the reverse order. All changes which do not satisfy these two conditions are termed irreversible.

because such a system provides a special insight to these postulates.

A particular reacting system is selected for this study. The arrangement consists of reactions which are "coupled" and display a behavior which is uncommon to chemical reacting systems. However, such an example demonstrates a behavior by which these postulates of non-equilibrium thermodynamics can be tested.

The study of non-equilibrium thermodynamics has been given a wide variety of names. Irreversible thermodynamics, thermodynamics of irreversible processes, thermodynamics of transport processes, and thermodynamics of the steady state are often used. The origin of these names will perhaps become apparent upon examination of the theory of non-equilibrium thermodynamics. The subject will be referred to as non-equilibrium thermodynamics throughout this thesis.

II. THEORY

A. General

The theory of non-equilibrium thermodynamics supplements the First and Second Laws of classical thermodynamics and the basic definitions with further postulates in order to describe a non-equilibrium system and correlate its properties. The basic postulates are: 1) local equilibrium, 2) the phenomenological rate laws, and 3) the Onsager Reciprocity Relations.

1) Local Equilibrium. The postulate of local equilibrium assumes that all thermodynamic state functions exist for each element of a system in which irreversible processes are taking place. Also, these state functions for the non-equilibrium system are the same functions of the local state variables as the corresponding equilibrium thermodynamic quantities treated in classical thermodynamics.

Prigogine[42] examined this postulate theoretically and found that it should be valid not only at equilibrium, but also at slight deviations from the equilibrium state. However, since he employed a particular gas model in his study, his conclusions apply only to special situations.

For any macroscopic system, the postulate must be verified by examining its consequences and comparing them with experimental results. A comparison between theory and experiment will then show the realm of validity of the postulate.

However, this postulate is expected to be valid for a system in which the gradients of the thermodynamic functions are small or in which the thermodynamic variables do not change with time at any particular point in the system, that is, under steady state conditions. Because this theory is particularly applicable to steady state processes, Denbigh[10] was prompted to call the subject "Thermodynamics of the Steady State." In addition, the postulate of local equilibrium is also expected to become a better approximation as the system approaches equilibrium[16].

The validity of this postulate has been usually implied without justification in most kinetic and transport property investigations through the years. The validity of this postulate has also been assumed in this study, primarily because the gradients in the system are very small.

Often implied in the assumption of local equilibrium is the so-called entropy balance equation. This equation states that the entropy of a volume element changes with time for two reasons; first, because entropy flows in and out of the element, and second, because an entropy source exists inside the volume element due to irreversible processes,

$$dS = d_e S + d_i S \,. \tag{1}$$

The entropy source, $d_i S$, is never negative, being positive for irreversible and zero for reversible phenomena.

The thermodynamic Gibbs equation is often used to relate this entropy source explicitly to the various irreversible processes that may occur in a system,

$$T\,dS = dE + P\,d\underline{V} - \sum_{k=1}^{n} \mu_k\,dm_k\,. \qquad (2)$$

This equation, of course, is identical in form to that which applies in the equilibrium case. In many instances, combination of the macroscopic conservation laws of mass, momentum and energy with this Gibbs' equation is useful.

For the example of a chemical reaction, the conservation of mass can be written for reaction i as

$$dm_{k,i} = \nu_{k,i}\,d\xi_i\,, \qquad (3)$$

where $\nu_{k,i}$ is the stoichiometric coefficient of component k in this reaction. The stoichiometric coefficient is considered positive when component k appears in the right-hand member of the stoichiometric reaction equation and negative when it appears in the left-hand member. ξ is called the degree of advancement or the extent of reaction. As an example, for the reaction

$$2NO + Cl_2 = 2NOCl\,, \qquad (4)$$

$$\nu_{NO} = -2\,,\quad \nu_{Cl_2} = -1\,,\quad \nu_{NOCl} = 2\,, \qquad (5)$$

so that

$$\frac{dm_{NO}}{-2} = \frac{dm_{Cl_2}}{-1} = \frac{dm_{NOCl}}{2} = d\xi\,. \qquad (6)$$

Obviously, ξ does not depend upon which component is selected.

The conservation of mass, equation (3), can be combined with the Gibbs equation for a closed system in which r chemical reactions are occurring to give

$$T\,dS = dE + P\,d\underline{V} - \sum_{i=1}^{r}\sum_{k=1}^{n} \nu_{k,i}\mu_k\,d\xi_i \,. \tag{7}$$

By introducing the definition of the chemical affinity of reaction i,

$$A_i = -\sum_{k=1}^{n} \nu_{k,i}\mu_k \,, \tag{8}$$

equation (7) can be simplified to

$$dS = \frac{dE + P\,dV}{T} + \frac{1}{T}\sum_{i=1}^{r} A_i\,d\xi_i \,. \tag{9}$$

The entropy supplied by the surroundings is usually identified for a closed system as[43]

$$d_e S = \frac{dE + P\,dV}{T} \,, \tag{10}$$

while the entropy production, resulting from the action of irreversible chemical reactions, is

$$d_i S = \frac{1}{T}\sum_{i=1}^{r} A_i\,d\xi_i \geq 0 \,. \tag{11}$$

The separation of equation (9) into equations (10) and (11) may seem somewhat arbitrary. However, these two parts of equation (9) must satisfy a number of requirements. De Groot and Mazur[7]

claim that this separation is determined uniquely.

In the general case, such an entropy production equation can usually be differentiated with respect to time to give the rate of production of entropy. The resulting equation has a very simple appearance[7]. The entropy production equation will be a sum of terms, each being a product of a flux characterizing a reversible process, and a quantity called the thermodynamic driving force, which is related to the non-uniformity of the system,

$$T\sigma \equiv T\, d_i S/dt = \sum_{i=1}^{n} J_i X_i \geq 0 \,. \tag{12}$$

For example, the force may be a function of a temperature gradient or a chemical affinity of the system. The force and flux in each particular product are said to be "conjugate" to each other.

Returning to the example of a chemical reaction, equation (11) can be differentiated to give the rate of entropy production

$$\sigma \equiv d_i S/dt = \frac{1}{T} \sum_{i=1}^{r} A_i V_i \geq 0 \,, \tag{13}$$

where V_i is the velocity of chemical reaction i. Multiplying equation (13) by the temperature, an expression is formed,

$$T\sigma = \sum_{i=1}^{r} A_i V_i \geq 0 \,, \tag{14}$$

which has this simple appearance of the product of a flux, the reaction velocity, times the force, the affinity. The product $T\sigma$ is sometimes called the "power" of a reaction[55].

In addition to providing another equation which can be used to put limits on the behavior of the system, the rate of entropy production equation is useful in selecting the proper conjugate fluxes and forces which appear in the Onsager theory. Prigogine[43] claims that the only general criterion of irreversibility is the internal entropy production.

Even with the entropy balance equation, the three conservation laws, and the equations of state, often sufficient information is not available to describe a system. Some relationship between the fluxes and forces is necessary. The phenomenological rate laws serve this purpose.

2) Phenomenological Rate Laws. As a first approximation, the fluxes are considered to be linear, homogeneous functions of the thermodynamic forces,

$$J_i = L_i X_i \,. \tag{15}$$

Fick's law of diffusion, Fourier's law of heat conduction, and Ohm's law of electrical conduction are common examples of this type of law.

When two or more of these phenomena occur simultaneously, they may interfere and give rise to new effects such that each force contributes to each flux. Mathematically, these effects are usually treated by the addition of new linear functions to the phenomenological laws given by equation (15),

$$J_i = \sum_{j=1}^{n} L_{ij} X_j \quad \text{where} \quad i = 1, 2, \ldots, n . \qquad (16)$$

The Soret or thermal diffusion effect, which results from diffusion due to a temperature gradient, is an example of such a "cross-effect."

The consequences of the assumption of these linear rate laws should be derived and checked by experiment. They are expected to be good approximations close to equilibrium and in systems with small space and time gradients of the thermodynamic variables. Ohm's and Fourier's laws have been found in some cases to be valid over large ranges of the driving forces[16]. However, except close to equilibrium, these linear reactions are considered to be very poor for the example of chemical reactions.

In its present state, non-equilibrium thermodynamics is primarily concerned with the description of such linear phenomena. However, in the last few years, a significant amount of work has been done on the non-linear problems.

Some important statements can be made about the phenomenological coefficients which appear in these rate laws. The Onsager Reciprocity Relations are the most well known relations between these coefficients.

3) Onsager Reciprocity Relations. These relations state that if a "proper" choice is made of the fluxes and forces, the entire array or matrix of phenomenological coefficients will be symmetric, that is,

$$L_{ik} = L_{ki} \cdot \tag{17}$$

The meaning of the " proper " choice of fluxes and forces has been the subject of some controversy in recent years. If the fluxes and forces are required to obey only the entropy production equation, equation (12), and the linear phenomenological laws, equation (16), Coleman and Truesdell[3] show that an infinite number of choices of fluxes and forces exist for which the Onsager relations are valid, and also an infinite number exist for which the Onsager relations are not valid. Although giving a much less general discussion, Gage and Kline[17] reach a similar conclusion. To minimize this problem, Coleman and Truesdell suggest that the flux should be selected as the time derivative of a thermodynamic quantity which measures the deviation of the system from equilibrium,

$$J_i = \frac{d}{dt}(b_i) \tag{18}$$

and the force be chosen so that

$$X_i = T\, \partial_i S/\partial b_i \cdot \tag{19}$$

Onsager[35, 36] originally derived his relations from statistical mechanical considerations. His derivation is based upon not only the principles of fluctuation theory and microscopic reversibility, but also upon his own hypothesis of the regression of fluctuations.

The principle of microscopic reversibility means that under equilibrium conditions, any molecular process and the reverse of that

process will be taking place on the average at the same rate. As an example, for the hypothetical reaction between monomeric substances

(20)

at equilibrium, the time rate of change in the concentrations of each of the three chemical species, A, B, and C, is equal to zero. "However," said Onsager, "the chemists are accustomed to impose a very interesting additional restriction, namely: when equilibrium is reached each individual reaction must balance itself. They require that the transition $A \rightarrow B$ must take place just as frequently as the reverse transition $B \rightarrow A$, etc." This detailed balancing of more than one chemical reaction occurring simultaneously is a special case of microscopic reversibility and, as Onsager points out, is not the result of thermodynamics.

In his derivation, Onsager introduced his hypothesis of the regression of fluctuations, which means that the microscopic fluctuations within a system decay toward equilibrium in the same manner as the macroscopic processes. Finally, Onsager applied his relations to the linear phenomenlogical laws. However, the Onsager theory makes no statements regarding the validity of these linear laws. It is simply concerned with the reciprocal relations between the coefficients when these equations are a satisfactory approximation.

From the microscopic viewpoint, the Onsager reciprocity

relations are well founded[16]. However, no adequate, general macroscopic derivation has been proposed.

A derivation of the Onsager relations is given in a subsequent section and the phenomenological coefficients are identified. This derivation treats the example of a chemically reacting system and assumes the overall rate expressions can be expressed in the form of the law of mass action. Not only is the reacting system assumed to be close to equilibrium, but also the principle of detailed balancing is assumed for each of the reactions.

Parlin, Marcus, and Eyring[37] use rate theory to verify the Onsager relations for a chemically reacting system. However, since they incorporate the results of Zwolinski and Marcus[60] in their argument, they tacitly make the same assumptions mentioned above.

Li[25], Pitzer[39, 40], and Verschaffelt[57] base their derivation on the hypothesis that an intrinsically independent set of forces and fluxes always exist in a system. However, as discussed in a subsequent section, this hypothesis may not embrace any of the physical systems usually analyzed by non-equilibrium thermodynamics.

Nims[34] examines diffusion through membranes and claims that the Onsager relations can be derived from Newton's three laws of motion. However, Nims arbitrarily assumes some empirical relationships between certain "forces" and the properties of his system. His results are questionable because the validity of these relationships are doubtful.

Sliepcevich and Finn[48] also recently presented a derivation. Their results are not valid because they assumed their answer in one of the last steps in the derivation. Their work has been often criticised in the literature[1, 11, 15].

The example of a chemically reacting system is also examined by Van Rysselberghe[54] in his derivation. However, the reasoning beyond equation (9) of his paper is questionable.

B. Chemical Reactions

Although the hypothetical system previously mentioned, involving a set of triangular reactions between monomeric substances, is a commonly quoted analytical model to demonstrate the Onsager reciprocity[10, 49], very little literature on the treatment of real reacting systems by irreversible thermodynamics exists. In a 1960 review article, Miller[33] pointed out that the chemical reaction was an obvious case of coupled phenomena which had not been directly studied experimentally. Except for several complicated biological systems discussed by Van Rysselberghe[50], few measurements dealing with coupled reactions have been reported, and no experimental verification of the Onsager reciprocity in a reacting system has been made.

1. Stoichiometry and Thermodynamics. For convenience, generalized stoichiometry[44] and rate notation can be used. Let the stoichiometry of the reactions, 1 and 2, be denoted by

$$1: \quad \sum_{i=1}^{n} \nu_{i1} M_i = 0 \tag{21}$$

$$2: \quad \sum_{i=1}^{n} \nu_{i2} M_i = 0 \ , \tag{22}$$

where M_i is the molecular weight of component i, and ν_{i1} and ν_{i2} are the stoichiometric coefficients of component i in reaction 1 and 2 respectively. As discussed in the previous section, these coefficients are positive for products, negative for reactants, and zero

for non-participants in a particular reaction.

The chemical affinities of the two reactions are defined as

$$A_1 = - \Delta G_1 = - \sum_{i=1}^{n} \nu_{i1} \mu_i \tag{23}$$

$$A_2 = - \Delta G_2 = - \sum_{i=1}^{n} \nu_{i2} \mu_i \, , \tag{24}$$

where μ_i is the chemical potential of component i. Generalized reaction velocities are selected as the time derivatives of the extent of reaction

$$V_1 = d\xi_1/dt = \frac{1}{\nu_{i,1}} \frac{dm_{i,1}}{dt} \tag{25}$$

$$V_2 = d\xi_2/dt = \frac{1}{\nu_{i,2}} \frac{dm_{i,2}}{dt} \, . \tag{26}$$

2. Linearization. If only one reaction is occurring, the reaction rate is proportional to the affinity[7] when the system is slightly displaced from equilibrium,

$$V_i = LA_i \,. \tag{27}$$

In addition to being analogous to other linear phenomenological rate laws, this equation has another basis. If the kinetic rate expression for the overall rate of this reaction can be expressed in the form of the law of mass action, the results of Appendix 1 show the rate of the reaction can be approximated by equation (27) near equilibrium.

The validity of these linear rate laws for chemical reactions is discussed by Prigogine and Hansen[45] and others[29]. Prigogine, Outer, and Herbo[46] verified these relations experimentally in the case of the hydrogenation of benzene and the dehydrogenation of cyclohexane.

Also, Appendix 1 shows that L can be explicitly identified as

$$L = \frac{k_f}{RT} \prod_{\text{reactants}} [a_i]_{eq.}^{\nu_i} \tag{28}$$

and therefore is a function of the equilibrium state of the system. If two reactions are proceeding without coupling, two equations of the type of equation (27) still continue to apply, each independently of the other.

3. Interference and Coupling. Although a pair of reactions are not coupled, they nevertheless will interfere: as one reaction proceeds, it will generally modify the concentration of a number of species present. This concentration change will have the inevitable effect of displacing other reactions from equilibrium, resulting in finite reaction rates. However, these secondary reactions presumably would not proceed if the affinities (free energy differences) of the secondary reactions were kept at their equilibrium value of zero.

Pings[38] suggests that the necessary and sufficient criterion of coupling is the non-disappearance of the following derivatives

$$(\partial V_i/\partial A_j)_{A_i} \neq 0 \qquad i \neq j \,. \tag{29}$$

Van Rysselberghe[50, 51, 52] also suggested sufficient but not necessary coupling criteria, the existence of a negative AV product. This criterion is discussed in more detail later in this section.

Figure 1 compares two hypothetical systems. One system exhibits only interference, while the other shows coupling. Both cases involve two reactions. Up to time t_o, the systems are assumed to be in equilibrium, that is, the affinities and reaction velocities of both reactions are zero. The system is disturbed at t_o by a step function increase in the affinity of reaction 1, without changing the affinity of reaction 2. This action causes a step function increase from zero to a finite value for the velocity of reaction 1. In the interference case, as the first reaction proceeds, it disturbs all

concentrations, thus probably perturbing the affinity of reaction 2 from its zero value. This phenomenon certainly would take place if the two reactions shared one or more components in common.

For the system exhibiting coupling, the step function change in the affinity of reaction 1 is also done in such a way as to not abruptly disturb the affinity of reaction 2. Although affinity 2 is not disturbed from a zero value, a discontinuous increase (or decrease) will occur in the velocity of reaction 2 from its zero value due to the non-zero value of the derivative. As both reactions proceed, concentration changes will cause affinity 2 to deviate from its equilibrium value. This deviation not only will cause further modification in the reaction velocity of reaction 2, but also will modify the velocity of reaction 1 due to the non-zero value of $\partial V_1/\partial A_2$.

A generalization of equation (27) to a system that formally encompasses the possibility of coupling is given by the following set of equations

$$V_1 = L_{11}A_1 + L_{12}A_2 \tag{30}$$

$$V_2 = L_{21}A_1 + L_{22}A_2 \,. \tag{31}$$

The Onsager reciprocity relations (35, 36) require that

$$L_{12} = L_{21} \,. \tag{32}$$

In the case of no coupling, this relationship is satisfied in a trivial sense

$$L_{12} = L_{21} = 0 \,. \tag{33}$$

Except for reports in 1937 by Van Rysselberghe[50], apparently no experimental study of coupling in a chemical reacting system has been made. Miller[33] mentions two very inconclusive attempts to analyze these same systems in an attempt to verify the Onsager relations. No report of a clearly identifiable simple system exhibiting nontrivial coupling or an experimental verification of the reciprocity for a chemical reacting system has been given.

In order to clarify these ideas, consider the particular system which is made by mixing iodine, chlorine, and nitric oxide in the gas phase. At equilibrium, only five chemical species will exist in appreciable quantities, iodine, chlorine, iodine monochloride, nitrosyl chloride, and nitric oxide[2]. Nitrosyl iodide has never been prepared and is considered to be incapable of existence[13]. Only three sub-species, that is, atoms or smaller molecules, are interchanged between the reactants to form the equilibrium mixtures. Therefore, as discussed by Denbigh[9], only two independent stoichiometric equations are necessary to describe the system. Providing that these two stoichiometric equations are linearly independent among themselves, they may be arbitrarily selected to be

$$1.\quad 2NO + Cl_2 = 2NOCl \tag{34}$$

$$2.\quad 2NOCl + I_2 = 2NO + 2ICl\,. \tag{35}$$

Since chlorine is only involved in reaction 1 and iodine is only involved in reaction 2, the fluxes which can be selected to describe the apparent reaction rates for a constant volume system are

$$V_1 = \partial\xi_1/\partial t = - \partial C_{Cl_2} / \partial t \qquad (36)$$

$$V_2 = \partial\xi_2/\partial t = - \partial C_{I_2} / \partial t \,, \qquad (37)$$

and the corresponding driving forces will be the chemical affinities of each reaction. These fluxes and forces can then be substituted into equations (30) and (31) to describe the system, providing it is close to equilibrium so that these equations will be adequate approximations.

If these reactions only interfere and do not couple, each equation will reduce to the form of equation (27). However, Beeson and Yost[2] observed that if these reactions are allowed to proceed together, that is, if iodine, chlorine, and nitric oxide are combined in a single container, the apparent rate of each reaction will be much greater than if these reactions were allowed to proceed separately. This phenomenon may be explained by considering that at least the following additional reaction is occurring,

$$3. \quad I_2 + Cl_2 = 2ICl \qquad (38)$$

which obviously cannot occur if reactions 1 and 2 were allowed to proceed separately. This latter reaction presumably has a kinetic path which is somewhat independent of reactions 1 and 2.

Note that this third reaction is stoichiometrically merely a linear combination of the first two reactions. Macroscopic thermodynamic analysis involves only the independent reactions. Therefore, any two of the three reactions may be regarded as the independent

reactions, as will be discussed later.

This example thus suggests a sufficient condition for the occurrence of nontrivial coupling, namely the existence of one or more reactions which are stoichiometrically redundant, but are kinetically independent. In a sense, this phenomenon is stoichiometric degeneracy. Another view is that the concealed reaction represents a kinetic short cut[38].

Van Rysselberghe[50, 51, 52] suggests that a reaction is coupled if it possesses a negative AV product. Equation (14) requires that the sum of all the AV products in the system must be positive, but does not exclude the possibility that one of these terms in the equation may be negative.

However, Van Rysselberghe's criterion of coupling has proved to be too narrow, involving a sufficient, but not necessary condition for coupling. For example, Koenig, Horne, and Mohilner[24] demonstrated a general technique by which a linear combination of coupled reactions may result in a new set of reactions devoid of coupling. This result was criticized by Hooyman[22], Van Rysselberghe[53], and Pings[38].

Hooyman gave stoichiometric criteria from which he concluded that the division into reactions with positive or negative entropy production is uniquely determined. Van Rysselberghe noted that Koenig, Horne, and Mohilner's transformations create stoichiometric equations which are devoid of the usual physical meaning. Manes[28] attempted to reply to the objections of Hooyman

and Van Rysselberghe and still demonstrate the suppression of coupling. Pings pointed out that the technique of Koenig, Horne, and Mohilner did not prove the suppression of coupling in the sense of a direct effect on the velocity of one reaction by the affinity of another reaction and suggested the criterion of coupling as presented in equation (29).

4. Kinetic Identification of the Phenomenological Coefficients for Coupled Reactions. The phenomenological coefficients for the reacting system discussed on Page 19 can be identified. Assume again that the kinetic expressions which describe the rates of reactions 1, 2, and 3 can be described by the form of the law of mass action,

$$-\partial a_{Cl_2}/\partial t = k_{1f} a_{NO}^2 a_{Cl_2} - k_{1r} a_{NOCl}^2 + k_{3f} a_{I_2} a_{Cl_2} - k_{3r} a_{ICl}^2 \tag{39}$$

$$-\partial a_{I_2}/\partial t = \frac{1}{2}\partial a_{ICl}/\partial t = k_{2f} a_{NOCl}^2 a_{I_2} - k_{2r} a_{NO}^2 a_{ICl}^2 + k_{3f} a_{I_2} a_{Cl_2} - k_{3r} a_{ICl}^2 \tag{40}$$

$$-\frac{1}{2}\partial a_{NO}/\partial t = \frac{1}{2}\partial a_{NOCl}/\partial t = k_{1f} a_{NO}^2 a_{Cl_2} - k_{1r} a_{NOCl}^2 - k_{2f} a_{NOCl}^2 a_{I_2} + k_{2r} a_{NO}^2 a_{ICl}^2 . \tag{41}$$

At equilibrium,

$$\partial a_{Cl_2}/\partial t = \partial a_{I_2}/\partial t = \partial a_{NO}/\partial t = 0 , \tag{42}$$

and therefore,

$$k_{1f} a_{NO}^2 a_{Cl_2} - k_{1r} a_{NOCl}^2 + k_{3f} a_{I_2} a_{Cl_2} - k_{3r} a_{ICl}^2 = 0 \tag{43}$$

$$k_{2f} a_{NOCl}^2 a_{I_2} - k_{2r} a_{NO}^2 a_{ICl}^2 + k_{3f} a_{I_2} a_{Cl_2} - k_{3r} a_{ICl}^2 = 0 \tag{44}$$

and

$$k_{1f}a_{NO}^{2}a_{Cl_2} - k_{1r}a_{NOCl}^{2} - k_{2f}a_{NOCl}^{2}a_{I_2} + k_{2r}a_{NO}^{2}a_{ICl}^{2} = 0 . \quad (45)$$

However, a stronger, additional condition for equilibrium must also be imposed, that is, that the velocity of each individual reaction is zero,

$$\partial\xi_1/\partial t = \partial\xi_2/\partial t = \partial\xi_3/\partial t = 0 \quad (46)$$

or

$$k_{1f}a_{NO}^{2}a_{Cl_2} - k_{1r}a_{NOCl}^{2} = k_{2f}a_{NOCl}^{2}a_{I_2} - k_{2r}a_{NO}^{2}a_{ICl}^{2} = k_{3f}a_{I_2}a_{Cl_2} - k_{3}a_{ICl}^{2} = 0 . \quad (47)$$

This detailed balancing of chemical reactions is a special case of the more general principle of microscopic reversibility discussed previously. Using this concept, equations (39) and (40) can be reduced to the following expressions in a manner identical to that by which equation (1-4) was reduced to equation (1-17),

$$V_1 = -\partial a_{Cl_2}/\partial t = \left(\frac{\partial\xi_1}{\partial t} + \frac{\partial\xi_3}{\partial t}\right) = \left(\frac{V_{1f}}{RT}\right)_{eq.} A_1 + \left(\frac{V_{3f}}{RT}\right)_{eq.} A_3 \quad (48)$$

$$V_2 = -\partial a_{I_2}/\partial t = \left(\frac{\partial\xi_2}{\partial t} + \frac{\partial\xi_3}{\partial t}\right) = \left(\frac{V_{2f}}{RT}\right)_{eq.} A_2 + \left(\frac{V_{3f}}{RT}\right)_{eq.} A_3 . \quad (49)$$

Recall that the rate of production of entropy for these three reactions will be

$$T\dot{S} = A_1 \partial\xi_1/\partial t + A_2 \partial\xi_2/\partial t + A_3 \partial\xi_3/\partial t \tag{50}$$

and that the affinities for the reactions are

$$A_1 = 2\mu_{NO} + \mu_{Cl_2} - 2\mu_{NOCl} \tag{51}$$

$$A_2 = 2\mu_{NOCl} + \mu_{I_2} - 2\mu_{NO} - 2\mu_{ICl} \tag{52}$$

$$A_3 = \mu_{I_2} + \mu_{Cl_2} - 2\mu_{ICl} . \tag{53}$$

The preceeding equations show that the affinities are related by

$$A_1 + A_2 = A_3 . \tag{54}$$

Arbitrarily selecting reactions 1 and 2 to be the independent reactions, equation (54) can be combined with equations (48), (49), and (50) to give

$$V_1 = \left(\frac{\partial\xi_1}{\partial t} + \frac{\partial\xi_3}{\partial t}\right) = \left(\frac{V_{1f} + V_{3f}}{RT}\right)_{eq.} A_1 + \left(\frac{V_{3f}}{RT}\right)_{eq.} A_2 \tag{55}$$

$$V_2 = \left(\frac{\partial\xi_2}{\partial t} + \frac{\partial\xi_3}{\partial t}\right) = \left(\frac{V_{3f}}{RT}\right)_{eq.} A_2 + \left(\frac{V_{2f} + V_{3f}}{RT}\right)_{eq.} A_2 \tag{56}$$

$$T\dot{S} = A_1\left(\frac{\partial\xi_1}{\partial t} + \frac{\partial\xi_3}{\partial t}\right) + A_2\left(\frac{\partial\xi_2}{\partial t} + \frac{\partial\xi_3}{\partial t}\right) \tag{57}$$

Choosing the reaction velocities or fluxes to be time derivatives of the thermodynamic variables, the following relations are obtained

$$V_1 = \left(\frac{\partial \xi_1}{\partial t} + \frac{\partial \xi_3}{\partial t} \right) = J_1 \tag{58}$$

$$V_2 = \left(\frac{\partial \xi_2}{\partial t} + \frac{\partial \xi_3}{\partial t} \right) = J_2 . \tag{59}$$

From equation (57) the corresponding conjugated forces appear to be

$$X_1 = A_1 \quad \text{and} \quad X_2 = A_2 . \tag{60}$$

This choice of fluxes and forces conforms with Coleman and Truesdell's[3] criteria. Also noting that this selection of fluxes and forces is in agreement with those used in the rate expressions given by equations (55) and (56), the following identification of the phenomenological coefficients can be made

$$L_{11} = \left(\frac{V_{1f} + V_{2f}}{RT} \right)_{eq.} \tag{61}$$

$$L_{12} = L_{21} = \left(\frac{V_{3f}}{RT} \right)_{eq.} \tag{62}$$

$$L_{22} = \left(\frac{V_{2f} + V_{3f}}{RT} \right)_{eq.} \tag{63}$$

Hence, close to equilibrium, the coupling coefficients, L_{12} and L_{21}, are equal, thereby obeying the Onsager Reciprocity Relations. These coupling coefficients involve only the constants characteristic of the redundant reactions. However, the diagonal coefficients, L_{11} and L_{22}, are functions not only of the kinetic constants of the independent reactions 1 and 2, but also of the kinetic constants of the redundant reaction 3. The above analysis

can obviously be extended to include any number of dependent stoichiometric equations.

If reactions 2 and 3 are arbitrarily selected to be the independent reactions, the following rate equations result

$$-\partial a_{Cl_2}/\partial t = \left(\frac{V_{1f} + V_{3f}}{RT}\right)_{eq.} A_3 + \left(\frac{-V_{1f}}{RT}\right)_{eq.} A_2 \quad (64)$$

$$+\frac{1}{2}\,\partial a_{NO}/\partial t = \left(\frac{-V_{1f}}{RT}\right)_{eq.} A_3 + \left(\frac{V_{1f} + V_{2f}}{RT}\right)_{eq.} A_2 \quad (65)$$

with the coefficients identified as

$$L_{11} = \left(\frac{V_{1f} + V_{3f}}{RT}\right)_{eq.} \quad (66)$$

$$L_{12} = L_{21} = \left(\frac{-V_{1f}}{RT}\right)_{eq.} \quad (67)$$

$$L_{22} = \left(\frac{V_{1f} + V_{2f}}{RT}\right)_{eq.} . \quad (68)$$

Finally, if reactions 1 and 3 are selected as the independent reactions,

$$-\partial a_{I_2}/\partial t = \left(\frac{V_{2f} + V_{3f}}{RT}\right)_{eq.} A_3 + \left(\frac{-V_{2f}}{RT}\right)_{eq.} A_1 \quad (69)$$

$$-\frac{1}{2}\,\partial a_{NO}/\partial t = \left(\frac{-V_{2f}}{RT}\right)_{eq.} A_3 + \left(\frac{V_{1f} + V_{2f}}{RT}\right)_{eq.} A_1 \quad (70)$$

with

$$L_{11} = \left(\frac{V_{2f} + V_{3f}}{RT} \right)_{eq.} \tag{71}$$

$$L_{12} = L_{21} = \left(\frac{-V_{2f}}{RT} \right)_{eq.} \tag{72}$$

$$L_{22} = \left(\frac{V_{1f} + V_{2f}}{RT} \right)_{eq.} . \tag{73}$$

Therefore, the anticipated magnitudes of the phenomenological coefficients depend upon the choice of independent reactions. Such a choice might affect the resulting experimental work.

Obviously, if any one or all of the three reactions were written in a reverse order, for example, if equation (2) were written,

$$2NO + 2ICl = 2NOCl + I_2 \tag{74}$$

no change in the results would occur.

However, the importance of combining the appropriate conjugate fluxes and forces cannot be minimized. For example, suppose that reactions 1 and 2 are considered to be the independent reactions. The rates would be given by equations (48) and (49). Making the substitution

$$A_1 = A_3 - A_2 , \tag{75}$$

the resulting linear rate expressions become

$$-\partial a_{Cl_2}/\partial t = \left(\frac{-V_{1f}}{RT} \right)_{eq.} A_2 + \left(\frac{V_{1f} + V_{3f}}{RT} \right)_{eq.} A_3 \tag{76}$$

$$-\partial a_{I_2}/\partial t = \left(\frac{V_{2f}}{RT}\right)_{eq.} A_2 + \left(\frac{V_{3f}}{RT}\right)_{eq.} A_3 . \qquad (77)$$

The resulting cross-coefficients are not equal because the conjugate fluxes and forces have not been used.

Some authors have claimed that if the fluxes and forces in a system are properly chosen, the coupling may be made to disappear. To accomplish this, they employ a particular type of linear transformation.

5. Destruction of Coupling. Several papers have inspected the theoretical implications of linear transformations which result in new sets of independent reactions with a diagonal matrix of phenomenological coefficients, that is, transformations which result in the elimination of coupling. A well-known algebraic theorem states that a real, symmetric matrix can be diagonalized[6, 30]. DeGroot[6], Manes[27], and de Groot and Mazur[7] point out that a transformation which diagonalizes such a matrix can always be found. This statement might appear to be in contradiction to the earlier assertion by Prigogine[41] that cases of intrinsic coupling exist which cannot be suppressed by simple linear transformations.

However, these points of view are reconcilable. Consider a general linear transformation of equations (21) and (22). A new independent reaction is created by multiplying reaction 1 by a_{11} and reaction 2 by a_{21} and adding. Then, a new second independent reaction is created by multiplying action 1 by a_{12} and reaction 2 by a_{22} and adding. These a_{ij} coefficients are real numbers, and the matrix or array of these coefficients is assumed to be non-singular. Obviously, an infinity of new pairs of independent reactions can be so created by an arbitrary selection of the coefficients, a_{ij}. However, unless these coefficients are integers or ratios of small integers, the resulting expressions will formally suggest rather strange stoichiometry.

De Donder[5] and Prigogine[41] have shown that the stoichiometric coefficients, velocities, and affinities for the two new reactions can be expressed as linear combinations of the previous quantities by

$$\nu'_{ij} = \sum_k a_{kj} \nu_{ik} \tag{78}$$

$$V'_j = \sum_i a^*_{ij} V_i \tag{79}$$

$$A'_j = \sum_i a_{ij} A_i \tag{80}$$

where a^*_{ij} is the cofactor of the matrix $||a_{ij}||$ divided by the determinant. The new rates and affinities can also be shown to be related by the linear rate laws as follows,

$$V'_1 = L'_{11} A'_1 + L'_{12} A'_2 \tag{81}$$

$$V'_2 = L'_{21} A'_1 + L'_{22} A'_2 . \tag{82}$$

The new phenomenological coefficients can be expressed in terms of the original phenomenological coefficients and elements of the transformation matrix by

$$L'_{11} = \frac{1}{D_a^2} (L_{11} a_{22}^2 - L_{12} a_{12} a_{22} - L_{21} a_{12} a_{22} + L_{22} a_{12}^2) \tag{83}$$

$$L'_{12} = \frac{1}{D_a^2} (-L_{11} a_{21} a_{22} + L_{12} a_{11} a_{22} + L_{21} a_{12} a_{21} - L_{22} a_{11} a_{22}) \tag{84}$$

$$L'_{21} = \frac{1}{D_a^2} (-L_{11} a_{21} a_{22} + L_{12} a_{12} a_{21} + L_{21} a_{11} a_{22} - L_{22} a_{11} a_{12}) \tag{85}$$

$$L'_{22} = \frac{1}{D_a^2} (L_{11} a_{21}^2 - L_{12} a_{11} a_{21} - L_{21} a_{11} a_{21} + L_{22} a_{11}^2) , \tag{86}$$

where D_a is the determinant of the $||a_{ij}||$ matrix. Note that, if the original matrix was symmetric, $L_{12} = L_{21}$, then obviously the new matrix is also symmetric, $L'_{12} = L'_{21}$.

Prigogine[41] noted the impossibility of finding a single transformation matrix $||a_{ij}||$ which would always result in a new diagonalized matrix. For the transformed matrix to be diagonal, L'_{12} and L'_{21} in equations (84) and (85) must be zero. Hence, these equations can be used to find the family of transformation matrices $||a_{ij}||$ which will make the phenomenological coefficient matrix diagonal.

However, note that the required transformation coefficients a_{ij} will involve the ratios of the original phenomenological coefficients, which will usually not be integers. As one example, the following linear combination of reactions appearing in equations (34) and (35) can be written,

$$2\left(1 - \frac{L_{21}}{L_{11}}\right)NO + Cl_2 + \frac{L_{21}}{L_{11}} I_2 = 2\left(1 - \frac{L_{21}}{L_{11}}\right)NOCl + 2\frac{L_{21}}{L_{11}} ICl \qquad (87)$$

$$2NOCl + I_2 = 2NO + 2ICl \,. \qquad (88)$$

This example results in a new pair of equations which are independent in the sense that the velocity of each reaction depends only on its own affinity. However, one of the new equations is a non-integer combination of the original chemistry and, therefore, would seem to lack the physical significance of chemical reactions as usually written.

Also, recall that the L_{ij} matrix elements, that is, the

original phenomenological coefficients, were identified as functions of the equilibrium composition and temperature of the system. In other words, they were functions of the state of the system; for any given initial or equilibrium conditions of the system, these coefficients would be expected to be different than for any other initial or equilibrium conditions. Therefore, since the numerical value of the a_{ij} transformation coefficients involve ratios of the L_{ij} coefficients, any diagonal transformation will be valid for only one particular state.

This result is consistent with Prigogine's analysis[41] that no general transformation can be found unless these original elements are linearly dependent. De Groot[6] and de Groot and Mazur[7] also questioned the physical importance of the fluxes and forces resulting from such diagonalization transformations.

Inspection of the transformed L'_{ij} matrix of equations (83) through (86) reveals that the new matrix is symmetric if the original matrix was symmetric. Even simpler, the new matrix is symmetric if the original system contained zero off-diagonal terms, that is,

$$L'_{12} = L'_{21} \quad \text{if} \quad L_{12} = L_{21} \tag{89}$$

and

$$L'_{12} = L'_{21} \quad \text{if} \quad L_{12} = L_{21} = 0 \, . \tag{90}$$

This latter result is essentially the proof of the Onsager reciprocity relations based on the "independent processes hypothesis" postulated

by Li[25], Pitzer[39, 40] and Verschaffelt[57].

Their conclusions certainly constitute a macroscopic proof for the Onsager reciprocity relations for that sub-group of systems which possess processes which are separable. However, that this sub-group embraces all, if any, of the physical systems usually annalyzed by non-equilibrium thermodynamics is not apparent. For example, the conclusion was reached in the previous section that certain chemical systems exhibited intrinsic chemical coupling. This coupling could only be suppressed by a state-by-state transformation involving ratios of rate constants.

6. Destruction of the Reciprocity. Meixner[32] originally investigated the invariance of the Onsager relations under simultaneous linear transformations of the fluxes and forces. For a given linear transformation of the fluxes, the compatible linear transformation of the forces was derived from the invariance of the entropy production. Using these resulting transformation formulas, the invariance of the Onsager relations was established. De Groot[6] later presented an analogous discussion. In both cases, the transformation matrices are related in the following manner,

$$\tilde{\mathfrak{P}} \cdot \mathfrak{Q} = \mathfrak{J} \tag{91}$$

where $\mathfrak{J}$ is the identity matrix, $\mathfrak{P}$ is the transformation matrix for the velocities or fluxes,

$$\mathfrak{v}' = \mathfrak{P} \cdot \mathfrak{v}, \tag{92}$$

and $\mathfrak{Q}$ is the transformation matrix for the affinities or forces,

$$\mathfrak{A}' = \mathfrak{Q} \cdot \mathfrak{A}. \tag{93}$$

However, Verschaffelt[56] later gave an example of linear transformations which destroy the Onsager relations. Davies[4] concurred that, if the transformations are only subject to the condition that the entropy production is invariant, the transformation matrices will be related by

$$\tilde{\mathfrak{P}} \cdot \mathfrak{Q} = \mathfrak{J} + \mathfrak{w}\,\mathfrak{L} \tag{94}$$

where $\mathfrak{w}$ is a skew symmetric matrix and $\mathfrak{L}$ is the original phenomenological coefficient matrix. Providing $\mathfrak{w} \neq 0$, such transformations will indeed destroy the Onsager relations. However, Davies argued that, since such transformations "depend explicitly on the flow coefficients contained in $\mathfrak{L}$," these transformations can have no physical importance. He then selected $\mathfrak{w} = 0$, which led again to the Onsager relation invariance transformation of Meixner and de Groot. Hooyman, de Groot, and Mazur[23] later showed that, if the deviation of the entropy from its equilibrium value as well as the entropy production are to remain invariant under these transformations, then $\mathfrak{w} = 0$.

Also, if $\mathfrak{w} \neq 0$, the resulting stoichiometry of the transformed reaction system is questionable. Recall that the $||a_{ij}||$ transformation, as given by equation (78), is a transformation of the stoichiometric equations, for example, equations (34) and (35). This linear stoichiometric transformation implies definite velocity and affinity transformations as given by equations (79) and (80). These velocity and affinity transformations were shown to result in the invariance of the Onsager relations. Inspection of equations (79) and (80) will show that they indeed obey equation (94) with $\mathfrak{w} = 0$.

Recently, Coleman and Truesdell[3] used the following example of the transformations expressed by equation (94),

$$\mathfrak{v}_i' = \mathfrak{v}_i + \sum_j \mathfrak{w}_{ij} \mathfrak{A}_j \tag{95}$$

$$\mathfrak{A}_i' = \mathfrak{A}_i \tag{96}$$

to demonstrate the destruction of the Onsager relations. Using the examples of reactions 1 and 2, an illustration of Coleman and Truesdell's velocity transformation, as expressed by equation (95) can be given by the following simple $||W_{ij}||$ skew symmetric matrix,

$$||W_{ij}|| = \left|\left| \begin{matrix} 0 & -1 \\ 1 & 0 \end{matrix} \right|\right| . \qquad (97)$$

This transformation is tantamount to using the following stoichiometric transformation matrix

$$||a_{ij}|| = (D_L - L_{21} + L_{12} + 1)^{-1} \left|\left| \begin{matrix} D_L - L_{12} & L_{11} \\ -L_{22} & D_L + L_{21} \end{matrix} \right|\right| , \qquad (98)$$

where D_L is the determinant of the original phenomenological coefficient matrix, $D_L = L_{11}L_{22} - L_{12}L_{21}$. This $||a_{ij}||$ matrix transforms the reactions of equation (34) and (35) into the following new pair of reactions,

$$2(D_L - L_{12} + L_{22})NO + (D_L - L_{12})Cl_2 + (-L_{22})I_2 \rightleftharpoons 2(D_L - L_{12} + L_{22})NOCl + (-L_{22})ICl \qquad (99)$$

$$2(L_{11} - D_L - L_{21})NO + (L_{11})Cl_2 + (D_L + L_{21})I_2 \rightleftharpoons 2(L_{11} - D_L - L_{21})NOCl + 2(D_L + L_{21})ICl . \qquad (100)$$

In contrast, consider Coleman and Truesdell's affinity

transformation, as given by equation (96). Equation (80) shows that this transformation is equivalent to the following $||a_{ij}||$ transformation

$$||a_{ij}|| = \mathcal{J} \tag{101}$$

which leaves the stoichiometric equations (34) and (35) invariant!

Hence, Coleman and Truesdell's particular example of a transformation satisfying equation (94) with $\mathfrak{b} \neq 0$, and thereby resulting in a destruction of the Onsager relations, requires different transformed stoichiometric equations, depending upon whether the flux or the force transformation is used to generate the $||a_{ij}||$ matrix. Obviously, a meaningful $||a_{ij}||$ stoichiometric transformation matrix cannot be generated to simultaneously satisfy a nontrivial flux and force transformation of the form of equation (94). In fact, such an $||a_{ij}||$ transformation matrix can only be made to simultaneously satisfy a flux and force transformation if these transformations are related by equation (91). Such transformations, in turn, will preserve the Onsager reciprocity.

III. EXPERIMENTAL METHOD

The immediate purpose of the experimental work is to determine the rates of the reactions and the concentrations of the macroscopic chemical species as functions of time. Using this information, various statements of the preceeding section can be examined.

Although the kinetics of reaction 1 have been studied[59], no rate data is available for reactions 2 and 3. However, Yost[59] indicated that both reaction 2 and 3 were rapid. Such a statement was quantitatively verified by some of our preliminary measurements.

Therefore, the objective of the experiment is to rapidly mix the reactants, iodine, chlorine, and nitric oxide and then measure the concentrations of the various chemical species as the system relaxes to equilibrium. The flow system accomplishes the former objective while the optical system together with the electrical system achieved the latter.

The flow system is shown schematically in Figure 3. Nitric oxide and chlorine gas are passed directly from cylinders to the rotameters, which served as flow rate measuring devices. Gas regulators are used to control the flow rates.

However, the problem is more complicated for iodine, since a sufficient quantity of iodine vapor is not available at room temperature due to the low vapor pressure of iodine. To overcome this problem, an argon carrier gas flows over finely ground iodine crystals which are packed in a jacketed glass column. The column

can be heated above room temperature by flowing hot water through the jacket. In this manner, appreciable quantities of iodine vapor can be transported into the vapor phase and passed through rotameters. The presence of the argon carrier gas tended to damp out thermal changes in the system. The temperature of all runs differed by less than 0.7 ^{o}C.

After exciting from their respective rotameters, the reactant streams are rapidly and thoroughly mixed in a tangential mixing chamber. The resulting mixture then flows through a transparent quartz reaction cell.

When a steady state condition is attained in the flow system, high-speed valves are closed, thereby trapping a homogeneous, reacting system in the reaction cell. The optical and electrical systems then measure data related to the concentrations as the system approached equilibrium.

The concentrations are determined by photometric methods using the optical and electrical systems. In this manner, the desired data can be taken without disturbing the reacting mixture.

A schematic diagram of the optical system is shown in Figure 5. White light is collimated and sent through a solution of cupric sulfate to attenuate the ultraviolet and infrared components. The light is then passed through the reaction cell. After being partially absorbed by the chemical species, the light emerges from the cell and is split into four wavelengths, as shown in Figure 5. Each light beam is directed upon a multiplier phototube, which is utilized to

to measure the amount of this light absorption in the reaction cell. The electrical output of each phototube is displayed on an oscilloscope and photographed. Using these photographs and the Lambert-Beer law, the concentrations of the chemical species can be determined as a function of time.

IV. EXPERIMENTAL APPARATUS AND REAGENTS

A. Primary Equipment

The primary equipment is designed to study the behavior of a particular chemical reacting system. However, due to its versatility, the equipment may be utilized to observe many liquid and gas phase reactions which can be followed photometrically.

A photograph of this equipment is shown in Figure 2. Two power supplies appear in the top portion of the picture, the high voltage supply on the left and the low voltage supply on the right. Directly below the high voltage power supply is a plug-board which can be used to connect various inputs to a potentiometer. Below the plug-board is the control panel which covers the majority of the electrical system.

In the right foreground of Figure 2 is the oscilloscope with its camera. The enclosure which houses the optical system is directly behind the oscilloscope. The light source is on one corner of the optical system enclosure, below the rotameters. In addition to the rotameters, the center of the photograph shows the control valves for the flow system, the light source control panel, and the packed iodine column.

1. Flow System

By means of the flow system, a homogeneous, gas phase, reacting mixture of nitric oxide, chlorine, and iodine is isolated in the reaction cell. Figure 3 shows a schematic diagram of this system.

Nitric oxide is passed through a Matheson Model 14-660 stainless steel regulator, needle valve, and check valve to a rotameter, which is used for approximate flow rate measurements. Monel tubing was used throughout this system in order to minimize attack by the corrosive chemicals. Similarly, a Matheson Model 15-660 nickel alloy regulator, needle valve, and monel check valve are utilized to control the flow of chlorine to a separate rotameter. For the nitric oxide and chlorine streams, the check valves are installed just downstream of the regulators and needle valves to prevent any flow back into the cylinders.

The flow of argon gas is controlled through a packed bed of iodine crystals and a rotameter by a Matheson Model 8-590 regulator and needle valve. The packed bed is constructed by packing finely crushed iodine crystals in a 3 cm. I. D. glass tube which is "necked-down" and fused onto heavy-walled 3/8 inch glass tubing at each end. Glass wool is inserted at each end of the 3/8 inch tubing to prevent the crystals from coming out. Around this 3 cm. packed tube is fused a 5 cm. I. D. glass tube so that the entire arrangement resembles a large laboratory condensor. Ports are put into the walls of the 5 cm. tube so that hot water can be passed through the jacket formed by the

3 cm. and 5 cm. tubes. A rectangular enclosure with a lucite front supports this column and also protects the operator in case of glass breakage. The column is attached to the enclosure with 3/8 inch, monel Swagelok bulkhead fittings. The seal to the glass 3/8 inch tubing is accomplished with a specially bored 3/8 inch Swagelok teflon ferrule.

All three rotameters are Fischer and Porter stainless steel Purge Meters Model 10A3135N, constructed with a needle valve on the inlet and a check valve at the outlet. However, the tubes and floats in these meters differ. The meters utilized for the nitric oxide and chlorine streams used FP-1/8"-08-P-3 tubes and 1/8" glass floats, while the meter which monitored the iodine-argon stream used a FP-1/4"-41-P-3 tube with a 1/4" GSS stainless steel float.

After leaving the rotameters, the nitric oxide and chlorine streams are each put into one port, and the iodine-argon stream is split and passed into two ports of a monel mixing chamber. This mixing chamber is designed from the recommendations of Hartridge and Roughton[18, 19, 20]. The chamber is made to utilize very large fluid velocities to improve mixing and to decrease the residence time of fluid in the chamber. The residence time is also minimized by keeping the chamber volume small.

From the mixing chamber, the stream passes through a high-speed valve, through the reaction cell, and out through another high-speed valve. The exhaust gas from the last valve is emptied into the atmosphere above the laboratory by means of a blower and a three-inch diameter polyvinyl chloride pipe.

The reaction cell is constructed from 12 mm. O. D. quartz tubing and can be seen in the left foreground of Figure 4. Optical flats, made of one-eighth inch thick, optical grade, Corning fused silica Code 7940, are fused on each end of the tubing.

The high-speed valves are non-destructive and can be opened and closed repeatedly. They are constructed by properly connecting and adapting three stainless steel valves purchased from the Vacco Valve Company. A solenoid valve, SD3-22-3, is used to control two pneumatic actuated control valves, COS-3P-401. A high pressure nitrogen line, maintained at 1000 psig. by a Matheson Model 3-590 high pressure regulator, is connected to the inlet port of the solenoid valve. Upon actuating the solenoid with 28 volt direct current, the solenoid valve poppet is dislodged from the valve seat allowing a shock wave of nitrogen gas to discharge from the outlet port. The pneumatic actuated control valves are connected in parallel to this outlet port. With this arrangement, the shock wave rams the poppet of each control valve down, thereby simultaneously closing both control valves. In this closed position, the control valves isolate the gaseous mixture in the reaction cell. When the current to the solenoid valve is turned off, the high pressure nitrogen loading the poppets of the control valves is vented to the atmosphere. A spring then returns the poppets of the control valves to their open position.

These valves were modified after they were received from the manufacturer. The control valves were supplied with female AN connections. To improve these connections and to eliminate leakage,

the inlet and outlet connections of each valve are machined to accept a specially designed monel fitting employing a confined teflon gasket seal. These fittings are used in conjunction with monel bulkhead fittings to connect each valve to the glass reaction cell. One of these valves is also connected to the mixing chamber, and the other is connected to the exit blower, as shown in Figure 3.

To stop leaks through the control valves when they are closed, the Kel-F seat washer is replaced by a softer washer of the same material. In addition, the metal surface below this washer is ground for a tight fit to the washer.

Due to the corrosive nature of chlorine, the O-rings of the control valves were replaced with O-rings made of Viton-A. Kel-F grease was also substituted as the poppet lubricant.

Three modifications are made to the resulting valve system to increase the speed of operation. The poppet position adjustment of the solenoid valve is altered from the manufacturer's recommendations to optimize operation under the 1000 psig. nitrogen pressure. In addition, the springs which returned the poppets of the control valves to their open position when the nitrogen pressure is released are replaced by springs with smaller spring constants. Finally, the effective length of the control valve poppets is increased in order to decrease the distance the poppet was required to travel to close the valve.

The final valve configuration was tested and timed by shining a light through each control valve onto two multiplier phototubes. The

outputs from the multiplier phototubes were displayed simultaneously on the screen of a Tektronix Type 531 oscilloscope equipped with a Type C-A Dual-Trace preamplifier. With the oscilloscope set on a calibrated sweep rate, the valves were closed and a photograph was made of the traces. The closing time was obtained directly from a measurement of the trace on these photographs.

The manufacturer of these valves claimed that the solenoid valve would open within 20 milliseconds. However, by using this solenoid valve to operate the high pressure nitrogen line to the control valves, the control valves can be closed within three milliseconds. The valves closed simultaneously within 0.5 millisecond.

A Sorenson Nobatron low voltage power supply, Model F-28-10, provides the 28 volt power to operate the solenoid valve. A schematic diagram of the associated wiring is shown in Figure 6.

The bulkhead fittings are specially designed and machined from monel. As shown in Figure 3, they are mounted on the wall of the optical system enclosure so that the reaction cell protrudes into the optical system. These fittings employ Viton-A O-ring seals to the valve fittings and also to the legs of the reaction cell. In addition, one bulkhead fitting is machined to accept a thermocouple probe and the other a pressure probe.

The thermocouple probe is made of monel and has a 0.040 inch diameter hole in the center. This hole is bored to accept a small quart tube which contains a copper-constantan thermocouple. The

quartz tube is fused at one end, and a drop of silicone oil is placed on the tip of the thermocouple junction to increase the effective heat transfer coefficient to the junction from the quartz wall.

The pressure tap is machined from monel and is used during leak tests of the reaction cell when the control valves are closed. During runs, the pressure tap is closed with a plug.

Using this flow system, the reactants can be mixed and isolated in the reaction cell very rapidly. At the lowest flow rate used in this work, the time required to mix and pass the reactants completely through the reaction cell was 0.06 seconds.

2. Optical System

After the flow system isolated the gaseous reacting system in the reaction cell, the purpose of the optical system is to work in conjunction with the electrical system to produce data which allow the calculation of concentrations during a run. The optical system is represented by a schematic diagram in Figure 5. Figure 4 gives a photograph of the interior of the optical system enclosure.

The light source is a General Electric Q 6.6A/T3/Cl, 100 watt, tungsten filament, quartz envelope, iodine filled lamp. The lamp is soldered into special mounting brackets which can be adjusted by set screws in a wide range of vertical and horizontal positions. In this way, the lamp can be placed in an optimum position in the light path.

A quartz envelope is needed for the lamp so that the weak ultraviolet radiation at 3343 Å will not be absorbed. Also, the lamp is designed to operate at high temperatures to enhance the emitted radiation at these low wavelengths. The intensity does not diminish over extended periods of time due to deposition or "blackening" of the quartz envelope with tungsten molecules. The manufacturer claims that the iodine allows a mechanism to occur which actually deposits the vaporizing tungsten molecules back on the hot filament.

A glowing filament lamp is desired in the experiment because a stable source is mandatory. Arc or discharge lamps, which produce an abundance of ultraviolet light, are unacceptable because they are too unstable. The stability of the light source is also aided by the power source, two Exide Type LL-57A lead-acid storage batteries. The

batteries are wired in series to produce sixteen volts. A steady current of approximately 6.5 amperes is drawn from these batteries for many hours preceeding and during a run. The batteries have ample storage capacity, being each about four cubic feet in volume and 600 pounds in weight. An electrical diagram of the light source controls is shown in Figure 6. When not used to actuate the solenoid valve, the Nobatron low voltage power supply is used to charge these batteries.

The light from the lamp is first partially collimated by a double convex lens with a focal length of 15 mm. and a diameter of 17 mm. This lens has sufficient transmittance in the near-ultraviolet region of the spectrum to pass the desired wavelength of 3343 Å. As shown in Figure 5, the lens is mounted in the opening of an enclosure so that the light must pass through the lens before entering the next stage in the optical path.

After leaving the lens, the light passes through a solution of cupric sulfate which is mounted in a transparent quartz cell. This solution attenuated most of the ultraviolet rays, which may cause photochemical effects, and also attenuated the red and infrared wavelengths which have a marked heating effect. Since this solution absorbed the majority of the heating rays, it is continuously cooled by passing dry air around the cell.

Next, the light enters a collimator which is made from a five inch long, one-half inch diameter tube. The tube contains disks with one-eighth inch diameter holes in their centers. The disks are

placed by hollow spacers every one inch along the tube. All inside surfaces of the collimator are pained with dull black Eastman Kodak No. 4 Brushing Lacquer to minimize any reflections which would degrade the collimation.

Leaving the collimator, the narrow beam of light passes through the reaction cell. Care is taken to align the beam so that it passes through the center of the reaction cell and no reflections or scattering occur on the sides or corners of the cell.

As shown in Figure 5, the beam is split into four separate beams of continuous light by three mirrors. Although the bottom mirror is made from quartz to transmit 3343 Å, the other mirrors are constructed from glass. They were made by Thin Film Products, Inc. of Cambridge, Massachusetts to reflect about fifty percent and to transmit about fifty percent of the incident radiation by depositing the proper thickness of inconel on the glass or quartz base. Inconel was chosen because it has a high reflectivity in the visible and near ultraviolet regions of the spectrum and also because it tarnishes much less than most common reflective materials. These mirrors are sealed in a quartz or glass cover material as an added protection against scratching or damage to the inconel layer.

The mirrors and interference filters are arranged in the manner shown in Figure 5 because the light reaching this system is richer in the longer wavelength radiation, such as 4900 Å, than in the near-ultraviolet radiation, such as 3343 Å. Therefore, each wavelength is separated in the order of increasing wavelength.

The narrow bandpass interference filters, which isolated the desired spectral regions from the continuum of each of the four beams, are examples of the recent achievements of optical technology. They are made by depositing more than forty extremely thin layers of dielectric material upon one another. The transmittance curves of these filters are shown in Figures 11 through 14. In addition to the characteristics shown in these figures, each filter is blocked to approximately 8000 Å. As shown in Figure 5, the filters are mounted in the openings of light-tight enclosures so that each multiplier phototube only encounters radiation transmitted by its own filter.

The entire optical system, including the reaction cell, is housed in the light system enclosure, thereby preventing any extraneous light from affecting the measurements. A photograph of the interior of this enclosure is shown by Figure 4. The interior is coated with dull black Eastman Kodak No. 4 Brushing Lacquer in order to absorb undesirable reflections.

3. Electrical System

The light intensity of each light beam incident on the multiplier phototubes is converted into electrical signals by the electrical system. The diagram of the main electrical system is shown in Figure 7.

The overall amplification of a multiplier phototube is highly dependent on the voltage per stage. Even slight changes in overall voltage will result in large changes in amplification. Therefore, only high quality, wire-wound resistors are used in the voltage divider circuits of the multiplier phototubes. Also, very stringent stability requirements are demanded of the power supply to these divider circuits and multiplier phototubes.

A regulated, high voltage power supply provides 1500 volts direct current to the multiplier phototubes and their voltage divider circuits. The power supply is a Model 132S, manufactured by the Calibration Standards Corporation. For this application, the manufacturer increased the current output of this unit to 50 milliamperes. The ripple and regulation of the unit are well within the manufacturer's specifications, which are excellent.

A ten-stage, Type 6292 multiplier phototube, manufactured by the Allen B. DuMont Laboratories, Inc., is used to monitor the wavelengths of 4900, 4716 and 3802 Å. This phototube is a member of a series of phototubes that has a silver-magnesium photocathode which gives very stable operating characteristics. Also, the spectral response of this tube is particularly suited for these wavelengths.

This Type 6292 tube is selected because it has a separate connection in the base so that the potential of the focusing shield can be independently adjusted to optimize the collection of photoelectrons on the first dynode. Smaller tubes in this series do not have this feature.

Due to the poor sensitivity of the Type 6292 tube at 3343 Å, a Radio Corporation of America 1P28 multiplier phototube is used to follow this wavelength. Although the tube has only nine stages, adequate amplification is obtained because the wavelength of maximum response is 3400 Å. This phototube has many industrial and laboratory applications and is very stable.

In selecting an individual tube, several tubes of the same type are purchased, and their output characteristics are examined from oscilloscope displays. Only the most stable tubes are retained and employed in the experimental work. After a tube is accepted, it is aged at least forty-eight hours in the dark at the operating voltage.

In operation, all the multiplier phototubes are shielded from magnetic and electrostatic fields by wrapping a high mu-metal shield around each tube and maintaining the shield at the high potential of the photocathode. The shield is also maintained at cathode potential to prevent charging of the glass envelope of the tube.

The measurement of the concentrations of the chemical species is complicated because extremely low light intensities and concentrations are used. In order to secure the desired amplification, the multiplier phototubes were operated close to their maximum rated output. Although the output current was unusually large, the voltage per stage was maintained at the values recommended by the manu-

facturers to secure the optimum signal-to-noise ratio. The large currents in the last stages of the phototubes caused voltage drops which must be considered in the design of the voltage divider circuits. Otherwise, the voltage ratios in these circuits and between dynodes would be upset, thereby causing a non-linear response of the multiplier phototube. This problem was avoided by keeping the current flow through the divider circuits about ten times the average anode current[12, 47].

The voltage divider circuits are shown in Figure 7. To be certain that most of the photoelectrons emitted by the photocathode were drawn into the multiplier section of the multiplier phototubes, a voltage drop between the photocathode and first dynode is twice the voltage drop between any two dynodes. By adjusting R_1, the focusing shield is maintained a few volts more positive than the photocathode in order to enhance this collection.

Due to the high currents in the voltage divider circuits, appreciable heat is produced. Therefore, the main electrical circuits are isolated in a separate enclosure from the multiplier phototubes in the optical system enclosure. Not only would excessive heat increase the undesirable thermionic emission of the multiplier phototubes, but also it would heat the gas mixture in the reaction cell.

To eliminate the high frequency noise components from the output signal of the multiplier phototubes, the anode is connected to a low-pass, Pi-type filter. The filter is designed so that attenuation frequencies beginning at 54, 416, or ∞ cycles per second can be

selected by turning the switch S_1. At the lower attenuation frequencies, rapid changes in the signal are damped out or distorted even though more noise is filtered out at lower than at higher attenuation frequencies. Therefore, the speed of the signal change dictates the particular filter attenuation frequency which is used. The noise level is also reduced by electrostatically shielding all the wiring which carries the signal.

The filtered signal then passes to the null and measuring circuits, which are shown in Figure 7. R_8 is a ten-turn Helipot and R_4, R_5, R_6, and R_7 are precision wirewound resistors. With the reactants flowing through the reaction cell, R_8 is adjusted so that the reading on the oscilloscope is zero. This means that the voltage drop across R_4 plus R_5 is equal to the voltage drop across R_6 plus R_7. When the valves are closed, thereby isolating the reacting system in the reaction cell, the voltage drop across R_6 and R_7 changes as the reaction progresses. This change in voltage is measured by the deflection of the oscilloscope trace because the voltage drop across R_4 and R_5 remains constant, as dictated by the setting of R_8.

A Leeds and Northrup K-3 potentiometer is used to measure the static voltage across R_4 plus R_5 and across R_6 and R_7. Actually, the voltage across these resistors together exceeds the range of this potentiometer. Therefore, the resistance ratios $R_5/(R_4 + R_5)$ and $R_6/(R_6 + R_7)$ are calibrated, and the potentiometer is connected to read the voltage drop across either R_5 or R_6.

Knowing these resistance ratios, the voltage drop across R_4 plus R_5 or R_6 plus R_7 can be determined by measuring the voltage drop across R_5 or R_6.

A Tektronix Type 531 oscilloscope with a Type M four-channel plug-in preamplifier is used. The four traces, representing the time behavior of each multiplier phototube output, are photographed with a Tektronix C-12 oscilloscope camera using a Polaroid Land Roll Film back with Polaroid Type 47, 3000 Speed film.

B. Vacuum System

The vacuum system is used to make mixtures of the various gaseous chemical species used in this experiment. Small optical cells used in the Cary Model 14 recording spectrophotometer and also large, five-liter bulbs, used to flow calibration mixtures through the flow system, are filled by means of this vacuum system.

A photograph of the vacuum system is shown in Figure 8. The system is mounted on a sturdy and light frame, thereby making the system portable. An Edwards Speedivac Model ISC50B single stage high vacuum pump is connected to the glass vacuum system by a Viton-A O-ring seal. This pump is protected from the vacuum system by a cold trap which is immersed in liquid nitrogen. When corrosive gases are used, Type AW500 Linde Molecular Sieves are placed in the cold trap to prevent any corrosive gas passing into the vacuum pump.

The main manifold of the system is 15 mm. tubing and can be isolated from the pump and cold trap by a 10 mm. high-vacuum stopcock. Two tapered joints, provided with 4 mm., high-vacuum stopcocks, are fused into the main manifold to allow connections for filling either the Cary optical cells or the five-liter bulbs.

Provisions for connecting the vacuum system to metal gas cylinders is also provided. Three connections, employing 2 mm., high-vacuum stopcocks and Kovar glass seals to 3/8 inch stainless steel tubing, are connected to monel Swagelok bulkhead fittings. These fittings are rigidly mounted to the frame of the vacuum

system. Lines from the cylinders can be easily connected to the vacuum system by means of these fittings without danger of undue stressing of the glass.

Low vacuum pressures are measured by a Todd Universal Vacuum Gauge, a three scale McLeod type gauge. A 160 cm. mercury manometer and a silicone oil manometer are also employed as pressure measuring devices. The McLeod gauge is fused directly into the main manifold, while the manometers are connected to the manifold by Viton-A O-ring vacuum seals. Each device can be connected to the main manifold by turning 2 mm., high-vacuum stopcocks.

The silicone oil manometer is an improvement on the design recommended by A. T. J. Hayward[21]. When oil manometers are used at low pressures or to measure pressures relative to a vacuum, errors are often introduced due to the release of small amounts of gases which are dissolved in the oil. Hayward's design avoids this problem by providing an arrangement which will permit the oil to be quickly freed of these dissolved gases before each measurement. A diagram of our manometer is shown in Figure 9.

Measurements are taken with the manometer in its upright position, as shown by the dashed lines. Preceeding a measurement, the manometer is tilted on its side by turning it in the specially designed, rotating O-ring vacuum seal. In this position, a maximum surface area of the oil is exposed to vacuum. By exposing the oil in this manner, and by slightly agitating the manometer, the dissolved gases are quickly expelled from the oil.

In our design, two "de-aeration" chambers are used to increase the surface area of the oil and also to allow a place for the oil to flow from each leg of the manometer when the manometer is turned on its side. With a "de-aeration" chamber connected to only one leg of a manometer, excessive time is consumed in adjusting the manometer so that the oil from both legs can flow into the one chamber. In addition, the "de-aeration" chambers are set about ten degrees to the axis of the legs to allow the oil to drain by gravity into the chambers while the chambers remain horizontal. The connecting tubing to the O-ring seal is only open at the bottom side so that oil cannot run into the vacuum system when the manometer was tilted.

DC 200 silicone oil, manufactured by the Dow Corning Corporation, is used as the manometer fluid. This oil possesses desirable viscosity, density and gas solubility properties.

C. Reagents

The iodine crystals which are used in the iodine column were Baker and Adamson Reagent Grade Resublimed iodine, claimed to have a minimum purity of 99.8%. The maximum limits on the impurities are stated to be 0.005% for chlorine and bromine, and 0.010% for non-volatile impurities.

The gaseous reagents were all purchased from The Matheson Company, Inc. The minimum purity for the argon is 99.98%, with typical impurity analysis on our sample of 1/2 to 1 ppm. of water, 1 to 2 ppm. of nitrogen, and 1/2 to 1 ppm. of oxygen.

The chlorine was specially prepared by The Matheson Company and is stated to have a purity of 99.9%. The impurities are claimed to be less than 200 ppm. of carbon dioxide, 50 ppm. of oxygen, and 100 ppm. of nitrogen.

Our nitric oxide sample has a minimum purity of 99.0%. The impurities were less than 400 ppm. of nitrogen dioxide, 0.42% nitrous dioxide, and 0.56% of nitrogen.

These analyses were only checked qualitatively by obtaining the absorption spectrum of each reagent in the infrared, visible, and ultraviolet regions of the spectrum. A Cary Model 14 recording spectrophotometer was used for this purpose. Nothing was found to discredit these analyses.

V. EXPERIMENTAL PROCEDURE

The high-voltage power supply to the voltage divider circuits and multiplier phototubes is turned on at least eight hours prior to a run to allow for temperature stabilization of the electronic equipment. Only two hours are needed to allow the system to stabilize after the light source is turned on.

Although the Tektronix equipment is very stable, adequate time is given the oscilloscope and four-channel preamplifier to warm up. Before the final series of runs, the oscilloscope and preamplifier were calibrated by the Tektronix Corporation. The "DC Balance" and "Gain Adjustment" for each channel of the preamplifier are checked before each run. The preamplifier is used only in its "chopped" mode. For each channel of the preamplifier, the variable gain control is set in the calibrated position, and the normal DC mode is used.

The initial oscilloscope traces are started at the moment the control valves are closed to isolate the reacting system. Such "triggering" is accomplished by connecting a line in parallel from the solenoid valve to the trigger input of the oscilloscope, as shown in Figure 6. Incidentally, the resistance value in this circuit is selected so that triggering will occur without disturbing the initial characteristics of the traces. In addition, the external DC triggering mode and a positive trigger slope are used. The triggering level and the stability of the trigger are adjusted for optimum conditions before each run.

With transparent argon gas flowing through the reaction cell, switches, S_3, are opened to disconnect the oscilloscope from the circuit. Under these conditions all of the anode current goes through R_6 and R_7. The voltage drop across R_6 is measured with the potentiometer. This voltage was proportional to v_o, which is discussed in a subsequent section.

With four simultaneous traces on the oscilloscope screen, the resulting photographs are somewhat confusing. To minimize this problem, each trace is started at a different point on the screen by adjusting the position controls for each channel of the preamplifier. Figure 15 gives an illustration of these photographs for Run 17.

The sweep rate of the oscilloscope and the vertical sensitivity of each channel of the preamplifier are then set. The current and voltage drop through the light source are recorded. The latter provided a warning when the tungsten filament is going to burn out. The output current from the anode of each multiplier phototube is recorded. The null point for each trace is then noted by shorting a wire across the inputs of each channel. With all the preliminary adjustments made, the equipment is ready for a run.

The reactants, iodine, chlorine, and nitric oxide are allowed to flow through the reaction cell. After steady state conditions are reached, the rotameter readings are recorded. The switches S_2 and S_3 are closed and R_8 is adjusted for each channel so that each trace is approximately at its null value. The camera shutter

is opened and the solenoid value is fired, thereby isolating the reacting mixture in the reaction cell and simultaneously triggering the sweep of the four traces on the oscilloscope screen.

With the oscilloscope traces recording the progress of the reaction, the triggering mode of the oscilloscope is changed from "external DC" to "automatic," so that the succeeding sweeps will be initiated automatically as each preceeding one is completed. In this manner, the entire progress of the reaction is followed. Polaroid photographs are taken of each sweep and the film is changed when necessary. If a trace progresses so far in a vertical direction that the trace goes off the screen, the vertical sensitivity of the particular channel is decreased in order to return the trace to the screen.

When the traces finally level off, the run is terminated. The temperature in the reaction cell is measured, the valves are opened, and the chemicals are flushed out of the reaction cell with argon gas. The voltage drop across R_5 for each channel is measured with the potentiometer. This voltage is proportional to the voltage set by R_8. As a final check for consistency and drift of the optical or electrical system, v_o is again measured by the method outlined above.

VI. ANALYSIS OF DATA

The raw data consisted primarily of the photographs of the oscilloscope traces, the potentiometer readings of the voltage drop across R_5 and across R_6, and the vertical sensitivity settings of each channel of the preamplifier. These data are used to calculate the concentration of each of the five chemical species and the velocities and affinities of each reaction as functions of time. Also, the coefficients in the phenomenological equations are eventually evaluated.

Light passing through the reaction cell produces a voltage by means of the electrical system. Preferably, this voltage should be a linear function of the intensity of the light. Fortunately, both the DuMont Type 6292 and the RCA 1P28 multiplier phototubes produce an anode current which is proportional to the incident light intensity on their photocathodes[12, 47],

$$i = sI , \tag{102}$$

where s is the overall sensitivity of the multiplier phototube. As shown in Figure 7, this current is passed through two fixed resistors, R_6 and R_7. The resulting voltage drop across these resistors, as given by equation (102) and Ohm's law, is

$$v = (R_6 + R_7)sI . \tag{103}$$

Therefore, the ratio of the transmitted to incident light intensity can be shown to be

$$v/v_o = I/I_o \qquad (104)$$

from equation (103).

With no absorbing species in the reaction cell, v_o is equal to the voltage drop across both R_6 and R_7. For each channel, v_o is easily calculated by multiplying the voltage drop across R_6, as measured by the potentiometer, by the resistance ratio $(R_6 + R_7)/R_6$. The calculation of v, however, is more complicated.

v for each channel is equal to the voltage drop across both R_6 and R_7 when absorbing species are present in the reaction cell. Since this voltage changed rapidly during a run as the reaction progressed, some means with an adequate time response was needed to record the dynamic behavior. As explained in the preceeding section, an oscilloscope with a camera is used to record this behavior.

The following relation exists between the voltages across R_6 and R_7, R_4 and R_5, and the oscilloscope,

$$v(t) = v_6 + v_7 = (v_4 + v_5) + v_{osc.}(t) . \qquad (105)$$

$(v_4 + v_5)$, as dictated by the setting of the variable resistor R_8, is simply calculated by multiplying the voltage drop across R_5 by the resistance ratio $(R_4 + R_5)/R_5$. At any time, $v_{osc.}$ is computed by multiplying the vertical sensitivity of the particular channel of the oscilloscope by the algebraic distance that the trace is displaced from the null point on the screen. If the trace is below the null point, $v_{osc.}$ is positive. Otherwise, $v_{osc.}$ is negative.

Before using the values of $v_{osc.}$ in equation (105) to calculate

v(t), these oscilloscope voltages are corrected for parallax error of the oscilloscope camera. This error arises because the phosphor of the cathode ray tube is not in the same plane as the oscilloscope graticule. Starting with the trace for each channel in its null position, various voltages were applied to the oscilloscope from a potentiometer and the resulting deflection of the trace was photographed. Also, a signal from a square wave generator was applied to the oscilloscope at various sweep rates and photographed. From these photographs, a parallax correction could be computed and applied to correct not only the magnitude, but also the time dependence of $v_{osc.}$.

These corrected oscilloscope voltages are then plotted as a function of time. Small gaps are present in this data because time is required to change film in the camera as the run progressed. A continuous curve is drawn through these points, and voltages are selected at five second intervals to be used in the calculations. The values of $(v_4 + v_5)$ and these oscilloscope voltages are then substituted into equation (105) in order to calculate v as a function of time for each channel.

The fundamental equation of the experimental work is the Lambert-Beer law, which is discussed in Appendix 5. Figure 10 illustrates the variation of the extinction coefficients with wavelength. Data for nitric oxide is not shown in this figure because nitric oxide is transparent in the visible and near-ultraviolet regions of the spectrum. Extinction coefficients which were used in the calculations are tabulated in Table IV and discussed in Appendix 3.

Unfortunately, as an examination of Figure 10 will show, none of the four species have a spectral region of absorption which is not shared by the others. Therefore, the simple Lambert-Beer law expression, equation (5-1) of Appendix 5, must be replaced by

$$I(\lambda) = I_o(\lambda) \exp \left\{ - \sum_{i=1}^{n} C_i \epsilon_i(\lambda) \ell \right\} . \qquad (106)$$

Since nitric oxide does not absorb light in the visible and near-ultraviolet regions, the concentrations of iodine, chlorine, iodine monochloride, and nitrosyl chloride can be found by solving the following equations simultaneously

$$(v(t)/v_o)_\lambda = \exp \left\{ - \sum_{i=1}^{4} C_i(t) \epsilon_{i,\lambda} \ell \right\} \quad \lambda = 1, 2, 3, 4 . \qquad (107)$$

The wavelengths used in this experiment were selected in order to minimize the possibility that the four-by-four matrix of extinction coefficients, shown in the equation above, will be singular.

The solution of equation (107) is possible, but often gives inaccurate concentrations due to large propagation of the error in the extinction coefficients. This problem can be minimized by using only two of the four equations given above with a material balance on the chlorine and iodine atoms. The initial concentration of iodine monochloride is assumed to be negligible compared to the initial concentration of iodine in the reaction cell. Also, the initial concentration of nitrosyl chloride is assumed to be negligible to that of chlorine. In this manner, the concentrations of iodine monochloride and nitrosyl chloride can be calculated as functions of

time from data taken on only the 4900 Å and 3802 Å channels. The equations which are used for this purpose are

$$C_{ICl}(t) = \left\{ \ln \left(v^i/v(t)\right)_{4900} + \left(\frac{\epsilon_{Cl_2,\,4900}}{\epsilon_{Cl_2,\,3802}}\right) \ln \left(v/v_o\right)^i_{3802} \right.$$

$$- \left(\frac{\epsilon_{NOCl,\,4900} - \frac{1}{2}\epsilon_{Cl_2,\,4900}}{\epsilon_{NOCl,\,3802} - \frac{1}{2}\epsilon_{Cl_2,\,3802}}\right)$$

$$\left. \times \left[\ln \left(v^i/v(t)\right)_{3802} + \left(\frac{\epsilon_{I_2,\,3802}}{\epsilon_{I_2,\,4800}}\right) \ln \left(v/v_o\right)^i_{4900} \right] \right\}$$

$$\div \left\{ \ell \left[\left(\epsilon_{ICl,\,4900} - \frac{1}{2}\epsilon_{I_2,\,4900} - \frac{1}{2}\epsilon_{Cl_2,\,4900}\right) \right.\right.$$

$$- \left(\frac{\epsilon_{NOCl,\,4900} - \frac{1}{2}\epsilon_{Cl_2,\,4900}}{\epsilon_{NOCl,\,3802} - \frac{1}{2}\epsilon_{Cl_2,\,3802}}\right)$$

$$\left.\left. \times \left(\epsilon_{ICl,\,3802} - \frac{1}{2}\epsilon_{Cl_2,\,3802} - \frac{1}{2}\epsilon_{I_2,\,3802}\right) \right] \right\} \qquad (108)$$

and

$$C_{NOCl}(t) = \left\{ \ln\left(v^i/v(t)\right)_{4900} + \left(\frac{\epsilon_{Cl_2,4900}}{\epsilon_{Cl_2,3802}} \ln\left(v/v_o\right)^i_{3802}\right.\right.$$

$$- \left(\frac{\epsilon_{ICl,4900} - \frac{1}{2}\epsilon_{I_2,4900} - \frac{1}{2}\epsilon_{Cl_2,4900}}{\epsilon_{ICl,3802} - \frac{1}{2}\epsilon_{Cl_2,3802} - \frac{1}{2}\epsilon_{I_2,3802}}\right)$$

$$\left.\left. \times \left[\ln\left(v^i/v(t)\right)_{3802} + \left(\frac{\epsilon_{I_2,3802}}{\epsilon_{I_2,4900}} \ln\left(v/v_o\right)^i_{4900}\right]\right]\right\}$$

$$\div \left\{ \ell \left[\left(\epsilon_{NOCl,4900} - \frac{1}{2}\epsilon_{Cl_2,4900}\right)\right.\right.$$

$$- \left(\epsilon_{NOCl,3802} - \frac{1}{2}\epsilon_{Cl_2,3802}\right)$$

$$\left.\left. \times \left(\frac{\epsilon_{ICl,4900} - \frac{1}{2}\epsilon_{I_2,4900} - \frac{1}{2}\epsilon_{Cl_2,4900}}{\epsilon_{ICl,3802} - \frac{1}{2}\epsilon_{Cl_2,3802} - \frac{1}{2}\epsilon_{I_2,3802}}\right)\right]\right\} . \quad (109)$$

The concentrations of iodine and chlorine can then be computed from

$$C_{I_2}(t) = \ln\left(v/v_o\right)^i_{4900} \Big/ \ell \epsilon_{I_2,4900} - \frac{1}{2} C_{ICl}(t) \quad (110)$$

$$C_{Cl_2}(t) = \ln\left(v/v_o\right)^i_{3802} \Big/ \ell \epsilon_{Cl_2,3802} - \frac{1}{2} C_{ICl}(t) - \frac{1}{2} C_{NOCl}(t) . \quad (111)$$

The time dependence of the concentration of nitric oxide is evaluated by first calculating the concentration at some point in the latter stages of a run. Knowing the nitrosyl chloride concentration as a function of time and using a material balance on the nitric oxide molecule, the nitric oxide concentration can be calculated as a function of time. The details of this computation and the assumptions involved are discussed in Appendix 2.

To find the velocities of reactions 1 and 2, the concentrations of chlorine and iodine are differentiated numerically. The first seven consecutive points in a run are fit by a parabola using the least squares method of Deming[8]. The slope at the first four points is found by analytically differentiating the resulting equation. The parabola is then fit to the second through eighth point, the third through ninth, etc., and the resulting equation of each fit is differentiated to find the slope at the midpoint of each fit. In this manner, the derivative was generated through the entire set of data points. For the last fit in a run, the resulting equation is differentiated to find the derivative for the final four points.

The method for calculating the affinities is discussed in Appendix 4. Equations (4-25) and (4-26) are used in this calculation.

All of the calculations which have been discussed were programmed and performed on a digital computer. For this purpose, an IBM 7094 high-speed digital computer was used.

In correlating the velocity and affinity data, other functional relationships in addition to the linear phenomenological equations,

equations (30) and (31), are examined. The velocity of a reaction can be expanded in a Taylor series expansion in terms of the two affinities as independent variables to give

$$V_i = \sum_{j=1}^{2} L_{ij}A_j + \frac{1}{2}\sum_{j=1}^{2}\sum_{k=1}^{2} L_{ijk}A_jA_k \quad i = 1, 2 . \tag{112}$$

This equation reduces to the linear phenomenological relations if the quadratic terms are neglected. The velocity and affinity data for each reaction of every run are fit to equation (112). Also, a fit is made to all other forms of this equation constructed by deleting one or more phenomenological coefficients in this equation.

These correlations are performed by the least squares method of Deming[8]. This method is programmed for general application of the IBM 7094 digital computer[58]. Using this approach, the least squares procedure can be applied to situations where several variables have error which is not uniformly distributed over the range of variables. Double precision arithmetic is employed in all matrix inversions of this program.

A convergence problem is encountered when each velocity and both affinities are assumed to have error. However, this problem can be overcome by first making a fit assuming only the velocity has error. Then the phenomenological coefficients obtained from this fit are used in a program which assumes that both the velocity and an affinity have error. Finally, the resulting coefficients from this fit are utilized to calculate the fit with the velocity and both affinities having error. The error in each variable is estimated by examining

the scatter in the velocity and affinity data.

The variance of each fit is computed. In this way, the goodness of each fit can be compared. Also, the 95% confidence limits based on a Student-t distribution are calculated for each coefficient. The details of these calculations are discussed by Deming[8].

Not only are many forms of equation (112) used in these correlations, but also different regions of data are examined in these fits. First, a fit is made using all the data of a run except the first few points that may show erratic behavior of the affinities. Then the fits are made using data from a later point through and including the last point of a run. Successively smaller regions of data are examined, always including the last point of a run, until only a small part of data at the end of a run is retained. In this way, the change in the phenomenological coefficients of each equation and the applicability of the equations themselves can be examined as the run approaches equilibrium.

VII. EXPERIMENTAL RESULTS

The results of the calculations discussed in the previous section are given for Runs 11, 12, 13, 16, and 17. Data for earlier runs are not shown because these runs were performed primarily to observe the behavior of the equipment. Electrical noise, presumably produced by some source which was external to the laboratory, adversely affected the oscilloscope traces for Runs 14 and 15. Therefore, the data for these runs are not comparable in quality to those of other runs and are rejected.

The tabulated results are not smoothed or adjusted to improve their appearance. They are taken directly from the computer output.

Run 17 is arbitrarily chosen to graphically illustrate the behavior and trends of the results. The results of this run are considered typical.

The calculated concentrations of iodine, chlorine, iodine monochlorine, nitrosyl chloride, and nitric oxide are shown in Table I. For Run 17, these results are also shown graphically in Figures 16 through 20.

The time dependence of the chemical affinities, velocities, and affinity-velocity products for reactions 1 and 2 are given in Table II. The affinities are scattered during the first few points of a run because the method of calculation is very sensitive to small fluctuations of the concentrations at these points. As a result, their entries have been omitted from Table II. For Run 17, the affinities are shown in Figures 21 and 22, and the velocities are illustrated in

Figures 23 and 24.

The significant results of the least squares correlations of the various functional relationships between the velocities and chemical affinities are shown in Tables IV and V. The results in Table IV are statistically the "best" values of the phenomenological coefficients for the last region of data used in the correlations. Table V gives the complete tabulation of the phenomenological coefficients.

The "best" values presented in Table IV are selected from Table V in the following manner. The variance of the fit for each correlation over a particular region of data are compared using a one-percent F-distribution[8]. Occassionally, this method of comparison shows that more than one correlation is equally significant. In these cases, the confidence limits of the phenomenological coefficients are examined to select the "best" fit. In addition, when the same correlation is the "best" fit for not only the last region of data, but also the preceeding region, the phenomenological coefficients for both regions are shown.

A discussion of the error associated with the experimental work is given in Appendix 6. The maximum uncertainties in the "best" phenomenological coefficients presented in Table IV are slightly better than those given in Table V. The maximum uncertainties in L_{11} and L_{21} in Table IV are less than 20% of the magnitude of the coefficient. The maximum uncertainties in L_{12}, L_{22}, and the coefficients of the quadratic terms are less than 40% of the magnitude of the coefficient.

The complete listing of the phenomenological coefficients is

presented in Table V. The first half of this table presents the coefficients of the least squares correlations with the velocity of reaction 1 as the dependent variable, that is, the coefficients L_{11}, L_{12}, L_{111}, L_{112}, and L_{122}. The coefficients for the correlations with the velocity of reaction 2, L_{21}, L_{22}, L_{211}, L_{212}, and L_{222}, are shown in the second half of the table. The variance for each fit is included.

As discussed in the previous section, various regions in the data are used in these correlations. However, when the number of data points becomes too small, the variance of the fit becomes several orders of magnitude larger than the variances using more points, or the confidence limits on the coefficients become larger than the magnitude of the coefficients. These fits with too few points are not shown.

The terms containing affinities in the first degree, that is, the terms with L_{11}, L_{12}, L_{21}, and L_{22}, are not arbitrarily assumed to be more significant than the terms with the affinities in the second degree, that is, terms containing L_{111}, L_{112}, L_{122}, L_{211}, L_{212}, and L_{222}. For almost all correlations, the confidence limits on the coefficients of the quadratic terms are a much greater percentage of the magnitude of the coefficients than the confidence limits for the coefficients of the first degree terms.

In addition, various fits are made deleting either one or both terms of first degree and substituting one of the three quadratic terms in its place. Such a substitution is done to see if the fit can be improved. In all cases, the variance of the fit increased greatly.

For these reasons, the terms containing the affinities in the

first degree appear to be more significant in attaining a good fit to the data than the quadratic terms. Therefore, Table V shows that as the number of terms included in a fit are decreased, the quadratic terms are deleted first while terms in the first degree are retained.

As more terms in the expansion, equation (112), are considered, eventually the least squares matrix becomes singular, the confidence limits on the coefficients become larger than the magnitude of the coefficients, or the least squares program fails to converge on values of the coefficients. Any of these phenomena may indicate that the functional relationships between each velocity and the affinities contain too many terms. These inferior correlations are also not included in Table V.

Figure 25 shows a graphical comparison for Run 17 of the velocity of reaction 1 measured experimentally with that predicted from the least squares correlations. The results of correlations made with data from 70 to 600 seconds are shown together with the results using data from only 470 to 600 seconds.

VIII. DISCUSSION OF EXPERIMENTAL RESULTS

The time dependence of the concentrations and velocities does not indicate simple kinetic behavior. Perhaps a rapid kinetic path is present initially which soon reaches equilibrium thereby allowing a slower path to determine the overall reaction rate. The rapid path appears to involve the macroscopic species iodine and iodine monochloride.

For all runs, reaction 1 is far from equilibrium, as shown by its chemical affinity. A_1/RT varied from about 20 to 10. However, reaction 2 seems to be close to equilibrium throughout a large portion of each run. A_2/RT varied between about 1.0 and 0.0. Since reaction 2 is so close to equilibrium conditions, small adjustments of the initial concentrations of a run can result in the existence of a negative ΔV product for this reaction. The affinities of both reactions relax monotonically toward their equilibrium values of zero as expected.

The sum of the ΔV products is always positive. This result agrees with the prediction of equation (13), which is a consequence of the Second Law of Thermodynamics.

Although the sum of the ΔV products is always positive, Table II shows that the ΔV product for reaction 2 is negative for Runs 12, 16, and 17. This result conforms to the ΔV product criterion for coupling discussed previously. However, since the ΔV product for reaction 2 in Runs 11 and 13 is positive, the ΔV product criterion for coupling appears to be a sufficient, but not necessary

condition. Such a criterion is not as general as the one proposed by equation (29).

Also, since the ΔV product of reaction 2 is negative in Runs 12, 13, and 17, reaction 2 appears to be running backward, that is, in a direction which is not spontaneous. Van Rysselberghe has mentioned that such phenomena exist in complex biological systems[50, 51, 52, 55], but this set of chemical reactions may be the first example of an inorganic system which shows this type of behavior. Although this fact may be interesting, it is certainly not profound because the entire system is proceeding in the proper direction as indicated by equation (13). The presence of the negative ΔV product may be physically explained by the existence of additional kinetic paths than those which occur in the presence of reaction 2 alone.

Figure 25 illustrates that the phenomenological rate expressions, given by various forms of equation (112), do not closely approximate the experimental data even when quadratic terms are used. However, the correlations agreed in most cases to approximately ten percent with the experimental data over the central portion of a fit.

Table V shows that the linear rate laws become better approximations as the system approaches equilibrium. In fact, the "best" fits, as shown in Table IV, are these linear relationships which describe V_1 for the last region of data in Runs 12, 13, and 16. The linear expressions describing V_2 are also the "best" representations

of the experimental data for the last regions of data in Runs 11, 16, and 17.

Over the regions in which these linear relations are "best," A_1/RT is as large as 13.5, but A_2/RT is no greater than 0.25. This result may indicate that the linear relationships can be useful in describing the behavior of a reaction in regions where A/RT is greater than 1.0. Prigogine, Outer, and Herbo[46] noted this same result during their study of the applicability of linear phenomenological laws for a single reaction.

The existence of the negative ΔV product shows the presence of coupling in this system. This conclusion is also substantiated by the statistical significance of the "coupling coefficients," L_{12} and L_{21}.

The Onsager reciprocity relations state that the coupling coefficients, L_{12} and L_{21}, should be equal when the linear rate laws are reasonable approximations of the behavior of a system. Inspection of the values of L_{12} and L_{21} in Table V where the linear rate laws have been used show a large discrepancy between these coefficients.

However, most of the correlations in Table V employing the linear rate law may not be adequate descriptions of the behavior of the system. By referring to Table IV, only in Run 16 do the linear rate laws appear to be the "best" correlations to describe the velocities of both reactions 1 and 2. Hence, a comparison of L_{12} and L_{21} is reasonable for this example. Even in this case the discrepancy between these coefficients is at least a factor of -200.

Although the linear rate laws may be adequate representations of the data over the regions which are fit, reaction 1 is not close enough to equilibrium to allow the curve which is produced by this fit to be extended through the origin.

In order to obtain adequate data to test the Onsager relations, reaction rates are needed which allow the affinities to remain about the same order of magnitude as the system approaches equilibrium. Also, the rates of the independent and dependent reactions must be about the same order of magnitude so that the apparent coupling effect of one reaction will not be obscured by another, more rapid reaction. Since the various kinetic rates involved in this system seem to differ greatly, adjusting the concentrations to achieve more satisfactory rates would be difficult.

IX. CONCLUSIONS

As discussed in the Theory section, the following conclusions are made.

1. After careful review and critical evaluation of the literature, no macroscopic derivation of the Onsager reciprocity relations which was examined is generally applicable. These derivations are either erroneous or are limited by the stringent assumptions which are used in their development.

2. Providing i) a simple expression for the overall rate of reaction which follows the law of mass action is applicable, ii) the independent stoichiometric equations can be identified for a reacting system, and iii) the assumption of the detailed balancing of each reaction close to equilibrium is valid, the phenomenological coefficients in the linear rate laws can be identifieid in terms of kinetic parameters. The coupling coefficients, L_{12} and L_{21}, are equal, as implied by the Onsager reciprocity relations. These coefficients involve only parameters of the reactions which are assumed to be stoichiometrically redundant. The diagonal coefficients, L_{11} and L_{22}, are functions not only of the parameters of the independent reactions, but also of the redundant reactions.

3. Linear transformations of the fluxes and forces which either diagonalize or destroy the symmetry of the phenomenological coefficient matrix are not generally applicable for a chemical reacting system. Such a transformation is only valid for a given equilibrium state of the system. Also, the stochiometric equations resulting

from such transformations are questionable.

The following conclusions are made after examining the experimental results.

1. The reacting system which is studied exhibits coupling as shown by the non-zero values of the coupling coefficients, L_{12} and L_{21}.

2. The reacting system also has a negative affinity-velocity product. The existence of a negative affinity-velocity product not only indicates that coupling exists but also shows that a reaction is occurring in a direction which is not spontaneous. The presence of a negative AV product is a sufficient but not necessary criterion of coupling. A more general criterion is given by equation (29).

3. The functional relationship between the velocity of a reaction and the chemical affinities, as expressed by equation (112), does not adequately describe the behavior of the system over an entire run. However, such relationships may be useful in describing the system over portions of a run. The linear rate laws become better approximations as the system approaches equilibrium.

4. The Onsager reciprocity relations have not been verified for this system. However, a conclusive test of this postulate could not be made.

REFERENCES

1. Andrews, F. C., Industrial and Engineering Chemistry Fundamentals, 3, 274 (1964).

2. Beeson, C. M. and Yost, D. M., Journal of the American Chemical Society, 61, 1432 (1939).

3. Coleman, B. D. and Truesdell, C., Journal of Chemical Physics, 33, 28 (1960).

4. Davies, R. O., Physica, 18, 182 (1952).

5. De Donder, Th., Bulletin de l'Academie Royale de Belgique (Classe des Sciences), 23, 770 (1937).

6. de Groot, S. R., Thermodynamics of Irreversible Processes, North-Holland Publishing Company, Amsterdam, 1961.

7. de Groot, S. R. and Mazur, P., Non-Equilibrium Thermodynamics, North-Holland Publishing Company, Amsterdam, 1962.

8. Deming, W. E., Statistical Adjustment of Data, John Wiley & Sons, Inc., New York, 1943.

9. Denbigh, K. G., The Principles of Chemical Equilibrium, Cambridge University Press, Cambridge, 1964.

10. Denbigh, K. G., The Thermodynamics of the Steady State, John Wiley & Sons, Inc., New York, 1958.

11. Duda, J. L. and Vrentas, J. S., Industrial and Engineering Chemistry Fundamentals, 3, 272 (1964).

12. DuMont Multiplier Phototubes, DuMont Laboratories, Clifton, New Jersey, 1963.

13. Dutzmann, A., Gasschutz und Luftschutz, 6, 163 (1936).

14. Engstrom, R. W., Journal of the Optical Society of America, 37, 420 (1947).

15. Fan, L. T. and Chan, C. H., Industrial and Engineering Chemistry Fundamentals, 3, 181 (1964).

16. Fitts, D. D., Nonequilibrium Thermodynamics, McGraw-Hill Book Company, Inc., New York, 1964.

17. Gage, D. H. and Kline, S. J., Office of Technical Services, Document Number AD607377, 1964.

18. Hartridge, H. and Roughton, F. J. W., Proceedings of the Royal Society of London, A 104, 376 (1923).

19. Hartridge, H. and Roughton, F. J. W., Proceedings of the Cambridge Philosophical Society, 22, 426 (1924).

20. Hartridge, H. and Roughton, F. J. W., Proceedings of the Cambridge Philosophical Society, 23, 450 (1926).

21. Hayward, A. T. J., Journal of Scientific Instruments, 40, 173 (1963).

22. Hooyman, G. T., Proceedings of the National Academy of Science, 47, 1169 (1961).

23. Hooyman, G. J., de Groot, S. R., and Mazur, P., Physics, 11, 360 (1955).

24. Koenig, F. O., Horne, F. H., and Mohilner, D. M., Journal of the American Chemical Society, 83, 1029 (1961).

25. Li, J. C. M., Journal of Chemical Physics, 29, 747 (1958).

26. Linden, B. R., Nucleonics, Vol. 11, No. 9, 30 (1953).

27. Manes, M., Journal of Chemical Physics, 39, 456 (1963).

28. Manes, M., Journal of Physical Chemistry, 67, 651 (1963).

29. Manes, M., Hofer, L. J. E., and Weller, S., Journal of Chemical Physics, 18, 1355 (1950).

30. Margenau, H. and Murphy, G. M., The Mathematics of Physics and Chemistry, D. Van Nostrand Company, Inc., New York, 1956.

31. Marmo, F. F., Journal of the Optical Society of America, 43, 1186 (1953).

32. Meixner, J., Annalen der Physik, 43, 244 (1943).

33. Miller, P. G., Chemical Review, 60, 15 (1960).

34. Nims, F. L., American Journal of Physiology, 201, 987 (1961).

35. Onsager, L., Physical Review, 37, 405 (1931).

36. Onsager, L., Physical Review, 38, 2265 (1931).

37. Parlin, R. B., Marcus, R. J., and Eyring, H., Proceedings of the National Academy of Science, 41, 900 (1955).

38. Pings, C. J., Physica, 29, 243 (1963).

39. Pitzer, K. S., Pure and Applied Chemistry, 2, 207 (1961).

40. Pitzer, K. S. and Brewer, L., Thermodynamics, by Lewis, G. N. and Randall, M., McGraw-Hill Book Company, New York (1961).

41. Prigogine, I., Bulletin de l'Academie Royale de Belgique (Classe des Sciences), 32, 30 (1946).

42. Prigogine, I., Physica, 15, 272 (1949).

43. Prigogine, I., Introduction to Thermodynamics of Irreversible Processes, Interscience Publishers, New York, 1961.

44. Prigogine, I., and Defay, R., Chemical Thermodynamics, Longmans Green and Company, New York, 1954.

45. Prigogine, I. and Hansen, R., Bulletin de l'Academie Royale de Belgique (Classe des Sciences), 28, 301 (1942).

46. Prigogine, I., Outer, P., and Herbo, Cl., Journal of Physical and Colloid Chemistry, 52, 321 (1948).

47. RCA Phototubes and Photocells, Technical Manual PT-60, Radio Corporation of America, Lancaster, Pennsylvania, 1963.

48. Sliepcevich, C. M. and Finn, D., Industrial and Engineering Chemistry Fundamentals, 2, 249 (1963).

49. Sommerfeld, A., Thermodynamics and Statistical Mechanics, Academic Press, Inc., New York, 1956.

50. Van Rysselberghe, P., Bulletin de l'Academie Royale de Belgique (Classe des Sciences), 23, 416 (1937).

51. Van Rysselberghe, P., Journal of Physical Chemistry, 41, 787 (1937).

52. Van Rysselberghe, P., Science, 85, 383 (1937).

53. Van Rysselberghe, P., Bulletin des Societes Chimiques Belges, 70, 592 (1961).

54. Van Rysselberghe, P., Journal of Chemical Physics, 36, 1329 (1962).

55. Van Rysselberghe, P., Thermodynamics of Irreversible Processes, Blaisdell Publishing Company, New York, 1963.

56. Verschaffelt, J. E., Bulletin de l'Academie Royale de Belgique (Classe des Sciences), 37, 853 (1951).

57. Verschaffelt, J. E., Bulletin de l'Academie Royale de Belgique (Classe des Sciences), 41, 316 (1955).

58. Woodward, J. W., doctoral thesis, California Institute of Technology, Pasadena, 1965.

59. Yost, D. M. and Russell, H., Systematic Inorganic Chemistry, Prentice-Hall, Inc., New York, 1944.

60. Zwolinski, B. J. and Marcus, R. J., Journal of Chemical Physics, 21, 2235 (1953).

APPENDIX 1

KINETIC IDENTIFICATION OF THE PHENOMENOLOGICAL COEFFICIENT FOR A SINGLE CHEMICAL REACTION

Providing a particular kinetic model is supplemented with appropriate additional assumptions, the linear phenomenological rate law for a chemical reaction can be derived. In addition, the phenomenological coefficient can be identified. Prigogine, Outer, and Herbo[1-2] present a similar, but less detailed derivation for the example of the synthesis of hydriodic acid.

As an example, consider the reaction

$$2NO + Cl_2 = 2NOCl \ . \tag{1-1}$$

Assume that the forward and reverse reaction rates can be written in the form of the law of mass action, that is,

$$V_f = k_f a_{NO}^2 a_{Cl_2} \tag{1-2}$$

$$V_r = k_r a_{NOCl}^2 \ . \tag{1-3}$$

This assumption is perhaps a stringent one in the general case because it presupposes that the kinetic expression for the overall reaction rate corresponds to the stoichiometry of the reaction. Although this assumption has been applied successfully for the example reaction[1-3], such an assumption may force a too restricted mathematical restraint on the actual physical process. For example, this assumption does not appear to be adequate in describing the

rate of formation of water or hydrogen bromide from their elements[1-1]. In using the assumption, care should also be taken that the mechanism of the reaction does not change as the system approaches or deviates from equilibrium so that the expressions for V_f and V_r remain valid.

The overall rate of reaction will then be the sum of the forward and reverse rates,

$$V = V_f - V_r = k_f a_{NO}^2 a_{Cl_2} - k_r a_{NOCl}^2. \tag{1-4}$$

At equilibrium, the overall rate of reaction will be zero, and equation (1-4) reduces to

$$k_f/k_r = \left[a_{NOCl}^2/(a_{NO}^2 a_{Cl_2}) \right]_{eq.} . \tag{1-5}$$

Therefore, equation (1-4) can also be written in the form

$$V = V_f \left\{ 1 - \left[\frac{a_{NO}^2 a_{Cl_2}}{a_{NOCl}^2} \right]_{eq.} \frac{a_{NOCl}^2}{a_{NO}^2 a_{Cl_2}} \right\} . \tag{1-6}$$

By introducing the activity of component k,

$$a_k = f_k/f_{k,0}^o \tag{1-7}$$

where $f_{k,0}^o$ is the fugacity of component k at the arbitrarily chosen standard state, equation (1-6) becomes

$$V = V_f \left\{ 1 - \left[\frac{(f_{NO}/f^{\circ}_{NO,0})^2 (f_{Cl_2}/f^{\circ}_{Cl_2,0})}{(f_{NOCl}/f^{\circ}_{NOCl,0})^2} \right]_{eq.} \frac{(f_{NOCl}/f^{\circ}_{NOCl,0})^2}{(f_{NO}/f^{\circ}_{NO,0})^2 (f_{Cl_2}/f^{\circ}_{Cl_2,0})} \right\}. \tag{1-8}$$

By choosing a standard state of unit fugacity for all the components, the above equation will simplify to

$$V = V_f \left\{ 1 - (f_{NO,eq.}/f_{NO})^2 (f_{Cl_2,eq.}/f_{Cl_2}) (f_{NOCl}/f_{NOCl,eq.})^2 \right\}. \tag{1-9}$$

The chemical potential of component k is given by

$$\mu_k = \mu^{\circ}_k + RT \ln f_k , \tag{1-10}$$

where μ°_k is the chemical potential of component k at the standard state at which the unit fugacities were chosen. Combining this expression with the analogous one at equilibrium, the following relation is obtained,

$$f_k/f_{k,eq.} = \exp \left[(\mu_k - \mu_{k,eq.})/RT \right]. \tag{1-11}$$

Equation (1-9) can now be written

$$V = V_f \left[1 - \left\{ \exp - \left(\frac{2\mu_{NOCl,eq.} - \mu_{Cl_2,eq.} - 2\mu_{NO,eq.}}{RT} \right) \right\} \times \left\{ \exp - \left(\frac{2\mu_{NO} + \mu_{Cl_2} - 2\mu_{NOCl}}{RT} \right) \right\} \right]. \tag{1-12}$$

Recalling that the chemical affinity of this reaction is

$$A = -(2\mu_{NOCl} - 2\mu_{NO} - \mu_{Cl_2}) , \tag{1-13}$$

equation (1-12) can be simplified to

$$V = V_f\left[1 - \left\{\exp(A_{eq.}/RT)\exp - (A/RT)\right\}\right] . \tag{1-14}$$

However, the chemical affinity at equilibrium is zero, so that

$$V = V_f\left[1 - \exp(-A/RT)\right] . \tag{1-15}$$

However, near equilibrium

$$|A/RT| << 1, \tag{1-16}$$

and equation (1-15) reduces to the linear form of the phenomenological rate law

$$V = \left(\frac{V_f}{RT}\right)_{eq.} A = LA . \tag{1-17}$$

Therefore, providing that the overall rate expression for a chemical reaction can be written in the form of the law of mass action, the introduction of the fugacity, activity, and chemical affinity and the assumption of a suitable standard state will reduce the rate expression to the form of equation (1-15). Near equilibrium, this rate expression reduces to the form of the linear phenomenological laws.

Notice that the phenomenological coefficient in the linear rate

law is identified with the temperature and forward rate of the reaction at equilibrium. Since the forward rate is a function of the equilibrium composition, this phenomenological coefficient is definitely a function of the equlibrium state of the system.

NOMENCLATURE

English Symbols

a	activity
A	chemical affinity
f	fugacity
f_0^o	fugacity of pure component in the standard state
k_f	forward reaction rate constant
k_r	reverse reaction rate constant
L	phenomenological coefficient
P	total pressure
R	universal gas constant
T	absolute temperature
V	overall reaction rate
V_f	forward reaction rate
V_r	reverse reaction rate

Greek Symbols

μ	chemical potential

Subscripts

eq.	at equilibrium conditions
k	for component k

REFERENCES

1-1. Frost, A. A. and Pearson, R. G., Kinetics and Mechanism, John Wiley & Sons, Inc., New York, 1958.

1-2. Prigogine, I., Outer, P., and Herbo, Cl., Journal of Physical and Colloid Chemistry, 52, 321 (1948).

1-3. Yost, D. M. and Russell, H., Systematic Inorganic Chemistry, Prentice-Hall, Inc., New York, 1944.

APPENDIX 2

CALCULATION OF THE NITRIC OXIDE CONCENTRATION

If the reacting system was allowed to reach equilibrium, the final nitric oxide concentration could be computed by using equilibrium constant expressions employing the final concentrations of iodine, chlorine, iodine monochloride, and nitrosyl chloride. Then, knowing this final nitric oxide concentration and also the concentration of nitrosyl chloride during a run, the nitric oxide concentration as a function of time could be calculated by means of a material balance on the nitric oxide molecule.

Unfortunately, due to the large difference in the rates of the reactions which were present, the system never came completely to equilibrium. However, the system did appear to closely approach equilibrium with respect to reaction 2, that is, the left-hand-side of equation (4-26) was negligible compared to each one of the two terms which are shown in square brackets on the right-hand-side. Therefore, knowing the concentration of iodine, iodine monochloride, and nitrosyl chloride at the termination of a run, the final nitric oxide concentration was calculated from this equation. Using this final value of the nitric oxide concentration and a material balance on the nitric oxide molecule, the nitric oxide concentration during a run was calculated from the expression

$$C_{NO}(t) = C_{NO}(\text{final}) + C_{NOCl}(\text{final}) - C_{NOCL}(t) . \qquad (2\text{-}1)$$

A comparison of these calculated nitric oxide concentrations with those determined by other means is interesting. A rotameter, calibrated with nitrogen gas, was used to monitor the entering flow rate of nitric oxide into the system. Since nitrogen and nitric oxide have almost identical viscosities and densities at the operating conditions, the rotameter calibration was also considered to be valid for nitric oxide.

As shown in Table 2-I, the entering nitric oxide concentration calculated from the rotameter reading agrees within ten percent of the initial concentration of nitric oxide as calculated using the material balance on the nitric oxide molecule. The agreement between these results is within the accuracy of the rotameter determination.

In addition, the iodine, iodine monochloride, and nitrosyl chloride concentrations at each point in a run were substituted into equation (4-26) with A_2 again neglected. In this manner, a "pseudo" nitric oxide concentration could be calculated as a function of time. Of course, at the end of a run, this "pseudo" concentration became identical to the nitric oxide concentration discussed above.

However, when these "pseudo" nitric oxide concentrations were compared with the nitric oxide concentrations calculated using the material balance, the two concentrations coincided throughout the latter portions of a run. Therefore, the final nitric oxide concentration, appearing in equation (2-1), could be selected at any time in the latter stages of a run. Figure 2-1 shows such a

comparison for Run 17. Obviously, C_{NO}(final) could be selected at any time from 500 to 600 seconds without introducing appreciable error in the calculation of the nitric oxide concentration.

TABLE 2-I

INITIAL NITRIC OXIDE CONCENTRATION

(gram-moles/liter)

Run	Rotameter Calculation	Material Balance Calculation
11	9.2×10^{-5}	8.48×10^{-5}
12	9.0×10^{-5}	1.00×10^{-4}
13	7.6×10^{-5}	8.36×10^{-5}
16	4.8×10^{-4}	5.12×10^{-4}
17	5.4×10^{-4}	5.10×10^{-4}

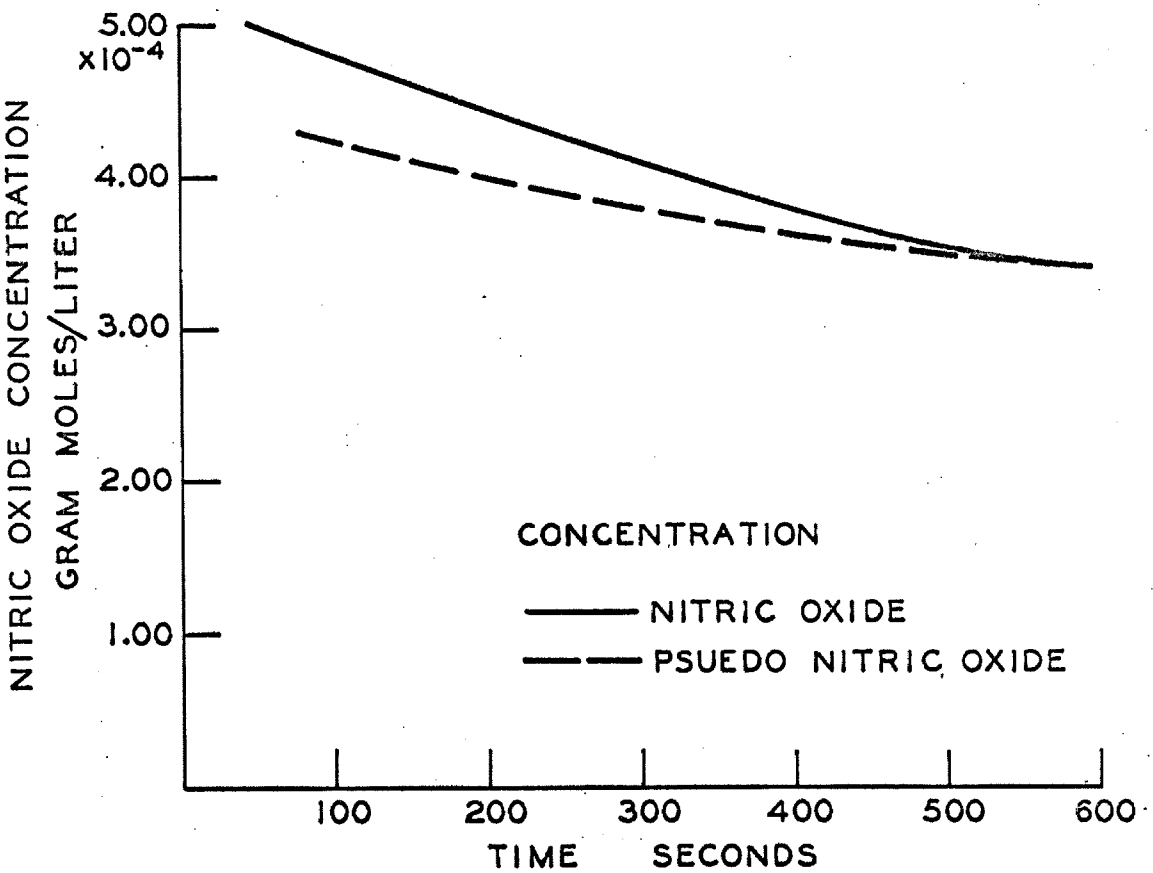

Figure 2-1. Comparison of Nitric Oxide Concentrations.

APPENDIX 3

SELECTION OF THE EXTINCTION COEFFICIENTS

Of the five macroscopic chemical species which are involved in this study, all but nitric oxide absorb light either in the visible or near-ultraviolet region of the spectrum. Nitric oxide has only discrete absorption beginning about 2250 Å and progressing to smaller wavelengths[3-9].

The behavior of the absorbing species is exemplified in Figure 10, which gives the extinction coefficients as functions of wavelength. The data shown in this figure represent regions of continuous absorption except for iodine above 4990 Å. Above this wavelength, the curve is only an approximation because the iodine absorption spectrum is discrete in this region.

The absorption spectrum of all five species was examined using a Cary Model 14 recording spectrophotometer. In most cases, the reported values of the extinction coefficients in the literature were verified quantitatively. However, if the literature values were found to be erroneous, they were either corrected, or better data were proposed.

In addition, the dependence of these extinction coefficients on the presence of inert gas was investigated. The absorption spectrum of the five components was examined with argon and nitrogen gas present. The absolute pressures of these inerts varied between zero and one and one-half atmospheres.

Over this range in pressures, the amount of inert gas did not

affect the absorption spectrum in the wavelength regions used in this experiment, that is, in the regions of continuous absorption. This result agrees with the observations of Rabinowitch and Wood[3-11] and Britton, Davidson, and Schott[3-3] for the continuous region of the iodine spectrum. In addition, the pressure dependence above 4990 Å for iodine, noted by Rabinowitch and Wood, was qualitatively confirmed.

The wavelengths which were used in the experimental work were 4900, 4716, 3802, and 3343 Å. The actual method of determining the extinction coefficients at these wavelengths for the absorbing species together with the necessary temperature corrections is discussed below. The resulting extinction coefficients are shown in Table IV.

Iodine

Vogt and Koenigsberger[3-15] quantitatively measured the absorption of saturated iodine vapor at 48 °C and 88 °C and superheated vapor at 400 °C over the spectral range of 4500 to 6000 Å. Bonhoeffer and Harteck[3-2] computed values of the extinction coefficient as a function of wavelength using the data of Vogt and Koenigsberger at 88 °C. However, Rabinowitch and Wood[3-11] felt that the Vogt and Koenigsberger data was incorrect and measured the decadic extinction coefficient themselves at 20 °C over the same spectral range.

In addition, Sulzer[3-13] reports decadic extinction coeffi-

cients between 3900 to 6000 Å at temperatures of 423, 873, and 1323 °K. Sulzer and Wieland[3-14] extended this data by measuring the extinction coefficient from 3570 to 6000 Å at temperatures of 423, 573, 723, 873, 1023, 1173 and 1323 °K and also from 6000 to 7400 Å at temperatures of 423, 873, and 1323 °K.

In measuring the extinction coefficient, Rabinowitch and Wood used an optical cell which was 12 centimeters in length. They apparently used a cell length of 10 centimeters in calculating the extinction coefficients, and therefore, their results should be "corrected" by dividing their coefficients by 1.2.

The tabulated results of Sulzer and Wieland at each temperature were graphically interpolated in order to find the extinction coefficient at the particular wavelengths of 4900, 4716, 3802, and 3343 Å. Although they reported extinction coefficients at elevated temperatures, the data could be readily extrapolated to room temperature. An examination of the interpolated values showed that the extinction coefficient of iodine was a linear function of temperature at these wavelengths. Therefore, a linear least squares fit was made to this extinction coefficient versus temperature data, and the data were extrapolated to 20 °C. The resulting extrapolated values agreed to 0.3% at 4900 Å and to 1.2% at 4716 Å with the "corrected" results of Rabinowitch and Wood. Since Rabinowitch and Wood did not report any results below 4500 Å, no data were available for comparison with Sulzer and Wieland's extrapolated data at 3802 and 3343 Å.

In addition, the spectrum of iodine at 25 °C was examined on the Cary Model 14 spectrophotometer, and the extinction coefficients agreed to 2% at 4900 Å and 0.7% at 4716 Å with the extrapolated values of Sulzer and Wieland. At 3802 and 3343 Å, the absorption of iodine vapor at 25 °C was too small to measure an extinction coefficient with this instrument.

The least squares equations which were employed in the temperature extrapolations were used to obtain values of the extinction coefficients at the operating temperature of 36 °C. The resulting extinction coefficients are shown in Table IV.

Chlorine

Halban and Siedentopf[3-6] measured the extinction coefficient of chlorine from 2540 to 6430 Å at an unknown temperature. The spectral range of 2618 to 4275 Å was investigated by Gibson and Bayliss[3-4] at 291, 441, 554, 699, 853, and 1038 °K. Then Aickin and Bayliss[3-1] extended the extinction coefficient curve to 5000 Å, making measurements at 18 and 580 °C. Finally, extinction coefficients from 5040 to 5320 Å were measured at 18 °C by Jones and Spooner[3-7]. Recently, Seery and Britton[3-12] measured these coefficients again from 2400 to 4500 Å at 25 °C.

The Cary Model 14 spectrophotometer was also used to observe the spectrum at 25 °C. The resulting extinction coefficients agreed to 0.3% at 3343 Å and to 1.5% at 3802 Å with Seery and Britton's results, agreed to 0.2% at 3343 Å and to 8.0% at 3802 Å

with Gibson and Bayliss' data at 25 °C, and agreed to 2% at 3343 Å and to 16% at 3802 Å with the results of Halban and Siedentopf.

Hence, the results of this investigation agreed well with Seery and Britton's data at 3343 and 3802 Å and also to the results of Gibson and Bayliss at 3343 Å. Our extinction coefficients at 3343 and 3802 Å at 25 °C were corrected slightly according to the temperature dependence observed by Gibson and Bayliss to give the corresponding values at the operating temperature of 36 °C.

Because of the low absorption of chlorine at 4716 and 4900 Å, extinction coefficients at these wavelengths could not be computed with any accuracy from our work. However, Aicken and Bayliss' data, adjusted to 36 °C, agreed to 5% at 4716 Å and to 17% at 4900 Å with the results of Halban and Siedentopf. Aickin and Bayliss' data were considered to be the more reliable, showing a temperature dependence and being more recent and complete. Table IV gives the values of these coefficients.

Iodine Monochloride

Nebeker and Pings[3-10] experimentally determined the extinction coefficient for iodine monochloride at 25 °C and compared their results to the existing literature values. Unfortunately, the temperature dependence of this coefficient has not been investigated.

However, Sulzer[3-13] and Sulzer and Wieland[3-14] have developed a simple theory for the continuous absorption spectra

of diatomic molecules which assumes that the continuous spectrum can be resolved into Gaussian peaks. Each peak can be described by

$$\epsilon(\omega, T) = \epsilon_m(T) e^{-[(\omega-\omega_o)/\Delta\omega(t)]^2} \qquad (3\text{-}1)$$

where

$$\epsilon_m(T) = \epsilon_{mo}[\tanh(hc\omega_v/2kT)]^{1/2} \qquad (3\text{-}2)$$

and

$$\Delta\omega(T) = \Delta\omega_o[\tanh(hc\omega_v/2kT)]^{-1/2}. \qquad (3\text{-}3)$$

Using these equations and the values of ω_v, ϵ_{mo}, ω_o, and $\Delta\omega_o$ presented by Seery and Britton, the extinction coefficients of Nebeker and Pings at 25 °C were adjusted to give extinction coefficients at 36 °C, as shown in Table IV.

Nitrosyl Chloride

Incidental to another problem, Leermakers and Ramsperger[3-8] measured the extinction coefficient of nitrosyl chloride from 4000 to 5000 Å at 25 and 50 °C. Goodeve and Katz[3-5] examined the spectrum from 1850 to 8000 Å at 293 °K and from 5260 to 6431 Å at temperatures of 233, 295, and 457.4 °K.

Leermakers and Ramsperger's data at 25 °C agreed to 10% at 4900 and 4716 Å with the results of Goodeve and Katz at 20 °C. Unfortunately, the data of Leermakers and Ramsperger does not

extend to wavelengths less than 4000 Å. Therefore, a direct comparison between these two sets of data cannot be made below this wavelength. However, Leermakers and Ramsperger's data at 25 °C can be extrapolated to 3802 Å to give an extinction coefficient which agrees to 8% with Goodeve and Katz's result for the same wavelength and at a temperature of 20 °C.

The results of Goodeve and Katz are probably more reliable because not only was their experiment performed very carefully, but also because their work was more recent. Therefore, they were able to profit from Leermakers and Ramsperger's earlier work.

Unfortunately, Goodeve and Katz did not investigate the temperature dependence of the extinction coefficient. However, their coefficients were corrected to the operating temperature of 36 °C by referring to the temperature dependency which Leermakers and Ramsperger observed between 25 and 50 °C. A slight dependency was observed at 4900 and 4716 Å, but a negligible dependency was observed at 4000 Å or after extrapolating their data to 3802 Å. The extinction coefficient of Goodeve and Katz at 3343 Å was used directly without a temperature correction. However, since this coefficient was not used in the main calculations but employed only in consistency checks, no error was introduced in this way into the main body of the calculations. Table IV shows the coefficients which were finally selected.

NOMENCLATURE

English Symbols

c	velocity of light
h	Planck's constant
k	Boltzmann's constant
T	absolute temperature

Greek Symbols

ϵ	extinction coefficient
ϵ_{mo}	maximum extinction coefficient of the Gaussian peak at 0 ^{o}K
ω	wave number
ω_o	wave number of the maximum of the Gaussian peak at 0 ^{o}K
$\Delta\omega_o$	half of the mean width of the Gaussian peak at 0 ^{o}K
ω_v	vibrational frequency of the molecule

REFERENCES

3-1. Aickin, R. G. and Bayliss, N. S., Transactions of the Faraday Society, 33, 1333 (1937).

3-2. Bonhoeffer, K. F. and Harteck, P., Grundlager der Photochemie, Theodor Steinkopff, Dresden and Leipzig, 1933.

3-3. Britton, D., Davidson, N., and Schott, G., Discussions of the Faraday Society, 17, 58 (1954).

3-4. Gibson, G. E. and Bayliss, N. S., Physical Review, 44, 188 (1933).

3-5. Goodeve, C. F. and Katz, S., Proceedings of the Royal Society of London, A172, 432 (1939).

3-6. Halban, H. v. and Siedentopf, K., Zeitschrift fur Physikalische Chemie, 103, 71 (1922).

3-7. Jones, F. W. and Spooner, W., Transactions of the Faraday Society, 31, 811 (1935).

3-8. Leermakers, J. A. and Ramsperger, H. C., Journal of the American Chemical Society, 54, 1837 (1932).

3-9. Marmo, F. F., Journal of the Optical Society of America, 43, 1186 (1953).

3-10. Nebeker, E. B. and Pings, C. J., Journal of Physical Chemistry, 69, (1965).

3-11. Rabinowitch, E. and Wood, W. C., Transactions of the Faraday Society, 32, 540 (1936).

3-12. Seery, D. J. and Britton, D. J., Journal of Physical Chemistry, 68, 2263 (1964).

3-13. Sulzer, von P., Helvetica Physica Acta, 23, 531 (1950).

3-14. Sulzer, von P. and Wieland, K., Helvetica Physica Acta, 25, 653 (1952).

3-15. Vogt, Von K. and Koenigsberger, J., Zeitschrift fur Physik, 13, 292 (1923).

APPENDIX 4

CALCULATION OF THE CHEMICAL AFFINITIES

Introduction and Derivation

Using the definition of the chemical affinity[4-16],

$$A = -\sum_{i=1}^{n} \nu_i \mu_i \,, \tag{4-1}$$

the following relation between the affinity and the standard affinity can be given for n components,

$$A - A^{o} = -\sum_{i=1}^{n} \nu_i \mu_i + \sum_{i=1}^{n} \nu_i \mu_i^{o} \,. \tag{4-2}$$

By introducing the definition of the fugacity[4-11],

$$\mu_i = \beta_i(T) + RT \ln f_i \,, \tag{4-3}$$

and by selecting the temperature of the standard state to be the temperature of the system, equation (4-2) may be written

$$A - A^{o} = - RT \ln \prod_{i=1}^{n} (f_i / f_{io}^{o})^{\nu_i} \,, \tag{A-4}$$

Assuming the validity of the Lewis Generalization[4-5, 4-12, 4-16, 4-17] for this system, the fugacity of component i at the temperature and pressure of the system is

$$f_i = n_i f^{o} \,, \tag{4-5}$$

or, in terms of concentrations,

$$f_i = C_i f_i^o / C \ . \tag{4-6}$$

The concentration of the system can be written as a function of the pressure and temperature of the system,

$$C = P/RT \ , \tag{4-7}$$

since the system is primarily argon gas, for which perfect gas behavior is valid for these conditions. Also, by arbitrarily specifying the standard state at the temperature of the system and one atmosphere pressure,

$$f_{io}^o = 1 \text{ atmosphere} \ , \tag{4-8}$$

Combining equations (4-4), (4-6), (4-7), and (4-8) gives the expression

$$A - A^o = - RT \ln \prod_{i=1}^{n} (C_i RT f_i^o / P)^{\nu_i} \ . \tag{4-9}$$

Referring to reactions 1, 2, and 3,

$$\begin{aligned} &1: \quad 2NO + Cl_2 = 2NOCl \\ &2: \quad 2NOCl + I_2 = 2ICl + 2NO \\ &3: \quad I_2 + Cl_2 = 2ICl \ , \end{aligned} \tag{4-10}$$

equation (4-9) can be written for each in the form

$$A_1 = A_1^o - RT \ln \left[(C_{NOCl} f^o_{NOCl}/P)^2 \div \right.$$
$$\left. \div (C_{NO} f^o_{NO}/P)^2 (C_{Cl_2} f^o_{Cl_2}/P) RT \right] \qquad (4\text{-}11)$$

$$A_2 = A_2^o - RT \ln \left[(C_{ICl} f^o_{ICl}/P)^2 (C_{NO} f^o_{NO}/P)^2 RT \div \right.$$
$$\left. \div (C_{NOCl} f^o_{NOCl}/P)^2 (C_{I_2} f^o_{I_2}/P) \right] \qquad (4\text{-}12)$$

$$A_3 = A_3^o - RT \ln \left[(C_{ICl} f^o_{ICl}/P)^2 \Big/ (C_{I_2} f^o_{I_2}/P)(C_{Cl_2} f^o_{Cl_2}/P) \right]. \qquad (4\text{-}13)$$

Evaluation of the Standard Affinity

The standard affinity is related to the standard free energy of a reaction by

$$A_k^o = - \Delta F_k^o . \qquad (4\text{-}14)$$

After carefully evaluating the literature values, an excellent review article[4-1] recommended the value of the free energy of formation of gaseous nitrosyl chloride which was calculated from the work of Beeson and Yost[4-2] at 25 °C. Such a recommendation is in agreement with the citation of the National Bureau of Standards[4-5]. This value was then combined with the free energy of formation of gaseous nitric oxide and chlorine[4-16] in order to calculate the standard free energy change of reaction 1. The result was identical to the standard free energy change for reaction 1 which was computed from the following equation at 25 °C given by McMorris and

Yost[4-14],

$$A_1^\circ = -\Delta F_1^\circ = 16429 - 18.967 \log_{10} T + 21.452\ T + 0.010708\ T^2 - 2.4208 \times 10^{-6} T^3 . \qquad (4\text{-}15)$$

Incidental to another problem, McMorris and Yost[4-14] studied the equilibrium of reaction 2 between 136.4 and 178.8 °C. Because their temperature range was small and because their experimental method was difficult, extrapolation of their data to 36 °C is uncertain.

However, the standard affinity of reaction 2 was determined indirectly by another method. By referring to equations (4-11), (4-12), and (4-13), this standard affinity can be shown to be the following function of the standard affinities of the other two reactions

$$A_2^\circ = A_3^\circ - A_1^\circ . \qquad (4\text{-}16)$$

Therefore, data for the standard free energy change of reaction 3 can be combined with equation (4-15) to calculate the standard free energy change of reaction 2.

The free energy of formation of iodine monochloride was first determined by McMorris and Yost[4-14]. However, their results were found to be erroneous and were analyzed again by Blair and Yost[4-3]. Greenwood[4-8] also evaluated McMorris and Yost's data and incorporated it with the most reliable spectroscopic data available at the time. Later Cole and Elverum[4-4] evaluated

various thermodynamic functions of iodine monochloride by statistical methods. Finally, Evans, Munson and Wagman[4-6] improved the calculations of Cole and Elverum by using more accurate constants.

Therefore, the value of the free energy of formation of Evans, Munson, and Wagman is considered to be the most reliable. At 25 °C, the value of Blair and Yost differs by 1.9%, of Greenwood by 1.2%, and of Cole and Elverum by 0.7% from the value of the free energy of formation of Evans, Munson, and Wagman.

Due to a fortuitous selection of standard states by Evans, Munson, and Wagman, the standard free energy of reaction 3 could be obtained directly from their results. By fitting their data from 273.16 to 400 °K with a straight line using the least squares technique, the following equation was obtained

$$A_3^o = -\Delta F_3^o = 6682 + 2.796\ T\ . \qquad (4\text{-}17)$$

The point at 250 °K in their data was not included in these calculations because it was obviously erroneous. By combining equations (4-15) and (4-17) in the manner suggested by equation (4-16), the following expression for the standard free energy change of reaction 2 results

$$A_2^o = -\Delta F_2^o = -9747 + 18{,}967\ T \log_{10} T - 18.656\ T - 0.010708\ T^2 + 2.4208 \times 10^{-6} T^3. \qquad (4\text{-}18)$$

Evaluation of Volumetric Behavior of the Gases

If the behavior of a gas can be expressed in terms of only the first two terms of the virial equation of state, Lewis and Randall[4-12] give the useful expression

$$f_i^o/P = e^{BP/RT} . \qquad (4\text{-}19)$$

Beeson and Yost[4-2] have evaluated the second virial coefficient for nitrosyl chloride. Substituting their results into equation (4-19) at the operating conditions gives

$$f_{NOCl}^o/P = 0.989 . \qquad (4\text{-}20)$$

The second virial coefficient has been determined by Johnston and Weimer[4-10] for nitric oxide. Similarly evaluating equation (4-19) using their data produces

$$f_{NO}^o/P = 1.00 . \qquad (4\text{-}21)$$

For lack of adequate data, the second virial coefficient for chlorine, iodine, and iodine monochloride was determined from the force constants of the Lennard-Jones (6-12) potential by a method outlined by Hirschfelder, Curtiss, and Bird[4-9]. In the case of chlorine and iodine, these constants had been determined from viscosity measurements. For iodine monochloride, the force constant data were not available and they were estimated by use of certain empirical combining laws[4-9].

The resulting second virial coefficient for chlorine was used to generate volumetric data for chlorine in the vicinity of the operating conditions. This data agreed well with the volumetric data for chlorine published by The Matheson Company[4-13]. No volumetric data was available for comparison in the cases of iodine and iodine monochloride. Using these calculated second virial coefficients, equation (4-19) was again evaluated to give

$$f^{o}_{Cl_2}/P = 0.990 , \qquad (4-22)$$

$$f^{o}_{I_2}/P = 0.957 , \qquad (4-23)$$

$$f^{o}_{ICl}/P = 0.980 . \qquad (4-24)$$

Results

Upon combining equations (4-11), (4-15), (4-20), (4-21), and (4-22), and also equations (4-12), (4-18), (4-20), (4-21), (4-23), and (4-24) with suitable values of the universal gas constant, the following expressions were obtained for the affinities of reactions 1 and 2 as functions of temperature

$$A_1 = 16429 - 18.967\ T \log_{10} T + 21.452\ T + 0.010708\ T^2 - 2.4208 \times 10^{-6} T^3 - 1.9872\ T \ln \left\{ (0.989\ C_{NOCl})^2 \div 0.082054\ T\ C^2_{NO}\ (0.990\ C_{Cl_2}) \right\} \qquad (4-25)$$

$$A_2 = \left[- 9747 + 18.967\ T \log_{10} T - 18.656\ T - 0.010708\ T^2 + 2.4208 \times 10^{-6} T^3 \right]$$

$$- \left[1.9872 T \ln \left\{ 0.082054\ T (0.980 C_{ICl})^2 C_{NO}^2 \div \div (0.989\ C_{NOCl})^2 0.957\ C_{I_2} \right\} \right] . \qquad (4\text{-}26)$$

NOMENCLATURE

English Symbols

A	chemical affinity
A^{o}	standard chemical affinity
C	concentration
f	fugacity
f^{o}	fugacity of pure component
f_{o}^{o}	fugacity of pure component in the standard state
ΔF^{o}	standard free energy change
n	mole fraction
P	total pressure
R	universal gas constant
T	absolute temperature

Greek Symbols

β	a function of temperature only for each component
μ	chemical potential
ν	stoichiometric coefficient

Subscripts

i	for component i
k	for eaction k

REFERENCES

4-1. Beckham, L. J., Fessler, W. A., and Kise, M. A., Chemical Reviews, 48, 319 (1951).

4-2. Beeson, C. M. and Yost, D. M., Journal of Chemical Physics, 7, 44 (1939).

4-3. Blair, C. M. and Yost, D. M., Journal of the American Chemical Society, 55, 4489 (1933).

4-4. Cole, L. G. and Elverum, G. W. Jr., Journal of Chemical Physics, 20, 1543 (1952).

4-5. Denbigh, K., The Principles of Chemical Equilibrium, Cambridge University Press, London, 1964.

4-6. Evans, W. H., Munson, T. R., and Wagman, D. D., National Bureau of Standards Journal of Research, 55, 147 (1955).

4-7. Fitts, D. D., Nonequilibrium Thermodynamics, McGraw-Hill Book Company, Inc., New York, 1962.

4-8. Greenwood, N. N., Reviews of Pure and Applied Chemistry, 1, 84 (1951).

4-9. Hirschfelder, J. O., Curtiss, C. F., and Bird, R. B., Molecular Theory of Gases and Liquids, John Wiley and Sons, Inc., New York, 1964.

4-10. Johnston, H. L. and Weimer, H. R., Journal of the American Chemical Society, 56, 625 (1934).

4-11. Klotz, I. M., Chemical Thermodynamics, Prentice-Hall, Inc., Englewood Cliffs, New Jersey, 1954.

4-12. Lewis, G. N. and Randall, M., Thermodynamics, revised by Pitzer, K. S. and Brewer, L., McGraw-Hill Book Company, Inc., New York, 1961.

4-13. Matheson Company, Gas Data Book, East Rutherford, New Jersey, 1963.

4-14. McMorris, J. and Yost, D. M., Journal of the American Chemical Society, 54, 2247 (1932).

4-15. National Bureau of Standards: Selected Values of Chemical Thermodynamic Properties, Washington, D. C.: Series I, Table 18-11, March, 1949.

4-16. Prigogine, I. and Defay, R., Chemical Thermodynamics, Longmans Green and Company, New York, 1954.

4-17. Sage, B. H. and Lacey, W. N., Volumetric and Phase Behavior of Hydrocarbons, Stanford University Press, Stanford, California, 1939.

APPENDIX 5

VALIDITY OF THE LAMBERT-BEER LAW

About two hundred years ago, J. H. Lambert[5-3] discovered that when a parallel beam of monochromatic light of intensity I_o enters a homogeneous absorbing material, the light which is transmitted through a layer of thickness ℓ will have the intensity

$$I(\lambda) = I_o(\lambda)e^{-k(\lambda)\ell} \qquad (5\text{-}1)$$

where k is a positive constant called the absorption coefficient of the material. A century later, Beer[5-1] and Bernard[5-2] found that the absorption coefficient is proportional to the concentration of the species present in the absorbing material, as given by the following linear expression for n species,

$$k(\lambda) = \sum_{i=1}^{n} C_i \epsilon_i(\lambda) \quad . \qquad (5\text{-}2)$$

Combination of equations (5-1) and (5-2) gives the Lambert-Beer law,

$$I(\lambda) = I_o(\lambda)e^{-\sum_{i=1}^{n} C_i \epsilon_i(\lambda)\ell} \quad , \qquad (5\text{-}3)$$

which is the fundamental equation of colorimetry and spectrophotometry.

Lambert's law can be derived by assuming that each infinitesimally thin layer of the absorbing material absorbs an amount of light which is proportional to the thickness of the layer and to the intensity of the monochromatic radiation reaching it. Similarly,

Beer's law follows from the assumption that each molecule of the absorbing material absorbs the radiation independently of every other molecule. Because these assumptions are not always valid, and because strictly monochromatic light is not employed, deviations from Lambert's and Beer's laws are sometimes observed.

In any particular situation, the experimental circumstances should be adjusted so that equation (5-3) is an adequate representation of the observations. For a general absorption experiment involving only one absorbing species, Nielson, Thornton, and Dale[5-4] have shown that the apparent intensity ratio is the quantity which is actually measured,

$$I(\lambda)^a/I_o(\lambda)^a = \int_o^\infty I_o(\lambda')\exp(-\epsilon(\lambda')C\ell)g(\lambda'-\lambda)\,d\lambda' \Big/ \int_o^\infty I_o(\lambda')g(\lambda'-\lambda)\,d\lambda' , \tag{5-4}$$

where $g(\lambda'-\lambda)$ is a properly normalized slit function[5-5] showing that the experimental instrument shows some response to light of wavelength λ' when set to wavelength λ. In this experiment, the slit function is determined primarily by the interference filters, with λ being the wavelength of maximum transmittance. Observing Figures 11 through 14, such a slit function would appear to be negligible for $|\lambda'-\lambda| \geq \Delta\lambda$. Therefore, equation (5-4) can be rewritten with new limits,

$$I(\lambda)^a/I_o(\lambda)^a = \int_{\lambda-\Delta\lambda}^{\lambda+\Delta\lambda} I_o(\lambda')\exp(-\epsilon(\lambda')C\ell)g(\lambda'-\lambda)\,d\lambda' \div \int_{\lambda-\Delta\lambda}^{\lambda+\Delta\lambda} I_o(\lambda')g(\lambda'-\lambda)\,d\lambda' \tag{5-5}$$

Providing a region in the absorption spectrum can be selected where the extinction coefficient is a weak function of wavelength, the extinction coefficient can be treated as a constant and equation (5-5) reduces to

$$I(\lambda)^a/I_o(\lambda)^a = e^{-\epsilon C\ell} \quad . \tag{5-6}$$

Often these conditions can be approximated by using optical filters or other devices which will give such a small wavelength region $2\Delta\lambda$ that the variation of the extinction coefficient over the region is negligible.

Equation (5-6) is also valid under other circumstances. If $2\Delta\lambda$ is reasonably small and in a wavelength region for which the incident light is continuous, often $I_o(\lambda')$ may be considered constant and removed from the integrals of equation (5-5). A tungsten filament light bulb is a common example of such a continuous source. Upon eliminating $I_o(\lambda')$ from equation (5-5) and making an appropriate change of variables, the equation can be simplified to

$$I(\lambda)^a/I_o(\lambda)^a = \int_{-\Delta\lambda}^{\Delta\lambda} \exp\left[-\epsilon(a+\lambda)C\ell\right] g(a)\, da \, . \tag{5-7}$$

If the extinction coefficient varies approximately linearly over this wavelength region, equation (5-7) may be approximated by

$$I(\lambda)^a/I_o(\lambda)^a = \exp\left[-\epsilon(\lambda)C\ell\right] \int_{-\Delta\lambda}^{\Delta\lambda} \exp\left[-\left(\frac{\Delta\epsilon}{2\Delta\lambda}\right) aC\ell\right] g(a)\, da \, . \tag{5-8}$$

In this experiment, the concentrations and path length are sufficiently small so that

$$(\Delta\epsilon/2\Delta\lambda)aC\ell \ll 1.00 \qquad (5\text{-}8)$$

Therefore, equation (5-8) may be expanded to give

$$I(\lambda)^a/I_o(\lambda)^a = \exp\left[-\epsilon(\lambda)C\ell\right]\left[1 - \left(\frac{\Delta\epsilon}{2\Delta\lambda}\right) C\ell \int_{-\Delta\lambda}^{\Delta\lambda} ag(a)\, da\right]. \qquad (5\text{-}9)$$

By referring to Figures 11 through 14, $g(a)$ appears to be very nearly a symmetrical (even) function. Therefore, the integral in equation (5-10) vanishes, and the equation reduces to the familiar form of the Lambert-Beer law shown by equation (5-6).

Experimentally, all of the references mentioned in Appendix 3 have verified the Lambert-Beer law over various ranges of concentration and temperature. In the initial stages of this experimental work, many mixtures of the chemical species were made in a vacuum system and examined with the photometric equipment. Providing the wavelengths examined were confined to regions of continuous absorption, a relationship in the form of equation (5-3) described the observations within the accuracy of the measurements. However, for iodine at wavelengths greater than 4990 Å, which represents the region of discrete absorption, the Lambert-Beer law definitely was not valid; however, this result is expected[5-5, 5-6].

NOMENCLATURE

English Symbols

C	concentration
g	normalized slit function
I	transmitted intensity
I_o	incident intensity
k	absorption index
ℓ	length of light path

Greek Symbols

α	variable equal to the difference $\lambda'-\lambda$
ϵ	extinction coefficient
$\Delta\epsilon$	infinitesimal increment of ϵ
λ, λ'	wavelength
$\Delta\lambda$	infinitesimal increment of λ

Superscripts

a	apparent
i	for component i

REFERENCES

5-1. Beer, A. v., Annalen der Physik, 86, 78 (1852).

5-2. Bernard, F., Annales de Chimie et de Physique, 35, 385 (1852).

5-3. Lambert, J. H., Photometria sive de mensura et gradibus luminus, colorum et umbrae, 1760.

5-4. Nielsen, J. R., Thornton, V., and Dale, E. B., Reviews of Modern Physics, 16, 307 (1944).

5-5. Penner, S. S., Quantitative Molecular Spectroscopy and Gas Emissivities, Addison-Wesley Publishing Company, Inc., Reading, Massachusetts, 1959.

5-6. Rabinowitch, E. and Wood, W. C., Transations of the Faraday Society, 32, 540 (1936).

APPENDIX 6

DISCUSSION OF ERROR

Although the data from the 4716 Å and 3343 Å channels are not used in the calculations, this data can be utilized to check the results of the concentration calculations which employed data from the 4900 Å and 3802 Å channels. Table 6-I shows a comparison of the initial concentrations of iodine, calculated from the data of the 4900 Å and 4716 Å channels, and also the initial concentration of chlorine, calculated from the 3802 Å and 3343 Å channels. From these comparisons, the iodine concentrations agree within seven percent, and the chlorine concentrations agree within six percent.

Appendix 2 discussed the validity of the calculations used to determine the nitric oxide concentrations. Also, a comparison of initial nitric oxide concentrations computed by two different methods is given.

A major concern in this experiment is the uncertainty in the determination of the phenomenological coefficients. The error or uncertainty in these coefficients occurs primarily from two sources: 1) the uncertainties in the data and various other information employed in the calculation of the concentrations, and 2) the statistical uncertainty in the least squares correlations as reflected by the confidence limits on these coefficients. The overall effect of errors in the data and associated information is estimated by using a typical propagation of error analysis[6-1, 6-2], employing a Taylor series expansion. The derivative of each phenomenological coefficient with

respect to each variable having error is computed numerically on the IBM 7094 computer. Each variable is perturbed, and the resulting change in the coefficient is noted. The uncertainties in the extinction coefficients are estimated from the discussion in Appendix 3. The maximum error in the initial nitric oxide concentration is assumed to be ten percent, as discussed in Appendix 2. The uncertainty in the other parameters is estimated from knowledge of the experimental equipment.

The results indicated that the uncertainty in the nitric oxide determination and the extinction coefficients, $\epsilon_{I_2,4900}$, $\epsilon_{ICl,4900}$, $\epsilon_{NOCl,4900}$, $\epsilon_{Cl_2,3802}$, $\epsilon_{ICl,3802}$, $\epsilon_{NOCl,3802}$, accounted for most of the error in the phenomenological coefficients. The contributions of the other extinction coefficients, oscilloscope and potentiometer voltages, temperature measurement, calibrated resistance ratios, eg. $(R_4 + R_5)/R_5$ and $(R_6 + R_7)/R_6$, measurement of the length of the optical cell, etc. are negligible in comparison. Therefore, if more accurate values of the extinction coefficients become available, these experimental data can be re-calculated with resulting smaller uncertainties in the phenomenological coefficients.

The results of the propagation of error analysis are combined with the confidence limits to give an estimate of the maximum uncertainty in the phenomenological coefficients. With the exceptions of the uncertainties in L_{11} and L_{21}, the uncertainties varied appreciably from one run to another. Also, the uncertainties varied according to the particular fit and data region used in each fit.

However, the maximum uncertainties in L_{11} and L_{21} are about 20% of the magnitude of the coefficients. Maximum uncertainty in L_{12} varies from 35% to 50%, while that in L_{22} ranged between 40% to 50% of the magnitude of the coefficient. The maximum uncertainties in the coefficients of the quadratic terms varied greatly, between 15% to 60% of the magnitude of the coefficient.

REFERENCES

6-1. Deming, W. E., Statistical Adjustment of Data, John Wiley & Sons, Inc., New York, 1943.

6-2. Mickley, H. S., Sherwood, T. K., and Reed, C. E., Applied Mathematics in Chemical Engineering, McGraw-Hill Book Company, Inc., New York, 1957.

TABLE 6-I

INITIAL IODINE CONCENTRATION
(gram-moles/liter)

RUN	CALCULATED USING DATA FROM 4900 Å CHANNEL	4716 Å CHANNEL
11	1.23×10^{-5}	1.32×10^{-5}
12	1.35×10^{-5}	1.26×10^{-5}
13	1.19×10^{-5}	1.23×10^{-5}
16	1.59×10^{-5}	1.71×10^{-5}
17	1.34×10^{-5}	1.40×10^{-5}

INITIAL CHLORINE CONCENTRATION
(gram-moles/liter)

RUN	CALCULATED USING DATA FROM 3802 Å CHANNEL	3343 Å CHANNEL
11	1.17×10^{-4}	1.23×10^{-4}
12	6.09×10^{-4}	5.82×10^{-4}
13	2.38×10^{-4}	2.20×10^{-4}
16	1.36×10^{-4}	1.30×10^{-4}
17	1.92×10^{-4}	1.81×10^{-4}

TABLE I

CONCENTRATIONS OF THE CHEMICAL SPECIES

RUN 11

Time (seconds)	Concentrations (moles/liter) Iodine	Chlorine	Iodine Monochloride	Nitrosyl Chloride	Nitric Oxide
0	1.23×10^{-5}	1.17×10^{-4}	0.00×10^{-5}	0.00×10^{-5}	8.48×10^{-5}
5	1.18	1.17	0.11	0.01	8.40
10	1.13	1.16	0.21	0.07	8.34
15	1.08	1.15	0.30	0.15	8.27
20	1.04	1.14	0.39	0.22	8.20
25	0.99	1.13	0.48	0.28	8.13
30	0.95	1.13	0.57	0.35	8.07
35	0.91	1.12	0.65	0.42	8.00
40	0.86	1.11	0.73	0.48	7.94
45	0.82	1.10	0.81	0.54	7.88
50	0.79	1.10	0.89	0.61	7.81
55	0.75	1.09	0.96	0.66	7.76
60	0.72	1.08	1.03	0.72	7.70
65	0.68	1.07	1.09	0.78	7.64
70	0.65	1.07	1.15	0.83	7.59
75	0.62	1.06	1.21	0.89	7.52
80	0.59	1.06	1.27	0.95	7.47
85	0.57	1.05	1.33	1.01	7.41
90	0.54	1.05	1.38	1.07	7.35
95	0.52	1.04	1.43	1.12	7.30
100	0.49	1.04	1.48	1.18	7.23
105	0.46	1.03	1.52	1.24	7.18
110	0.45	1.03	1.57	1.30	7.12

RUN 11 (Continued)

Time (seconds)	Concentrations (moles/liter) Iodine	Chlorine	Iodine Monochloride	Nitrosyl Chloride	Nitric Oxide
115	0.42×10^{-5}	1.02×10^{-4}	1.61×10^{-5}	1.35×10^{-5}	7.07×10^{-5}
120	0.41	1.02	1.65	1.39	7.02
125	0.38	1.02	1.69	1.45	6.97
130	0.37	1.01	1.73	1.50	6.92
135	0.35	1.01	1.76	1.55	6.86
140	0.33	1.00	1.80	1.61	6.81
145	0.32	1.00	1.82	1.66	6.76
150	0.30	0.99	1.86	1.71	6.71
155	0.29	0.99	1.89	1.75	6.66
160	0.27	0.99	1.91	1.80	6.62
165	0.26	0.98	1.94	1.85	6.56
170	0.25	0.98	1.96	1.90	6.51
175	0.24	0.98	1.98	1.95	6.47
180	0.23	0.97	2.01	2.00	6.41
185	0.22	0.97	2.02	2.06	6.38
190	0.21	0.96	2.05	2.10	6.31

RUN 12

Time (seconds)	Concentrations (moles/liter) Iodine	Chlorine	Iodine Monochloride	Nitrosyl Chloride	Nitric Oxide
0	1.35×10^{-5}	6.09×10^{-5}	0.00×10^{-5}	0.00×10^{-5}	10.04×10^{-5}
5	1.33	6.06	0.04	0.01	10.01
10	1.31	6.03	0.08	0.02	9.99
15	1.29	6.00	0.12	0.03	9.96
20	1.27	5.96	0.16	0.05	9.93
25	1.25	5.93	0.19	0.07	9.91
30	1.23	5.89	0.23	0.11	9.88
35	1.21	5.86	0.27	0.13	9.85
40	1.19	5.83	0.31	0.16	9.82
45	1.18	5.80	0.35	0.19	9.79
50	1.16	5.76	0.38	0.22	9.77
55	1.14	5.73	0.42	0.25	9.74
60	1.12	5.70	0.46	0.28	9.71
65	1.10	5.66	0.50	0.30	9.68
70	1.08	5.63	0.53	0.33	9.65
75	1.06	5.60	0.57	0.36	9.62
80	1.05	5.57	0.61	0.39	9.59
85	1.03	5.53	0.65	0.41	9.56
90	1.01	5.50	0.68	0.44	9.54
95	0.99	5.47	0.72	0.47	9.51
100	0.97	5.44	0.75	0.50	9.48
105	0.95	5.40	0.79	0.53	9.45
110	0.94	5.37	0.83	0.56	9.42
115	0.92	5.34	0.86	0.59	9.39
120	0.90	5.30	0.90	0.62	9.36
125	0.88	5.27	0.93	0.65	9.33
130	0.86	5.24	0.97	0.68	9.30

RUN 12 (Continued)

Time (seconds)	Concentrations (moles/liter) Iodine	Chlorine	Iodine Monochloride	Nitrosyl Chloride	Nitric Oxide
135	0.85×10^{-5}	5.20×10^{-5}	1.00×10^{-5}	0.72×10^{-5}	9.26×10^{-5}
140	0.83	5.17	1.04	0.75	9.23
145	0.81	5.14	1.07	0.78	9.20
150	0.80	5.10	1.11	0.82	9.17
155	0.78	5.07	1.14	0.85	9.14
160	0.76	5.04	1.17	0.88	9.10
165	0.74	5.01	1.21	0.91	9.07
170	0.73	4.97	1.24	0.95	9.03
175	0.72	4.94	1.27	0.98	9.00
180	0.70	4.90	1.30	1.02	8.96
185	0.68	4.87	1.34	1.05	8.92
190	0.66	4.84	1.37	1.09	8.89
195	0.65	4.80	1.40	1.12	8.86
200	0.63	4.77	1.43	1.16	8.82
205	0.62	4.73	1.46	1.20	8.78
210	0.60	4.70	1.49	1.24	8.75
215	0.59	4.66	1.52	1.28	8.70
220	0.57	4.63	1.55	1.32	8.67
225	0.56	4.59	1.58	1.36	8.62
230	0.54	4.56	1.61	1.40	8.59
235	0.53	4.53	1.64	1.43	8.55
240	0.51	4.49	1.67	1.47	8.51
245	0.50	4.46	1.69	1.52	8.46
250	0.49	4.42	1.72	1.56	8.43

RUN 13

Time (seconds)	Concentrations (moles/liter) Iodine	Chlorine	Iodine Monochloride	Nitrosyl Chloride	Nitric Oxide
0	1.19×10^{-5}	2.38×10^{-4}	0.00×10^{-5}	0.00×10^{-5}	8.36×10^{-5}
5	1.15	2.37	0.07	0.02	8.28
10	1.10	2.36	0.19	0.07	8.21
15	1.06	2.35	0.27	0.15	8.14
20	1.02	2.35	0.35	0.24	8.04
25	0.98	2.34	0.43	0.34	7.94
30	0.94	2.33	0.51	0.44	7.84
35	0.90	2.32	0.59	0.53	7.75
40	0.87	2.31	0.66	0.61	7.67
45	0.83	2.30	0.74	0.69	7.60
50	0.79	2.30	0.82	0.76	7.52
55	0.75	2.29	0.90	0.82	7.46
60	0.71	2.28	0.97	0.89	7.39
65	0.67	2.27	1.05	0.96	7.33
70	0.64	2.27	1.12	1.03	7.25
75	0.61	2.26	1.18	1.10	7.18
80	0.57	2.25	1.25	1.17	7.11
85	0.54	2.24	1.32	1.24	7.05
90	0.51	2.24	1.38	1.31	6.97
95	0.48	2.23	1.45	1.37	6.92
100	0.45	2.23	1.50	1.43	6.86
105	0.42	2.22	1.55	1.48	6.80
110	0.39	2.22	1.61	1.53	6.75
115	0.37	2.21	1.65	1.59	6.70
120	0.35	2.21	1.69	1.64	6.65
125	0.33	2.20	1.73	1.69	6.60
130	0.31	2.20	1.77	1.75	6.53

RUN 13 (Continued)

Time (seconds)	Concentrations (moles/liter) Iodine	Chlorine	Iodine Monochloride	Nitrosyl Chloride	Nitric Oxide
135	0.30×10^{-5}	2.20×10^{-4}	1.80×10^{-5}	1.80×10^{-5}	6.48×10^{-5}
140	0.28	2.19	1.83	1.86	6.42
145	0.27	2.19	1.86	1.92	6.36
150	0.25	2.18	1.89	1.98	6.30
155	0.24	2.18	1.92	2.05	6.23
160	0.23	2.17	1.94	2.12	6.16
165	0.21	2.17	1.97	2.17	6.11
170	0.20	2.16	1.99	2.24	6.05
175	0.20	2.16	2.00	2.29	6.00
180	0.19	2.16	2.02	2.33	5.95
185	0.18	2.15	2.04	2.38	5.90
190	0.17	2.15	2.06	2.43	5.85
195	0.16	2.15	2.07	2.47	5.81
200	0.15	2.15	2.09	2.50	5.78
205	0.15	2.14	2.10	2.54	5.74
210	0.14	2.14	2.12	2.58	5.70
215	0.13	2.14	2.13	2.61	5.67
220	0.13	2.14	2.14	2.65	5.63
225	0.12	2.13	2.15	2.68	5.60
230	0.12	2.13	2.16	2.72	5.57
235	0.11	2.13	2.17	2.75	5.54
240	0.11	2.13	2.18	2.78	5.50
245	0.11	2.13	2.19	2.81	5.47
250	0.10	2.12	2.19	2.85	5.43
255	0.10	2.12	2.20	2.88	5.40
260	0.09	2.12	2.21	2.91	5.37
265	0.09	2.12	2.21	2.94	5.34

RUN 13 (Continued)

Time (seconds)	Concentrations (moles/liter) Iodine	Chlorine	Iodine Monochloride	Nitrosyl Chloride	Nitric Oxide
270	0.09×10^{-5}	2.12×10^{-4}	2.22×10^{-5}	2.98×10^{-5}	5.30×10^{-5}
275	0.09	2.11	2.22	3.01	5.27
280	0.08	2.11	2.23	3.05	5.23
285	0.08	2.11	2.23	3.08	5.20
290	0.08	2.11	2.24	3.12	5.16
295	0.07	2.11	2.24	3.15	5.13
300	0.07	2.10	2.25	3.19	5.09
305	0.07	2.10	2.25	3.23	5.06
310	0.07	2.10	2.25	3.23	5.05

RUN 16

Concentrations (moles/liter)

Time (seconds)	Iodine	Chlorine	Iodine Mono-Chloride	Nitrosyl Chloride	Nitric Oxide
0	1.59×10^{-5}	1.36×10^{-4}	0.00×10^{-5}	0.00×10^{-4}	5.12×10^{-4}
5	1.55	1.35	0.07	0.00	5.11
10	1.53	1.34	0.13	0.02	5.10
15	1.50	1.33	0.19	0.03	5.09
20	1.47	1.32	0.25	0.04	5.07
25	1.44	1.31	0.30	0.05	5.06
30	1.41	1.30	0.36	0.07	5.05
35	1.38	1.30	0.42	0.08	5.04
40	1.35	1.29	0.48	0.09	5.02
45	1.32	1.28	0.54	0.11	5.01
50	1.29	1.27	0.59	0.12	5.00
55	1.27	1.26	0.63	0.14	4.98
60	1.23	1.25	0.71	0.15	4.97
65	1.21	1.24	0.77	0.16	4.96
70	1.18	1.23	0.83	0.17	4.95
75	1.15	1.22	0.89	0.18	4.93
80	1.12	1.21	0.95	0.19	4.92
85	1.09	1.20	1.00	0.20	4.91
90	1.06	1.19	1.06	0.22	4.90
95	1.03	1.18	1.12	0.23	4.88
100	1.00	1.17	1.18	0.25	4.87
105	0.97	1.16	1.23	0.26	4.85
110	0.95	1.16	1.28	0.27	4.84
115	0.92	1.15	1.33	0.29	4.83
120	0.90	1.14	1.38	0.30	4.81
125	0.88	1.13	1.42	0.32	4.80
130	0.86	1.12	1.47	0.33	4.78

RUN 16 (Continued)

Time (seconds)	Concentrations (moles/liter) Iodine	Chlorine	Iodine Monochloride	Nitrosyl Chloride	Nitric Oxide
135	0.83×10^{-5}	1.10×10^{-4}	1.51×10^{-5}	0.34×10^{-4}	4.77×10^{-4}
140	0.82	1.10	1.55	0.36	4.75
145	0.80	1.09	1.59	0.38	4.74
150	0.78	1.08	1.62	0.39	4.72
155	0.76	1.07	1.66	0.41	4.71
160	0.74	1.06	1.70	0.42	4.69
165	0.72	1.05	1.73	0.44	4.68
170	0.71	1.04	1.76	0.46	4.66
175	0.69	1.03	1.80	0.47	4.64
180	0.68	1.02	1.83	0.49	4.63
185	0.66	1.01	1.86	0.50	4.61
190	0.65	1.00	1.89	0.52	4.59
195	0.63	0.99	1.91	0.54	4.58
200	0.62	0.98	1.94	0.55	4.56
205	0.61	0.97	1.97	0.57	4.54
210	0.59	0.96	1.99	0.59	4.53
215	0.58	0.95	2.02	0.61	4.51
220	0.57	0.94	2.04	0.62	4.49
225	0.56	0.93	2.06	0.64	4.48
230	0.55	0.92	2.09	0.66	4.46
235	0.54	0.91	2.11	0.67	4.44
240	0.53	0.90	2.13	0.69	4.42
245	0.52	0.89	2.15	0.71	4.41
250	0.51	0.88	2.17	0.73	4.38
255	0.50	0.87	2.19	0.75	4.36
260	0.49	0.86	2.20	0.76	4.35
265	0.48	0.86	2.22	0.78	4.34

RUN 16 (Continued)

Time (seconds)	Concentrations (moles/liter) Iodine	Chlorine	Iodine Monochloride	Nitrosyl Chloride	Nitric Oxide
270	0.47×10^{-5}	0.85×10^{-4}	2.24×10^{-5}	0.80×10^{-4}	4.32×10^{-4}
275	0.46	0.84	2.25	0.81	4.30
280	0.46	0.83	2.27	0.83	4.28
285	0.45	0.82	2.28	0.85	4.27
290	0.44	0.81	2.30	0.86	4.25
295	0.43	0.80	2.31	0.88	4.23
300	0.43	0.79	2.32	0.90	4.22
305	0.42	0.78	2.34	0.92	4.20
310	0.41	0.77	2.35	0.94	4.17
315	0.41	0.76	2.36	0.95	4.17
320	0.40	0.76	2.38	0.97	4.15
325	0.40	0.75	2.39	0.98	4.14
330	0.39	0.74	2.40	1.00	4.12
335	0.38	0.73	2.41	1.02	4.10
340	0.38	0.72	2.42	1.03	4.09
345	0.37	0.71	2.44	1.05	4.07
350	0.37	0.70	2.45	1.06	4.05
355	0.36	0.69	2.46	1.08	4.04
360	0.36	0.69	2.46	1.09	4.02
365	0.35	0.68	2.47	1.11	4.00
370	0.34	0.67	2.47	1.12	3.99
375	0.34	0.66	2.49	1.13	3.98
380	0.33	0.65	2.50	1.15	3.96
385	0.33	0.65	2.51	1.17	3.95
390	0.32	0.64	2.52	1.18	3.93
395	0.32	0.63	2.53	1.20	3.92
400	0.31	0.62	2.54	1.21	3.90

RUN 16 (Continued)

Time (seconds)	Concentrations (moles/liter) Iodine	Chlorine	Iodine Monochloride	Nitrosyl Chloride	Nitric Oxide
405	0.31×10^{-5}	0.62×10^{-4}	2.55×10^{-5}	1.23×10^{-4}	3.89×10^{-4}
410	0.30	0.61	2.56	1.24	3.87
415	0.30	0.60	2.57	1.25	3.86
420	0.30	0.59	2.58	1.27	3.85
425	0.29	0.59	2.59	1.28	3.83
430	0.29	0.58	2.60	1.30	3.82
435	0.28	0.57	2.60	1.31	3.80
440	0.28	0.56	2.61	1.33	3.79
445	0.28	0.56	2.62	1.34	3.78
450	0.27	0.55	2.63	1.35	3.76
455	0.27	0.54	2.63	1.37	3.75
460	0.27	0.53	2.64	1.38	3.74
465	0.26	0.53	2.65	1.39	3.73
470	0.26	0.52	2.65	1.41	3.71
475	0.26	0.51	2.66	1.42	3.70
480	0.25	0.51	2.67	1.43	3.68
485	0.25	0.50	2.68	1.45	3.67
490	0.24	0.49	2.68	1.46	3.66
495	0.24	0.49	2.69	1.47	3.64
500	0.24	0.48	2.69	1.48	3.63

RUN 17

Concentrations (moles/liter)

Time (seconds)	Iodine	Chlorine	Iodine Monochloride	Nitrosyl Chloride	Nitric Oxide
0	1.34×10^{-5}	1.92×10^{-4}	0.00×10^{-5}	0.00×10^{-4}	5.10×10^{-4}
5	1.32	1.91	0.06	0.01	5.08
10	1.30	1.91	0.11	0.02	5.07
15	1.27	1.90	0.16	0.04	5.05
20	1.25	1.89	0.20	0.05	5.04
25	1.23	1.88	0.25	0.07	5.02
30	1.20	1.87	0.29	0.08	5.01
35	1.18	1.86	0.34	0.10	4.99
40	1.16	1.85	0.39	0.12	4.97
45	1.13	1.84	0.43	0.13	4.96
50	1.11	1.83	0.48	0.15	4.94
55	1.09	1.82	0.52	0.16	4.93
60	1.07	1.81	0.57	0.18	4.91
65	1.04	1.80	0.61	0.20	4.90
70	1.02	1.79	0.66	0.21	4.88
75	0.99	1.78	0.70	0.23	4.86
80	0.98	1.77	0.74	0.24	4.85
85	0.95	1.76	0.79	0.26	4.83
90	0.93	1.74	0.83	0.27	4.82
95	0.91	1.73	0.88	0.29	4.80
100	0.88	1.71	0.92	0.31	4.79
105	0.87	1.70	0.96	0.32	4.77
110	0.85	1.69	1.01	0.34	4.75
115	0.83	1.68	1.05	0.35	4.74
120	0.81	1.67	1.09	0.37	4.73
125	0.79	1.66	1.13	0.39	4.71
130	0.77	1.65	1.16	0.40	4.69

RUN 17 (Continued)

Time (seconds)	Concentrations (moles/liter) Iodine	Chlorine	Iodine Monochloride	Nitrosyl Chloride	Nitric Oxide
135	0.75×10^{-5}	1.64×10^{-4}	1.20×10^{-5}	0.42×10^{-4}	4.67×10^{-4}
140	0.73	1.64	1.24	0.43	4.66
145	0.71	1.63	1.27	0.45	4.64
150	0.70	1.62	1.31	0.47	4.62
155	0.68	1.61	1.34	0.48	4.61
160	0.66	1.60	1.37	0.50	4.59
165	0.65	1.59	1.40	0.52	4.58
170	0.63	1.58	1.43	0.53	4.56
175	0.62	1.57	1.46	0.55	4.54
180	0.60	1.56	1.49	0.57	4.53
185	0.59	1.55	1.52	0.58	4.51
190	0.58	1.54	1.55	0.60	4.50
195	0.56	1.53	1.58	0.61	4.48
200	0.55	1.52	1.60	0.63	4.46
205	0.53	1.51	1.63	0.65	4.44
210	0.52	1.50	1.65	0.66	4.43
215	0.51	1.49	1.68	0.68	4.41
220	0.50	1.48	1.70	0.69	4.40
225	0.49	1.47	1.73	0.71	4.38
230	0.48	1.46	1.75	0.73	4.36
235	0.46	1.45	1.77	0.74	4.35
240	0.45	1.44	1.79	0.76	4.33
245	0.44	1.43	1.81	0.78	4.32
250	0.43	1.43	1.83	0.79	4.30
255	0.42	1.42	1.85	0.81	4.28
260	0.41	1.41	1.87	0.82	4.27
265	0.40	1.40	1.89	0.84	4.25

RUN 17 (Continued)

Time (seconds)	Concentrations (moles/liter) Iodine	Chlorine	Iodine Monochloride	Nitrosyl Chloride	Nitric Oxide
270	0.40×10^{-5}	1.39×10^{-4}	1.91×10^{-5}	0.86×10^{-4}	4.24×10^{-4}
275	0.39	1.38	1.93	0.87	4.22
280	0.38	1.37	1.94	0.89	4.20
285	0.37	1.36	1.96	0.90	4.19
290	0.36	1.36	1.98	0.92	4.17
295	0.35	1.35	1.99	0.93	4.16
300	0.35	1.34	2.01	0.95	4.14
305	0.34	1.33	2.02	0.97	4.12
310	0.33	1.32	2.04	0.98	4.11
315	0.32	1.31	2.05	1.00	4.09
320	0.32	1.30	2.07	1.01	4.08
325	0.31	1.30	2.08	1.03	4.06
330	0.30	1.29	2.10	1.05	4.05
335	0.30	1.28	2.11	1.06	4.03
340	0.29	1.27	2.12	1.08	4.01
345	0.28	1.26	2.13	1.09	4.00
350	0.28	1.25	2.15	1.11	3.98
355	0.27	1.24	2.16	1.12	3.97
360	0.27	1.24	2.17	1.14	3.95
365	0.26	1.23	2.18	1.15	3.94
370	0.25	1.22	2.19	1.17	3.92
375	0.25	1.21	2.20	1.18	3.91
380	0.24	1.20	2.21	1.19	3.89
385	0.24	1.20	2.22	1.21	3.88
390	0.23	1.19	2.23	1.22	3.87
395	0.23	1.18	2.24	1.24	3.85
400	0.22	1.18	2.25	1.25	3.84

RUN 17 (Continued)

Time (seconds)	Concentrations (moles/liter) Iodine	Chlorine	Iodine Monochloride	Nitrosyl Chloride	Nitric Oxide
405	0.22×10^{-5}	1.17×10^{-4}	2.26×10^{-5}	1.27×10^{-4}	3.83×10^{-4}
410	0.22	1.16	2.27	1.28	3.81
415	0.21	1.15	2.27	1.29	3.80
420	0.21	1.15	2.28	1.30	3.79
425	0.21	1.14	2.29	1.32	3.77
430	0.20	1.13	2.29	1.33	3.76
435	0.20	1.13	2.30	1.34	3.75
440	0.20	1.12	2.31	1.35	3.74
445	0.19	1.12	2.31	1.37	3.73
450	0.19	1.11	2.32	1.38	3.71
455	0.19	1.10	2.32	1.39	3.70
460	0.19	1.10	2.33	1.40	3.69
465	0.18	1.09	2.33	1.41	3.68
470	0.18	1.09	2.34	1.42	3.67
475	0.18	1.08	2.34	1.43	3.66
480	0.18	1.08	2.35	1.44	3.65
485	0.17	1.07	2.35	1.45	3.64
490	0.17	1.06	2.36	1.46	3.63
495	0.17	1.06	2.36	1.48	3.62
500	0.17	1.05	2.37	1.49	3.61
505	0.17	1.05	2.37	1.50	3.60
510	0.16	1.04	2.37	1.50	3.59
515	0.16	1.04	2.38	1.51	3.58
520	0.16	1.03	2.38	1.53	3.57
525	0.16	1.03	2.39	1.54	3.56
530	0.16	1.02	2.39	1.55	3.55
535	0.15	1.02	2.39	1.56	3.54

RUN 17 (Continued)

Time (seconds)	Concentrations (moles/liter) Iodine	Chlorine	Iodine Monochloride	Nitrosyl Chloride	Nitric Oxide
540	0.15×10^{-5}	1.01×10^{-4}	2.40×10^{-5}	1.57×10^{-4}	3.53×10^{-4}
545	0.15	1.01	2.40	1.58	3.52
550	0.15	1.00	2.40	1.59	3.51
555	0.15	1.00	2.41	1.60	3.50
560	0.14	0.99	2.41	1.61	3.49
565	0.14	0.99	2.41	1.62	3.48
570	0.14	0.98	2.42	1.63	3.47
575	0.14	0.98	2.42	1.64	3.46
580	0.14	0.97	2.42	1.65	3.45
585	0.14	0.96	2.43	1.66	3.43
590	0.13	0.96	2.43	1.66	3.43
595	0.13	0.96	2.43	1.67	3.42
600	0.13	0.95	2.43	1.68	3.41

TABLE II

CHEMICAL AFFINITIES, VELOCITIES, AND AFFINITY-VELOCITY PRODUCTS OF THE REACTIONS

RUN 11

Time (seconds)	Affinities (Calories/Gram-Mole) Reaction 1	Affinities (Calories/Gram-Mole) Reaction 2	Velocities (Gram-Mole/Liter-Seconds) Reaction 1	Velocities (Gram-Mole/Liter-Seconds) Reaction 2	Affinity-Velocity Products (Calories/Liter-Second) Reaction 1	Affinity-Velocity Products (Calories/Liter-Second) Reaction 2
0	-	-	1.74×10^{-7}	10.28×10^{-8}	-	-
5	-	-	1.70	9.98	-	-
10	-	-	1.66	9.68	-	-
15	-	-	1.62	9.38	-	-
20	-	-	1.58	9.09	-	-
25	-	-	1.55	8.77	-	-
30	-	-	1.51	8.51	-	-
35	-	-	1.47	8.23	-	-
40	-	-	1.43	7.94	-	-

RUN 11 (Continued)

Time (seconds)	Affinities (Calories/Gram-Mole) Reaction 1	Reaction 2	Velocities (Gram-Mole/Liter-Seconds) Reaction 1	Reaction 2	Affinity-Velocity Products (Calories/Liter-Second) Reaction 1	Reaction 2
45	-	-	1.38×10^{-7}	7.65×10^{-8}	-	-
50	8958	56	1.33	7.34	11.9×10^{-4}	41×10^{-7}
55	8841	54	1.29	7.04	11.4	38
60	8723	53	1.25	6.72	10.9	36
65	8615	53	1.22	6.43	10.5	34
70	8519	52	1.19	6.12	10.1	32
75	8417	52	1.17	5.85	9.8	30
80	8335	50	1.14	5.59	9.5	30
85	8242	50	1.12	5.36	9.2	27
90	8157	50	1.10	5.15	9.0	26
95	8082	49	1.08	4.94	8.7	24
100	8006	48	1.05	4.77	8.4	23
105	7935	46	1.01	4.56	8.0	21
110	7870	46	0.98	4.37	7.7	20
115	7807	45	0.94	4.19	7.3	19

RUN 11 (Continued)

Time (seconds)	Affinities (Calories/Gram-Mole) Reaction 1	Reaction 2	Velocities (Gram-Mole/Liter-Seconds) Reaction 1	Reaction 2	Affinity-Velocity Products (Calories/Liter-Second) Reaction 1	Reaction 2
120	7752	38	0.92×10^{7}	4.01×10^{-8}	7.1×10^{-4}	15×10^{-7}
125	7695	35	0.89	3.80	6.8	13
130	7644	30	0.87	3.60	6.7	11
135	7588	24	0.86	3.42	6.5	8
140	7536	20	0.83	3.24	6.3	7
145	7485	19	0.81	3.08	6.1	6
150	7438	12	0.79	2.92	5.9	4
155	7393	6	0.77	2.76	5.7	2
160	7349	4	0.75	2.62	5.5	1
165	7302	4	0.74	2.46	5.4	1
170	7256	2	0.73	2.30	5.3	0.5
175	7216	2	0.72	2.14	5.2	0.4
180	7171	2	0.70	2.00	5.0	0.4
185	7126	1	0.70	1.88	5.0	0.2
190	7087	0	0.68	1.78	4.8	0.0

RUN 12

Time (seconds)	Affinities (Calories/Gram-Mole) Reaction 1	Affinities (Calories/Gram-Mole) Reaction 2	Velocities (Gram-Mole/Liter-Seconds) Reaction 1	Velocities (Gram-Mole/Liter-Seconds) Reaction 2	Affinity-Velocity Products (Calories/Liter-Second) Reaction 1	Affinity-Velocity Products (Calories/Liter-Second) Reaction 2
0	-	-	6.68×10^{-8}	3.87×10^{-8}	-	-
5	-	-	6.65	3.85	-	-
10	-	-	6.62	3.84	-	-
15	-	-	6.59	3.82	-	-
20	-	-	6.57	3.81	-	-
25	11418	-644	6.56	3.79	7.49×10^{-4}	-2.44×10^{-5}
30	11015	-472	6.55	3.77	7.21	-1.78
35	10737	-391	6.52	3.76	7.00	-1.47
40	10484	-341	6.56	3.76	6.88	-1.28
45	10292	-274	6.58	3.75	6.77	-1.03
50	10106	-227	6.63	3.75	6.70	-0.85
55	9941	-191	6.66	3.75	6.62	-0.72
60	9795	-163	6.66	3.74	6.52	-0.61
65	9662	-141	6.64	3.74	6.42	-0.53

RUN 12 (Continued)

Time (seconds)	Affinities (Calories/Gram-Mole) Reaction 1	Reaction 2	Velocities (Gram-Mole/Liter-Seconds) Reaction 1	Reaction 2	Affinity-Velocity Products (Calories/Liter-Second) Reaction 1	Reaction 2
70	9540	-122	6.60×10^{-8}	3.73×10^{-8}	6.30×10^{-4}	-0.46×10^{-5}
75	9439	-118	6.55	3.72	6.18	-0.44
80	9334	-106	6.49	3.72	6.06	-0.39
85	9246	-103	6.45	3.71	5.96	-0.38
90	9163	-101	6.47	3.69	5.91	-0.37
95	9083	- 97	6.48	3.65	5.89	-0.35
100	9008	- 94	6.53	3.63	5.88	-0.34
105	8922	- 92	6.57	3.60	5.86	-0.33
110	8848	- 86	6.58	3.57	5.82	-0.31
115	8775	- 83	6.60	3.55	5.79	-0.29
120	8707	- 80	6.62	3.54	5.76	-0.28
125	8642	- 77	6.64	3.52	5.74	-0.27
130	8573	- 69	6.67	3.48	5.72	-0.24
135	8506	- 63	6.72	3.47	5.72	-0.22

RUN 12 (Continued)

(seconds)	Affinities (Calories/Gram-Mole) Reaction 1	Reaction 2	Velocities (Gram-Mole/Liter-Seconds) Reaction 1	Reaction 2	Affinity-Velocity Products (Calories/Liter-Second) Reaction 1	Reaction 2
140	8448	-60	6.73×10^{-8}	3.45×10^{-8}	5.69×10^{-4}	-0.21×10^{-5}
145	8382	-53	6.69	3.43	5.61	-0.18
150	8322	-49	6.66	3.40	5.54	-0.16
155	8270	-48	6.67	3.37	5.52	-0.16
160	8215	-47	6.65	3.35	5.46	-0.16
165	8161	-45	6.67	3.31	5.44	-0.15
170	8105	-43	6.74	3.29	5.46	-0.14
175	8054	-43	6.77	3.27	5.45	-0.14
180	8000	-38	6.78	3.24	5.42	-0.12
185	7948	-35	6.78	3.20	5.39	-0.11
190	7898	-32	6.80	3.14	5.37	-0.10
195	7850	-30	6.77	3.09	5.31	-0.09
200	7798	-24	6.79	3.05	5.30	-0.07
205	7749	-19	6.81	3.01	5.28	-0.06

RUN 12 (Continued)

Time (seconds)	Affinities (Calories/Gram-Mole) Reaction 1	Reaction 2	Velocities (Gram-Mole/Liter-Seconds) Reaction 1	Reaction 2	Affinity-Velocity Products (Calories/Liter-Second) Reaction 1	Reaction 2
210	7704	-18	6.85×10^{-8}	2.98×10^{-8}	5.28×10^{-4}	-0.05×10^{-5}
215	7653	-12	6.85	2.95	5.24	-0.04
220	7607	- 9	6.86	2.94	5.22	-0.03
225	7559	- 4	6.85	2.91	5.18	-0.01
230	7514	- 3	6.84	2.89	5.14	-0.008
235	7471	- 3	6.85	2.88	5.12	-0.008
240	7429	- 2	6.83	2.88	5.07	-0.006
245	7381	0	6.85	2.85	5.06	0.0
250	7340	0	6.85	2.80	5.03	0.0

RUN 13

Time (seconds)	Affinities (Calories/Gram-Mole) Reaction 1	Reaction 2	Velocities (Gram-Mole/Liter-Seconds) Reaction 1	Reaction 2	Affinity-Velocity Products (Calories/Liter-Second) Reaction 1	Reaction 2
0	-	-	2.05×10^{-7}	8.55×10^{-8}	-	-
5	-	-	1.97	8.42	-	-
10	-	-	1.91	8.30	-	-
15	-	-	1.85	8.17	-	-
20	-	-	1.79	8.05	-	-
25	-	-	1.75	7.93	-	-
30	-	-	1.70	7.91	-	-
35	-	-	1.65	7.90	-	-
40	9388	487	1.59	7.85	1.49×10^{-3}	3.82×10^{-5}
45	9238	464	1.53	7.76	1.41	3.60
50	9099	451	1.48	7.71	1.35	3.48
55	8984	427	1.45	7.58	1.30	3.24
60	8876	403	1.42	7.35	1.26	2.96
65	8777	372	1.41	7.18	1.24	2.67

RUN 13 (Continued)

Time (seconds)	Affinities (Calories/Gram-Mole) Reaction 1	Reaction 2	Velocities (Gram-Mole/Liter-Seconds) Reaction 1	Reaction 2	Affinity-Velocity Products (Calories/Liter-Second) Reaction 1	Reaction 2
70	8671	365	1.39×10^{-7}	7.00×10^{-8}	1.21×10^{-3}	2.65×10^{-5}
75	8576	359	1.38	6.81	1.18	2.44
80	8488	337	1.35	6.63	1.15	2.23
85	8407	317	1.31	6.43	1.10	2.04
90	8324	304	1.26	6.21	1.05	1.89
95	8258	273	1.20	5.90	0.99	1.61
100	8193	255	1.13	5.51	0.93	1.41
105	8134	230	1.07	5.19	0.87	1.19
110	8081	202	1.01	4.79	0.82	0.97
115	8030	181	0.97	4.43	0.78	0.80
120	7981	165	0.94	4.08	0.75	0.67
125	7933	149	0.92	3.77	0.73	0.56
130	7877	146	0.91	3.53	0.72	0.52
135	8730	131	0.91	3.33	0.71	0.44

RUN 13 (Continued)

Time (seconds)	Affinities (Calories/Gram-Mole) Reaction 1	Reaction 2	Velocities (Gram-Mole/Liter-Seconds) Reaction 1	Reaction 2	Affinity-Velocity Products (Calories/Liter-Second) Reaction 1	Reaction 2
140	7778	127	0.90×10^{-7}	3.11×10^{-8}	0.70×10^{-3}	0.40×10^{-5}
145	7725	128	0.90	2.90	0.70	0.37
150	7671	126	0.89	2.72	0.68	0.34
155	7616	125	0.89	2.55	0.68	0.32
160	7561	126	0.86	2.36	0.65	0.30
165	7517	124	0.81	2.21	0.61	0.27
170	7470	124	0.75	2.06	0.56	0.26
175	7426	123	0.70	1.90	0.52	0.23
180	7398	122	0.66	1.77	0.49	0.22
185	7359	122	0.61	1.69	0.45	0.21
190	7325	116	0.58	1.61	0.42	0.19
195	7297	104	0.56	1.51	0.41	0.16
200	7270	94	0.53	1.44	0.39	0.14
205	7243	83	0.50	1.35	0.36	0.11

RUN 13 (Continued)

Time (seconds)	Affinities (Calories/Gram-Mole) Reaction 1	Reaction 2	Velocities (Gram-Mole/Liter-Seconds) Reaction 1	Reaction 2	Affinity-Velocity Products (Calories/Liter-Second) Reaction 1	Reaction 2
210	7215	75	0.48×10^{-7}	1.26×10^{-8}	0.35×10^{-3}	0.09×10^{-5}
215	7192	62	0.47	1.20	0.34	0.07
220	7167	54	0.45	1.12	0.32	0.06
225	7145	43	0.44	1.04	0.31	0.05
230	7121	33	0.43	0.96	0.31	0.03
235	7100	23	0.42	0.89	0.30	0.02
240	7075	22	0.41	0.82	0.29	0.02
245	7053	18	0.40	0.77	0.28	0.01
250	7031	13	0.40	0.73	0.28	0.01
255	7009	11	0.39	0.79	0.27	0.008
260	6990	11	0.38	0.62	0.27	0.007
265	6967	9	0.38	0.57	0.26	0.005
270	6942	10	0.37	0.54	0.26	0.005
275	6920	9	0.37	0.51	0.26	0.005

RUN 13 (Continued)

Time (seconds)	Affinities (Calories/Gram-Mole) Reaction 1	Reaction 2	Velocities (Gram-Mole/Liter-Seconds) Reaction 1	Reaction 2	Affinity-Velocity Products (Calories/Liter-Second) Reaction 1	Reaction 2
280	6897	7	0.36×10^{-7}	0.50×10^{-8}	0.25×10^{-3}	0.004×10^{-5}
285	6875	4	0.36	0.49	0.25	0.002
290	6851	4	0.36	0.47	0.25	0.002
295	6829	5	0.35	0.43	0.24	0.002
300	6805	0	0.34	0.42	0.23	0.0
305	6784	0	0.34	0.41	0.23	0.0
310	6782	0	0.34	0.39	0.23	0.0

RUN 16

Time (seconds)	Affinities (Calories/Gram-Mole) Reaction 1	Reaction 2	Velocities (Gram-Mole/Liter-Seconds) Reaction 1	Reaction 2	Affinity-Velocity Products (Calories/Liter-Second) Reaction 1	Reaction 2
0	-	-	1.80×10^{-7}	5.98×10^{-8}	-	-
5	-	-	1.82	5.95	-	-
10	-	-	1.83	5.91	-	-
15	-	-	1.84	5.88	-	-
20	-	-	1.83	5.84	-	-
25	11499	-698	1.85	5.82	2.13×10^{-3}	-4.06×10^{-5}
30	11222	-651	1.87	5.80	2.10	-3.78
35	11012	-647	1.88	5.79	2.07	-3.75
40	10813	-645	1.91	5.56	2.07	-3.59
45	10626	-646	1.89	5.66	2.01	-3.66
50	10492	-642	1.89	5.76	1.98	-3.70
55	10310	-638	1.86	5.86	1.92	-3.74
60	10238	-634	1.83	5.85	1.87	-3.71
65	10122	-624	1.82	5.84	1.84	-3.64
70	10026	-620	1.77	5.83	1.78	-3.61

RUN 16 (Continued)

Time (seconds)	Affinities (Calories/Gram-Mole) Reaction 1	Reaction 2	Velocities (Gram-Mole/Liter-Seconds) Reaction 1	Reaction 2	Affinity-Velocity Products (Calories/Liter-Second) Reaction 1	Reaction 2
75	9930	-614	1.81×10^{-7}	5.85×10^{-8}	1.80×10^{-3}	-3.59×10^{-5}
80	9841	-610	1.82	5.83	1.79	-3.56
85	9776	-606	1.84	5.79	1.80	-3.51
90	9678	-602	1.91	5.73	1.85	-3.45
95	9598	-596	1.91	5.73	1.83	-3.36
100	9522	-593	1.91	5.47	1.82	-3.24
105	9429	-589	1.87	5.27	1.76	-3.10
110	9376	-587	1.87	5.08	1.75	-2.98
115	9311	-585	1.86	4.83	1.73	-2.83
120	9241	-586	1.86	4.66	1.72	-2.73
125	9171	-582	1.91	4.44	1.75	-2.58
130	9106	-578	1.93	4.25	1.76	-2.46
135	9043	-580	1.92	4.08	1.74	-2.37
140	8980	-575	1.93	3.94	1.73	-2.27
145	8917	-569	1.93	3.80	1.72	-2.16

RUN 16 (Continued)

Time (seconds)	Affinities (Calories/Gram-Mole) Reaction 1	Reaction 2	Velocities (Gram-Mole/Liter-Seconds) Reaction 1	Reaction 2	Affinity-Velocity Products (Calories/Liter-Second) Reaction 1	Reaction 2
150	8860	-567	1.93×10^{-7}	3.66×10^{-8}	1.71×10^{-3}	-2.08×10^{-5}
155	8800	-568	1.94	3.60	1.71	-2.05
160	8746	-563	1.93	3.47	1.69	-1.95
165	8689	-579	1.93	3.35	1.68	-1.94
170	8635	-568	1.93	3.23	1.67	-1.84
175	8583	-557	1.95	3.14	1.67	-1.75
180	8530	-545	1.95	3.04	1.66	-1.66
185	8478	-533	1.96	2.94	1.66	-1.57
190	8428	-522	1.96	2.86	1.65	-1.49
195	8377	-509	1.96	2.78	1.64	-1.42
200	8329	-497	1.95	2.69	1.62	-1.34
205	8284	-488	1.95	2.60	1.62	-1.27
210	8236	-475	1.94	2.52	1.60	-1.20
215	8190	-464	1.94	2.44	1.59	-1.13
220	8144	-452	1.94	2.35	1.58	-1.06

RUN 16 (Continued)

Time (seconds)	Affinities (Calories/Gram-Mole) Reaction 1	Reaction 2	Velocities (Gram-Mole/Liter-Seconds) Reaction 1	Reaction 2	Affinity-Velocity Products (Calories/Liter-Second) Reaction 1	Reaction 2
225	8102	-442	1.94×10^{-7}	2.28×10^{-8}	1.57×10^{-3}	-1.01×10^{-5}
230	8057	-429	1.93	2.19	1.56	-0.94
235	8015	-418	1.91	2.12	1.53	-0.89
240	7971	-405	1.91	2.06	1.52	-0.83
245	7930	-393	1.90	1.97	1.51	-0.77
250	7872	-368	1.90	1.89	1.50	-0.70
255	7833	-359	1.90	1.80	1.49	-0.65
260	7805	-354	1.85	1.72	1.44	-0.61
265	7765	-341	1.77	1.63	1.37	-0.56
270	7729	-331	1.80	1.57	1.39	-0.52
275	7691	-318	1.85	1.54	1.42	-0.49
280	7654	-306	1.85	1.50	1.42	-0.46
285	7618	-295	1.86	1.46	1.42	-0.43
290	7580	-283	1.88	1.43	1.43	-0.40
295	7544	-271	1.91	1.42	1.44	-0.38

RUN 16 (Continued)

Time (seconds)	Affinities (Calories/Gram-Mole) Reaction 1	Affinities (Calories/Gram-Mole) Reaction 2	Velocities (Gram-Mole/Liter-Seconds) Reaction 1	Velocities (Gram-Mole/Liter-Seconds) Reaction 2	Affinity-Velocity Products (Calories/Liter-Second) Reaction 1	Affinity-Velocity Products (Calories/Liter-Second) Reaction 2
300	7508	-259	1.91×10^{-7}	1.38×10^{-8}	1.43×10^{-3}	-0.36×10^{-5}
305	7470	-246	1.84	1.33	1.37	-0.33
310	7419	-225	1.74	1.28	1.29	-0.29
315	7405	-223	1.70	1.25	1.26	-0.28
320	7373	-218	1.66	1.22	1.22	-0.27
325	7347	-212	1.65	1.21	1.21	-0.26
330	7307	-198	1.75	1.22	1.28	-0.24
335	7274	-189	1.74	1.21	1.27	-0.23
340	7245	-182	1.74	1.20	1.26	-0.22
345	7215	-175	1.69	1.17	1.22	-0.21
350	7185	-168	1.68	1.00	1.21	-0.17
355	7153	-159	1.68	1.03	1.20	-0.16
360	7124	-152	1.61	1.05	1.15	-0.16
365	7091	-147	1.61	1.08	1.14	-0.16
370	7067	-140	1.60	1.11	1.13	-0.16

RUN 16 (Continued)

Time (seconds)	Affinities (Calories/Gram-Mole) Reaction 1	Reaction 2	Velocities (Gram-Mole/Liter-Seconds) Reaction 1	Reaction 2	Affinity-Velocity Products (Calories/Liter-Second) Reaction 1	Reaction 2
375	7045	-137	1.61×10^{-7}	1.00×10^{-8}	1.13×10^{-3}	-0.14×10^{-5}
380	7009	-127	1.61	1.00	1.13	-0.13
385	6982	-121	1.61	0.99	1.12	-0.12
390	6952	-114	1.61	0.98	1.12	-0.11
395	6926	-108	1.56	0.94	1.08	-0.10
400	6900	-103	1.53	0.92	1.06	-0.10
405	6872	- 97	1.50	0.89	1.03	-0.09
410	6846	- 91	1.50	0.87	1.03	-0.08
415	6822	- 87	1.50	0.85	1.02	-0.07
420	6796	- 81	1.49	0.83	1.01	-0.07
425	6768	- 74	1.51	0.82	1.02	-0.06
430	6743	- 69	1.51	0.81	1.02	-0.06
435	6717	- 64	1.50	0.79	1.01	-0.05
440	6688	- 56	1.48	0.76	0.99	-0.04
445	6666	- 53	1.44	0.74	0.96	-0.04

RUN 16 (Continued)

Time (seconds)	Affinities (Calories/Gram-Mole) Reaction 1	Affinities (Calories/Gram-Mole) Reaction 2	Velocities (Gram-Mole/Liter-Seconds) Reaction 1	Velocities (Gram-Mole/Liter-Seconds) Reaction 2	Affinity-Velocity Products (Calories/Liter-Second) Reaction 1	Affinity-Velocity Products (Calories/Liter-Second) Reaction 2
450	6640	-47	1.34×10^{-7}	0.70×10^{-8}	0.89×10^{-3}	-0.03×10^{-5}
455	6614	-41	1.36	0.70	0.90	-0.03
460	6595	-35	1.38	0.70	0.91	-0.02
465	6581	-28	1.38	0.70	0.91	-0.02
470	6541	-20	1.40	0.70	0.92	-0.01
475	6520	-14	1.41	0.69	0.92	-0.01
480	6497	-10	1.41	0.69	0.92	-0.007
485	6467	- 6	1.41	0.68	0.91	-0.005
490	6447	- 4	1.39	0.67	0.90	-0.003
495	6422	- 4	1.39	0.67	0.89	-0.003
500	6392	0	1.39	0.66	0.89	0.0

RUN 17

Time (seconds)	Affinities (Calories/Gram-Mole) Reaction 1	Reaction 2	Velocities (Gram-Mole/Liter-Seconds) Reaction 1	Reaction 2	Affinity-Velocity Products (Calories/Liter-Second) Reaction 1	Reaction 2
0	-	-	2.03×10^{-7}	4.74×10^{-8}	-	-
5	-	-	2.01	4.72	-	-
10	-	-	1.99	4.69	-	-
15	-	-	1.97	4.65	-	-
20	11710	-263	1.97	4.64	2.31×10^{-3}	-12.20×10^{-6}
25	11425	-246	1.99	4.61	2.27	-11.34
30	11172	-218	2.02	4.59	2.26	-10.01
35	10955	-196	2.04	4.58	2.23	- 8.98
40	10738	-194	2.06	4.56	2.21	- 8.85
45	10572	-193	2.06	4.54	2.18	- 8.76
50	10432	-189	2.05	4.53	2.14	- 8.56
55	10295	-190	2.02	4.52	2.08	- 8.59
60	10175	-189	2.02	4.50	2.06	- 8.51
65	10065	-188	2.03	4.48	2.04	- 8.42
70	9965	-186	2.02	4.47	2.01	- 8.31
75	9866	-186	2.02	4.46	1.99	- 8.30

RUN 17 (Continued)

Time (seconds)	Affinities (Calories/Gram-Mole) Reaction 1	Affinities (Calories/Gram-Mole) Reaction 2	Velocities (Gram-Mole/Liter-Seconds) Reaction 1	Velocities (Gram-Mole/Liter-Seconds) Reaction 2	Affinity-Velocity Products (Calories/Liter-Second) Reaction 1	Affinity-Velocity Products (Calories/Liter-Second) Reaction 2
80	9774	-184	2.02×10^{-7}	4.45×10^{-8}	1.97×10^{-3}	-8.19×10^{-6}
85	9689	-183	2.02	4.44	1.96	-8.13
90	9611	-180	2.02	4.41	1.94	-7.94
95	9534	-177	2.02	4.35	1.93	-7.70
100	9459	-178	2.02	4.28	1.91	-7.62
105	9388	-177	2.02	4.20	1.90	-7.43
110	9321	-176	2.01	4.11	1.87	-7.23
115	9255	-174	2.00	4.02	1.85	-6.99
120	9195	-173	1.99	3.94	1.83	-6.82
125	9134	-175	1.99	3.86	1.82	-6.76
130	9075	-172	1.98	3.77	1.80	-6.48
135	9020	-170	1.98	3.68	1.79	-6.26
140	8965	-168	1.97	3.58	1.77	-6.01
145	8913	-166	1.97	3.48	1.76	-5.78
150	8860	-165	1.97	3.37	1.75	-5.56

RUN 17 (Continued)

Time (seconds)	Affinities (Calories/Gram-Mole) Reaction 1	Affinities (Calories/Gram-Mole) Reaction 2	Velocities (Gram-Mole/Liter-Seconds) Reaction 1	Velocities (Gram-Mole/Liter-Seconds) Reaction 2	Affinity-Velocity Products (Calories/Liter-Second) Reaction 1	Affinity-Velocity Products (Calories/Liter-Second) Reaction 2
155	8811	-162	1.97×10^{-7}	3.28×10^{-8}	1.74×10^{-3}	-5.31×10^{-6}
160	8761	-159	1.96	3.18	1.72	-5.06
165	8713	-161	1.96	3.10	1.71	-4.99
170	8666	-159	1.94	3.02	1.68	-4.80
175	8622	-157	1.92	2.93	1.66	-4.60
180	8574	-155	1.90	2.87	1.63	-4.45
185	8536	-153	1.89	2.82	1.61	-4.32
190	8492	-154	1.89	2.77	1.61	-4.27
195	8452	-153	1.88	2.71	1.59	-4.15
200	8411	-151	1.88	2.65	1.58	-4.00
205	8372	-150	1.87	2.59	1.57	-3.89
210	8333	-149	1.87	2.50	1.56	-3.73
215	8295	-148	1.87	2.43	1.55	-3.60
220	8258	-146	1.85	2.36	1.53	-3.45
225	8221	-145	1.86	2.30	1.53	-3.34

RUN 17 (Continued)

Time (seconds)	Affinities (Calories/Gram-Mole) Reaction 1	Reaction 2	Velocities (Gram-Mole/Liter-Seconds) Reaction 1	Reaction 2	Affinity-Velocity Products (Calories/Liter-Second) Reaction 1	Reaction 2
230	8183	-142	1.86×10^{-7}	2.23×10^{-8}	1.52×10^{-3}	-3.17×10^{-6}
235	8152	-140	1.84	2.17	1.50	-3.04
240	8112	-137	1.84	2.12	1.49	-2.90
245	8078	-135	1.84	2.07	1.49	-2.80
250	8046	-136	1.83	2.01	1.47	-2.73
255	8011	-132	1.79	1.95	1.43	-2.57
260	7978	-130	1.79	1.89	1.43	-2.46
265	7947	-128	1.78	1.84	1.41	-2.36
270	7915	-126	1.76	1.78	1.39	-2.24
275	7884	-125	1.75	1.74	1.38	-2.18
280	7854	-122	1.75	1.70	1.37	-2.07
285	7824	-121	1.75	1.66	1.37	-2.01
290	7793	-119	1.75	1.61	1.36	-1.92
295	7763	-116	1.74	1.58	1.35	-1.83
300	7734	-114	1.74	1.54	1.35	-1.76

RUN 17 (Continued)

Time (seconds)	Affinities (Calories/Gram-Mole) Reaction 1	Reaction 2	Velocities (Gram-Mole/Liter-Seconds) Reaction 1	Reaction 2	Affinity-Velocity Products (Calories/Liter-Second) Reaction 1	Reaction 2
305	7705	-112	1.73×10^{-7}	1.50×10^{-8}	1.33×10^{-3}	-1.68×10^{-6}
310	7678	-111	1.73	1.49	1.33	-1.65
315	7647	-107	1.72	1.45	1.32	-1.55
320	7620	-106	1.73	1.41	1.32	-1.50
325	7593	-108	1.73	1.38	1.31	-1.49
330	7565	-102	1.71	1.34	1.29	-1.37
335	7537	-100	1.70	1.30	1.28	-1.30
340	7510	- 98	1.68	1.26	1.26	-1.24
345	7484	- 98	1.66	1.24	1.24	-1.22
350	7459	- 97	1.64	1.21	1.22	-1.17
355	7433	- 96	1.62	1.18	1.20	-1.13
360	7408	- 93	1.61	1.14	1.19	-1.06
365	7383	- 93	1.61	1.09	1.19	-1.01
370	7360	- 93	1.58	1.05	1.16	-0.98
375	7336	- 92	1.55	1.03	1.14	-0.95

RUN 17 (Continued)

Time (seconds)	Affinities (Calories/Gram-Mole) Reaction 1	Reaction 2	Velocities (Gram-Mole/Liter-Seconds) Reaction 1	Reaction 2	Affinity-Velocity Products (Calories/Liter-Second) Reaction 1	Reaction 2
380	7309	-85	1.52×10^{-7}	0.99×10^{-8}	1.11×10^{-3}	-0.84×10^{-6}
385	7290	-85	1.49	0.96	1.09	-0.82
390	7268	-86	1.48	0.94	1.08	-0.81
395	7246	-85	1.45	0.91	1.05	-0.77
400	7224	-84	1.45	0.86	1.05	-0.72
405	7202	-83	1.43	0.82	1.03	-0.68
410	7181	-83	1.42	0.78	1.02	-0.65
415	7161	-81	1.38	0.74	0.99	-0.60
420	7141	-79	1.35	0.70	0.96	-0.55
425	7118	-75	1.31	0.66	0.93	-0.50
430	7102	-74	1.28	0.63	0.91	-0.47
435	7084	-72	1.25	0.61	0.89	-0.44
440	7066	-70	1.23	0.59	0.87	-0.41
445	7048	-67	1.23	0.58	0.87	-0.39
450	7030	-66	1.21	0.56	0.85	-0.37

RUN 17 (Continued)

Time (seconds)	Affinities (Calories/Gram-Mole) Reaction 1	Reaction 2	Velocities (Gram-Mole/Liter-Seconds) Reaction 1	Reaction 2	Affinity-Velocity Products (Calories/Liter-Second) Reaction 1	Reaction 2
455	7012	-63	1.19×10^{-7}	0.54×10^{-8}	0.83×10^{-3}	-0.34×10^{-6}
460	6996	-61	1.17	0.52	0.82	-0.32
465	6980	-59	1.15	0.50	0.80	-0.30
470	6964	-57	1.14	0.49	0.79	-0.28
475	6946	-54	1.13	0.48	0.78	-0.26
480	6931	-52	1.12	0.47	0.78	-0.24
485	6915	-50	1.11	0.46	0.77	-0.23
490	6900	-49	1.08	0.44	0.75	-0.22
495	6884	-47	1.07	0.43	0.74	-0.20
500	6868	-43	1.05	0.42	0.72	-0.18
505	6855	-41	1.05	0.41	0.72	-0.17
510	6840	-41	1.04	0.40	0.71	-0.16
515	6825	-40	1.04	0.40	0.71	-0.16
520	6811	-37	1.06	0.40	0.72	-0.15
525	6796	-35	1.05	0.38	0.71	-0.13

RUN 17 (Continued)

Time (seconds)	Affinities (Calories/Gram-Mole) Reaction 1	Reaction 2	Velocities (Gram-Mole/Liter-Seconds) Reaction 1	Reaction 2	Affinity-Velocity Products (Calories/Liter-Second) Reaction 1	Reaction 2
530	6780	-32	1.05×10^{-7}	0.37×10^{-8}	0.71×10^{-3}	-0.12×10^{-6}
535	6766	-30	1.05	0.36	0.71	-0.11
540	6751	-27	1.03	0.35	0.70	-0.10
545	6737	-25	1.03	0.35	0.69	-0.09
550	6723	-23	1.03	0.34	0.69	-0.08
555	6709	-21	1.02	0.33	0.68	-0.07
560	6694	-18	1.02	0.33	0.68	-0.06
565	6680	-15	1.02	0.33	0.68	-0.05
670	6666	-13	1.04	0.33	0.69	-0.04
575	6652	-11	1.03	0.33	0.69	-0.04
580	6638	- 9	1.02	0.33	0.68	-0.03
585	6621	- 6	1.01	0.32	0.67	-0.02
590	6610	- 6	1.01	0.31	0.67	-0.02
595	6596	- 3	1.00	0.31	0.66	-0.01
600	6581	0	1.00	0.31	0.66	0.0

TABLE III

EXTINCTION COEFFICIENTS
(liter/gram-mole-centimeter)
36 °C

	4900 Å	4716 Å	3802 Å	3343 Å
Iodine	1189.	667.3	0.9	negligible
Chlorine	0.295	0.893	29.7	147.
Iodine Monochloride	229.	268.	44.7	negligible
Nitrosyl Chloride	9.77	12.3	36.0	74.7

TABLE IV

SELECTED PHENOMENOLOGICAL COEFFICIENTS

$$V_1 = L_{11}A_1 + L_{12}A_2 + \frac{1}{2}L_{111}A_1^2 + L_{112}A_1A_2 + \frac{1}{2}L_{122}A_2^2$$

$$V_2 = L_{21}A_1 + L_{22}A_2 + \frac{1}{2}L_{211}A_1^2 + L_{212}A_1A_2 + \frac{1}{2}L_{222}A_2^2$$

	L_{11}	L_{12}	L_{111}	L_{112}	L_{122}	L_{21}	L_{22}	L_{211}	L_{212}	L_{222}
RUN 11										
95 - 190 secs.	1.02×10^{-11}	-1.94×10^{-9}	-	2.96×10^{-13}	-	3.23×10^{-12}	4.05×10^{-10}	-	-	-
RUN 12										
120 - 250 secs.	9.25×10^{-12}	1.81×10^{-10}	-	-	-					
170 - 250 secs.	9.23×10^{-12}	1.63×10^{-10}	-	-	-	3.89×10^{-12}	3.86×10^{-11}	-	-	3.70×10^{-12}

TABLE IV (Continued)

$$V_1 = L_{11}A_1 + L_{12}A_2 + \frac{1}{2}L_{111}A_1^2 + L_{112}A_1A_2 + \frac{1}{2}L_{122}A_2^2$$

$$V_2 = L_{21}A_1 + L_{22}A_2 + \frac{1}{2}L_{211}A_1^2 + L_{212}A_1A_2 + \frac{1}{2}L_{222}A_2^2$$

	L_{11}	L_{12}	L_{111}	L_{112}	L_{122}	L_{21}	L_{22}	L_{211}	L_{212}	L_{222}
RUN 13										
195 - 310 secs.	5.47×10^{-12}	1.31×10^{-10}	-	-	-	7.90×10^{-13}	-5.49×10^{-9}	-	7.99×10^{-13}	-4.79×10^{-12}
RUN 16										
270 - 500 secs.	2.14×10^{-11}	-7.82×10^{-11}	-	-	-	9.78×10^{-13}	-2.48×10^{-11}	-	-	-
370 - 500 secs.	2.15×10^{-11}	-6.35×10^{-11}	-	-	-	9.39×10^{-13}	-2.93×10^{-11}	-	-	-
RUN 17										
370 - 600 secs.	1.59×10^{-11}	3.23×10^{-10}	-	-	1.59×10^{-11}	2.70×10^{-13}	-6.98×10^{-11}	-	-	-
470 - 600 secs.	1.56×10^{-11}	2.42×10^{-10}	-	-	1.02×10^{-11}	4.35×10^{-13}	-2.81×10^{-11}	-	-	-

TABLE V

PHENOMENOLOGICAL COEFFICIENTS

$$V_1 = L_{11}A_1 + L_{12}A_2 + \tfrac{1}{2} L_{111}A_1^2 + L_{122}A_1A_2 + \tfrac{1}{2} L_{122}A_2^2$$

RUN 11

Data from 45 to 190 seconds were used in the following Correlations

$L_{11}^{*} = 1.01 \times 10^{-11}$	$L_{11} = -7.44 \times 10^{-12}$	$L_{11} = 1.02 \times 10^{-11}$
$L_{12}^{*} = -4.09 \times 10^{-9}$	$L_{12} = 1.52 \times 10^{-10}$	$L_{12} = -3.62 \times 10^{-9}$
$L_{111}^{**} = 0.0$	$L_{111} = 4.84 \times 10^{-15}$	$L_{111} = 0.0$
$L_{112}^{**} = 6.03 \times 10^{-13}$	$L_{112} = 0.0$	$L_{112} = 5.13 \times 10^{-13}$
$L_{122}^{**} = -1.14 \times 10^{-11}$	$L_{122} = 0.0$	$L_{122} = 0.0$
$\sigma^2 = 1.47$	$\sigma^2 = 5.39$	$\sigma^2 = 2.86$
$L_{11} = 1.03 \times 10^{-11}$	$L_{11} = 1.24 \times 10^{-11}$	$L_{11} = 0.0$
$L_{12} = 5.79 \times 10^{-10}$	$L_{12} = 0.0$	$L_{12} = 2.03 \times 10^{-9}$
$L_{111} = 0.0$	$L_{111} = 0.0$	$L_{111} = 0.0$
$L_{112} = 0.0$	$L_{112} = 0.0$	$L_{112} = 0.0$
$L_{122} = 0.0$	$L_{122} = 0.0$	$L_{122} = 0.0$
$\sigma^2 = 24.4$	$\sigma^2 = 734.$	$\sigma^2 = 31.4$

*Units of L_{11} and L_{12} are (gram-moles)^2/calorie-liter-second

**Units of L_{111}, L_{112}, and L_{122} are (gram-moles)^3/calorie^2-liter-second

RUN 11 (Continued)

Data from 95 to 190 seconds were used in the following Correlations

$L_{11} = 1.01 \times 10^{-11}$	$L_{11} = 1.02 \times 10^{-11}$	$L_{11} = 1.01 \times 10^{-11}$
$L_{12} = -5.47 \times 10^{-9}$	$L_{12} = -1.94 \times 10^{-9}$	$L_{12} = 2.72 \times 10^{-10}$
$L_{111} = 7.90 \times 10^{-13}$	$L_{111} = 0.0$	$L_{111} = 0.0$
$L_{112} = 0.0$	$L_{112} = 2.96 \times 10^{-13}$	$L_{112} = 0.0$
$L_{122} = -1.55 \times 10^{-11}$	$L_{122} = 0.0$	$L_{122} = 5.64 \times 10^{-12}$
$\sigma^2 = 0.54$	$\sigma^2 = 1.20$	$\sigma^2 = 1.39$

$L_{11} = 1.01 \times 10^{-11}$	$L_{11} = 1.13 \times 10^{-11}$	$L_{11} = 0.0$
$L_{12} = 4.12 \times 10^{-10}$	$L_{12} = 0.0$	$L_{12} = 2.37 \times 10^{-9}$
$L_{111} = 0.0$	$L_{111} = 0.0$	$L_{111} = 0.0$
$L_{112} = 0.0$	$L_{112} = 0.0$	$L_{112} = 0.0$
$L_{122} = 0.0$	$L_{122} = 0.0$	$L_{122} = 0.0$
$\sigma^2 = 2.21$	$\sigma^2 = 27.6$	$\sigma^2 = 52.1$

RUN 12

Data from 20 to 250 seconds were used in the following Correlations

$L_{11} = 9.37 \times 10^{-12}$	$L_{11} = 1.81 \times 10^{-11}$	$L_{11} = 8.93 \times 10^{-12}$
$L_{12} = 8.62 \times 10^{-10}$	$L_{12} = -2.74 \times 10^{-11}$	$L_{12} = 4.22 \times 10^{-10}$
$L_{111} = 0.0$	$L_{111} = -2.42 \times 10^{-15}$	$L_{111} = 0.0$
$L_{112} = -7.51 \times 10^{-14}$	$L_{112} = 0.0$	$L_{112} = -3.17 \times 10^{-14}$
$L_{122} = -1.91 \times 10^{-13}$	$L_{122} = 0.0$	$L_{122} = 0.0$
$\sigma^2 = 0.46$	$\sigma^2 = 7.25$	$\sigma^2 = 1.58$

RUN 12 (Continued)

$L_{11} = 8.54 \times 10^{-12}$	$L_{11} = 8.29 \times 10^{-12}$	$L_{11} = 7.48 \times 10^{-12}$
$L_{12} = 8.82 \times 10^{-11}$	$L_{12} = 5.19 \times 10^{-11}$	$L_{12} = 0.0$
$L_{111} = 0.0$	$L_{111} = 0.0$	$L_{111} = 0.0$
$L_{112} = 0.0$	$L_{112} = 0.0$	$L_{112} = 0.0$
$L_{122} = 1.08 \times 10^{-13}$	$L_{122} = 0.0$	$L_{122} = 0.0$
$\sigma^2 = 10.4$	$\sigma^2 = 42.4$	$\sigma^2 = 5876.$

$L_{11} = 0.0$

$L_{12} = -1.83 \times 10^{-10}$

$L_{111} = 0.0$

$L_{112} = 0.0$

$L_{122} = 0.0$

$\sigma^2 = 407.$

Data from 70 to 250 seconds were used in the following Correlations

$L_{11} = 9.27 \times 10^{-12}$	$L_{11} = 8.03 \times 10^{-12}$	$L_{11} = 0.0$
$L_{12} = 1.87 \times 10^{-10}$	$L_{12} = 0.0$	$L_{12} = -8.32 \times 10^{-10}$
$L_{111} = 0.0$	$L_{111} = 0.0$	$L_{111} = 0.0$
$L_{112} = 0.0$	$L_{112} = 0.0$	$L_{112} = 0.0$
$L_{122} = 0.0$	$L_{122} = 0.0$	$L_{122} = 0.0$
$\sigma^2 = 0.068$	$\sigma^2 = 2493.$	$\sigma^2 = 10.5$

RUN 12 (Continued)

Data from 120 to 250 seconds were used in the following Correlations

$L_{11} = 9.25 \times 10^{-12}$	$L_{11} = 8.46 \times 10^{-12}$	$L_{11} = 0.0$
$L_{12} = 1.81 \times 10^{-10}$	$L_{12} = 0.0$	$L_{12} = -1.30 \times 10^{-9}$
$L_{111} = 0.0$	$L_{111} = 0.0$	$L_{111} = 0.0$
$L_{112} = 0.0$	$L_{112} = 0.0$	$L_{112} = 0.0$
$L_{122} = 0.0$	$L_{122} = 0.0$	$L_{122} = 0.0$
$\sigma^2 = 0.046$	$\sigma^2 = 1056.$	$\sigma^2 = 4.45$

Data from 170 to 250 seconds were used in the following Correlations

$L_{11} = 9.23 \times 10^{-12}$	$L_{11} = 8.83 \times 10^{-12}$	$L_{11} = 0.0$
$L_{12} = 1.63 \times 10^{-10}$	$L_{12} = 0.0$	$L_{12} = -2.20 \times 10^{-9}$
$L_{111} = 0.0$	$L_{111} = 0.0$	$L_{111} = 0.0$
$L_{112} = 0.0$	$L_{112} = 0.0$	$L_{112} = 0.0$
$L_{122} = 0.0$	$L_{122} = 0.0$	$L_{122} = 0.0$
$\sigma^2 = 0.027$	$\sigma^2 = 349.$	$\sigma^2 = 1.87$

RUN 13

Data from 45 to 310 seconds were used in the following Correlations

$L_{11} = 5.02 \times 10^{-12}$	$L_{11} = 4.71 \times 10^{-12}$	$L_{11} = 5.61 \times 10^{-12}$
$L_{12} = 6.81 \times 10^{-10}$	$L_{12} = 3.78 \times 10^{-10}$	$L_{12} = 2.46 \times 10^{-10}$
$L_{111} = 0.0$	$L_{111} = 0.0$	$L_{111} = 0.0$
$L_{112} = -4.88 \times 10^{-14}$	$L_{112} = 0.0$	$L_{112} = 0.0$
$L_{122} = 0.0$	$L_{122} = -6.26 \times 10^{-13}$	$L_{122} = 0.0$
$\sigma^2 = 2.62$	$\sigma^2 = 2.48$	$\sigma^2 = 5.03$

$L_{11} = 1.05 \times 10^{-11}$	$L_{11} = 0.0$
$L_{12} = 0.0$	$L_{12} = 4.18 \times 10^{-10}$
$L_{111} = 0.0$	$L_{111} = 0.0$
$L_{112} = 0.0$	$L_{112} = 0.0$
$L_{122} = 0.0$	$L_{122} = 0.0$
$\sigma^2 = 3720.$	$\sigma^2 = 20.0$

Data from 95 to 310 seconds were used in the following Correlations

$L_{11} = 5.41 \times 10^{-12}$	$L_{11} = 5.08 \times 10^{-12}$	$L_{11} = 8.75 \times 10^{-12}$
$L_{12} = -5.97 \times 10^{-10}$	$L_{12} = 2.97 \times 10^{-10}$	$L_{12} = 0.0$
$L_{111} = 0.0$	$L_{111} = 0.0$	$L_{111} = 0.0$
$L_{112} = 1.12 \times 10^{-13}$	$L_{112} = 0.0$	$L_{112} = 0.0$
$L_{122} = 0.0$	$L_{122} = 0.0$	$L_{122} = 0.0$
$\sigma^2 = 3.56$	$\sigma^2 = 2.88$	$\sigma^2 = 1910.$

RUN 13 (Continued)

$L_{11} = 0.0$

$L_{12} = 5.56 \times 10^{-10}$

$L_{111} = 0.0$

$L_{112} = 0.0$

$L_{122} = 0.0$

$\sigma^2 = 8.35$

Data from 145 to 310 seconds were used in the following Correlations

$L_{11} = 5.68 \times 10^{-12}$	$L_{11} = 5.72 \times 10^{-12}$	$L_{11} = 5.08 \times 10^{-12}$
$L_{12} = -4.98 \times 10^{-9}$	$L_{12} = -3.88 \times 10^{-9}$	$L_{12} = 2.77 \times 10^{-10}$
$L_{111} = 0.0$	$L_{111} = 0.0$	$L_{111} = 0.0$
$L_{112} = 7.12 \times 10^{-13}$	$L_{112} = 5.52 \times 10^{-13}$	$L_{112} = 0.0$
$L_{122} = -1.52 \times 10^{-12}$	$L_{122} = 0.0$	$L_{122} = 0.0$
$\sigma^2 = 0.040$	$\sigma^2 = 0.048$	$\sigma^2 = 3.24$

$L_{11} = 7.39 \times 10^{-12}$	$L_{11} = 0.00$
$L_{12} = 0.0$	$L_{12} = 6.32 \times 10^{-10}$
$L_{111} = 0.0$	$L_{111} = 0.0$
$L_{112} = 0.0$	$L_{112} = 0.0$
$L_{122} = 0.0$	$L_{122} = 0.0$
$\sigma^2 = 1002.$	$\sigma^2 = 6.90$

RUN 13 (Continued)

Data from 195 to 310 seconds were used in the following Correlations

$L_{11} = 5.47 \times 10^{-12}$	$L_{11} = 6.03 \times 10^{-12}$	$L_{11} = 0.0$
$L_{12} = 1.31 \times 10^{-10}$	$L_{12} = 0.0$	$L_{12} = 7.49 \times 10^{-10}$
$L_{111} = 0.0$	$L_{111} = 0.0$	$L_{111} = 0.0$
$L_{112} = 0.0$	$L_{112} = 0.0$	$L_{112} = 0.0$
$L_{122} = 0.0$	$L_{122} = 0.0$	$L_{122} = 0.0$
$\sigma^2 = 0.59$	$\sigma^2 = 0.0$	$\sigma^2 = 6.39$

RUN 16

Data from 70 to 500 seconds were used in the following Correlations

$L_{11} = 3.80 \times 10^{-11}$	$L_{11} = 2.08 \times 10^{-11}$	$L_{11} = 4.88 \times 10^{-11}$
$L_{12} = -2.09 \times 10^{-10}$	$L_{12} = -4.57 \times 10^{-10}$	$L_{12} = -1.46 \times 10^{-10}$
$L_{111} = -5.22 \times 10^{-15}$	$L_{111} = 0.0$	$L_{111} = -8.18 \times 10^{-15}$
$L_{112} = 0.0$	$L_{112} = 4.61 \times 10^{-14}$	$L_{112} = 0.0$
$L_{122} = -3.46 \times 10^{-13}$	$L_{122} = -1.06 \times 10^{-13}$	$L_{122} = 0.0$
$\sigma^2 = 12.8$	$\sigma^2 = 17.0$	$\sigma^2 = 11.3$

$L_{11} = 2.12 \times 10^{-11}$	$L_{11} = 1.99 \times 10^{-11}$	$L_{11} = 2.33 \times 10^{-11}$
$L_{12} = -4.70 \times 10^{-10}$	$L_{12} = -2.03 \times 10^{-10}$	$L_{12} = 2.36 \times 10^{-11}$
$L_{111} = 0.0$	$L_{111} = 0.0$	$L_{111} = 0.0$
$L_{112} = 5.18 \times 10^{-14}$	$L_{112} = 0.0$	$L_{112} = 0.0$
$L_{122} = 0.0$	$L_{122} = -5.92 \times 10^{-13}$	$L_{122} = 0.0$
$\sigma^2 = 18.6$	$\sigma^2 = 34.0$	$\sigma^2 = 461.$

RUN 16 (Continued)

Data from 270 to 500 seconds were used in the following Correlations

$L_{11} = 2.14 \times 10^{-11}$	$L_{11} = 2.29 \times 10^{-11}$	$L_{11} = 0.0$
$L_{12} = -7.82 \times 10^{-11}$	$L_{12} = 0.0$	$L_{12} = -8.57 \times 10^{-10}$
$L_{111} = 0.0$	$L_{111} = 0.0$	$L_{111} = 0.0$
$L_{112} = 0.0$	$L_{112} = 0.0$	$L_{112} = 0.0$
$L_{122} = 0.0$	$L_{122} = 0.0$	$L_{122} = 0.0$
$\sigma^2 = 17.0$	$\sigma^2 = 245.$	$\sigma^2 = 38.6$

Data from 370 to 500 seconds were used in the following Correlations

$L_{11} = 2.15 \times 10^{-11}$	$L_{11} = 2.21 \times 10^{-11}$	$L_{11} = 0.0$
$L_{12} = -6.35 \times 10^{-11}$	$L_{12} = 0.0$	$L_{12} = -1.65 \times 10^{-9}$
$L_{111} = 0.0$	$L_{111} = 0.0$	$L_{111} = 0.0$
$L_{112} = 0.0$	$L_{112} = 0.0$	$L_{112} = 0.0$
$L_{122} = 0.0$	$L_{122} = 0.0$	$L_{122} = 0.0$
$\sigma^2 = 16.1$	$\sigma^2 = 84.3$	$\sigma^2 = 9.15$

RUN 17

Data from 70 to 600 seconds were used in the following Correlations

$L_{11} = 1.35 \times 10^{-11}$	$L_{11} = 1.19 \times 10^{-11}$	$L_{11} = 1.38 \times 10^{-11}$
$L_{12} = -7.12 \times 10^{-10}$	$L_{12} = -9.27 \times 10^{-10}$	$L_{12} = -5.01 \times 10^{-10}$
$L_{111} = 0.0$	$L_{111} = 0.0$	$L_{111} = 0.0$
$L_{112} = 2.31 \times 10^{-14}$	$L_{112} = 0.0$	$L_{112} = 0.0$
$L_{122} = 0.0$	$L_{122} = -4.46 \times 10^{-12}$	$L_{122} = 0.0$
$\sigma^2 = 0.86$	$\sigma^2 = 0.71$	$\sigma^2 = 1.04$

$L_{11} = 2.03 \times 10^{-11}$	$L_{11} = 0.0$
$L_{12} = 0.0$	$L_{12} = -1.42 \times 10^{-9}$
$L_{111} = 0.0$	$L_{111} = 0.0$
$L_{112} = 0.0$	$L_{112} = 0.0$
$L_{122} = 0.0$	$L_{122} = 0.0$
$\sigma^2 = 7261.$	$\sigma^2 = 3.42$

Data from 170 to 600 seconds were used in the following Correlations

$L_{11} = 1.60 \times 10^{-11}$	$L_{11} = 1.31 \times 10^{-11}$	$L_{11} = 1.35 \times 10^{-11}$
$L_{12} = -4.73 \times 10^{-9}$	$L_{12} = -9.18 \times 10^{-10}$	$L_{12} = -5.35 \times 10^{-10}$
$L_{111} = 0.0$	$L_{111} = 0.0$	$L_{111} = 0.0$
$L_{112} = 7.89 \times 10^{-13}$	$L_{112} = 4.44 \times 10^{-14}$	$L_{112} = 0.0$
$L_{122} = 3.06 \times 10^{-11}$	$L_{122} = 0.0$	$L_{122} = 0.0$
$\sigma^2 = 0.11$	$\sigma^2 = 0.77$	$\sigma^2 = 0.97$

RUN 17 (Continued)

$L_{11} = 1.99 \times 10^{-11}$	$L_{11} = 0.0$
$L_{12} = 0.0$	$L_{12} = 1.49 \times 10^{-9}$
$L_{111} = 0.0$	$L_{111} = 0.0$
$L_{112} = 0.0$	$L_{112} = 0.0$
$L_{122} = 0.0$	$L_{122} = 0.0$
$\sigma^2 = 8406.$	$\sigma^2 = 3.46$

Data from 270 to 600 seconds were used in the following Correlations

$L_{11} = 1.54 \times 10^{-11}$	$L_{11} = 1.56 \times 10^{-11}$	$L_{11} = 1.30 \times 10^{-11}$
$L_{12} = 4.44 \times 10^{-9}$	$L_{12} = 3.10 \times 10^{-10}$	$L_{12} = -6.09 \times 10^{-10}$
$L_{111} = 0.0$	$L_{111} = 0.0$	$L_{111} = 0.0$
$L_{112} = -6.53 \times 10^{-13}$	$L_{112} = 0.0$	$L_{112} = 0.0$
$L_{122} = 0.0$	$L_{122} = 1.44 \times 10^{-11}$	$L_{122} = 0.0$
$\sigma^2 = 2.99$	$\sigma^2 = 0.22$	$\sigma^2 = 0.79$

$L_{11} = 1.89 \times 10^{-11}$	$L_{11} = 0.0$
$L_{12} = 0.0$	$L_{12} = -1.71 \times 10^{-9}$
$L_{111} = 0.0$	$L_{111} = 0.0$
$L_{112} = 0.0$	$L_{112} = 0.0$
$L_{122} = 0.0$	$L_{122} = 0.0$
$\sigma^2 = 8292.$	$\sigma^2 = 2.51$

RUN 17 (Continued)

Data from 370 to 600 seconds were used in the following Correlations

$L_{11} = 1.59 \times 10^{-11}$	$L_{11} = 1.59 \times 10^{-11}$	$L_{11} = 1.37 \times 10^{-11}$
$L_{12} = 7.62 \times 10^{-9}$	$L_{12} = 3.23 \times 10^{-10}$	$L_{12} = -4.59 \times 10^{-10}$
$L_{111} = 0.0$	$L_{111} = 0.0$	$L_{111} = 0.0$
$L_{112} = -1.10 \times 10^{-12}$	$L_{112} = 0.0$	$L_{112} = 0.0$
$L_{122} = 0.0$	$L_{122} = 1.59 \times 10^{-11}$	$L_{122} = 0.0$
$\sigma^2 = 0.44$	$\sigma^2 = 0.13$	$\sigma^2 = 1.06$

$L_{11} = 1.71 \times 10^{-11}$	$L_{11} = 0.0$
$L_{12} = 5.84 \times 10^{-13}$	$L_{12} = -1.93 \times 10^{-9}$
$L_{111} = 0.0$	$L_{111} = 0.0$
$L_{112} = 0.0$	$L_{112} = 0.0$
$L_{122} = 0.0$	$L_{122} = 0.0$
$\sigma^2 = 4078.$	$\sigma^2 = 2.42$

Data from 470 to 600 seconds were used in the following Correlations

$L_{11} = 1.56 \times 10^{-11}$	$L_{11} = 1.52 \times 10^{-11}$	$L_{11} = 1.55 \times 10^{-11}$
$L_{12} = 2.42 \times 10^{-10}$	$L_{12} = -7.36 \times 10^{-11}$	$L_{12} = 0.0$
$L_{111} = 0.0$	$L_{111} = 0.0$	$L_{111} = 0.0$
$L_{112} = 0.0$	$L_{112} = 0.0$	$L_{112} = 0.0$
$L_{122} = 1.02 \times 10^{-11}$	$L_{122} = 0.0$	$L_{122} = 0.0$
$\sigma^2 = 0.37$	$\sigma^2 = 2.37$	$\sigma^2 = 99.9$

RUN 17 (Continued)

$L_{11} = 0.0$

$L_{12} = -2.73 \times 10^{-9}$

$L_{111} = 0.0$

$L_{112} = 0.0$

$L_{122} = 0.0$

$\sigma^2 = 1.56$

$$V_2 = L_{21}A_1 + L_{22}A_2 + \tfrac{1}{2}L_{211}A_1^2 + L_{212}A_1A_2 + \tfrac{1}{2}L_{222}A_2^2$$

RUN 11

Data from 45 to 190 seconds were used in the following Correlations

$L_{21}^{*} = -1.55 \times 10^{-11}$	$L_{21} = 3.15 \times 10^{-12}$	$L_{21} = -1.56 \times 10^{-11}$
$L_{22}^{*} = 1.71 \times 10^{-10}$	$L_{22} = -3.71 \times 10^{-9}$	$L_{22} = 1.12 \times 10^{-10}$
$L_{211}^{**} = 5.16 \times 10^{-15}$	$L_{211} = 0.0$	$L_{211} = 5.20 \times 10^{-15}$
$L_{212}^{**} = 0.0$	$L_{212} = 5.83 \times 10^{-13}$	$L_{212} = 0.0$
$L_{222}^{**} = -2.22 \times 10^{-12}$	$L_{222} = -2.04 \times 10^{-11}$	$L_{222} = 0.0$
$\sigma^2 = 0.46$	$\sigma^2 = 1.07$	$\sigma^2 = 0.52$

$L_{21} = 3.36 \times 10^{-12}$	$L_{21} = 3.49 \times 10^{-12}$	$L_{21} = 5.58 \times 10^{-12}$
$L_{22} = -3.64 \times 10^{-9}$	$L_{22} = 5.71 \times 10^{-10}$	$L_{22} = 0.0$
$L_{211} = 0.0$	$L_{211} = 0.0$	$L_{211} = 0.0$
$L_{212} = 5.15 \times 10^{-13}$	$L_{212} = 0.0$	$L_{212} = 0.0$
$L_{222} = 0.0$	$L_{222} = 0.0$	$L_{222} = 0.0$
$\sigma^2 = 4.06$	$\sigma^2 = 22.9$	$\sigma^2 = 193.$

*Units of L_{21} and L_{22} are (gram-moles)^2/calorie-liter-second

**Units of L_{211}, L_{212}, and L_{222} are (gram-moles)^3/calorie^2-liter-second

RUN 11 (Continued)

L_{21} = 0.0

L_{22} = 1.26×10^{-9}

L_{211} = 0.0

L_{212} = 0.0

L_{222} = 0.0

σ^2 = 19.6

Data from 95 to 190 seconds were used in the following Correlations

L_{21} = 3.18×10^{-12}	L_{21} = 3.23×10^{-12}	L_{21} = 4.40×10^{-12}
L_{22} = -3.25×10^{-9}	L_{22} = 4.05×10^{-10}	L_{22} = 0.0
L_{211} = 0.0	L_{211} = 0.0	L_{211} = 0.0
L_{212} = 5.08×10^{-13}	L_{212} = 0.0	L_{212} = 0.0
L_{222} = -1.52×10^{-11}	L_{222} = 0.0	L_{222} = 0.0
σ^2 = 0.56	σ^2 = 1.01	σ^2 = 66.1

L_{21} = 0.0

L_{22} = 1.03×10^{-9}

L_{211} = 0.0

L_{212} = 0.0

L_{222} = 0.0

σ^2 = 25.8

RUN 12

Data from 20 to 250 seconds were used in the following Correlations

$L_{21} = 2.54 \times 10^{-12}$	$L_{21} = 3.84 \times 10^{-12}$	$L_{21} = 4.06 \times 10^{-12}$
$L_{22} = 3.81 \times 10^{-11}$	$L_{22} = -2.45 \times 10^{-10}$	$L_{22} = 1.25 \times 10^{-11}$
$L_{211} = 4.00 \times 10^{-16}$	$L_{211} = 0.0$	$L_{211} = 0.0$
$L_{212} = 0.0$	$L_{212} = 2.61 \times 10^{-14}$	$L_{212} = 0.0$
$L_{222} = 3.30 \times 10^{-14}$	$L_{222} = 1.31 \times 10^{-13}$	$L_{222} = 0.0$
$\sigma^2 = 0.59$	$\sigma^2 = 0.11$	$\sigma^2 = 0.86$

$L_{21} = 3.86 \times 10^{-12}$	$L_{21} = 0.0$
$L_{22} = 0.0$	$L_{22} = -1.03 \times 10^{-10}$
$L_{211} = 0.0$	$L_{211} = 0.0$
$L_{212} = 0.0$	$L_{212} = 0.0$
$L_{222} = 0.0$	$L_{222} = 0.0$
$\sigma^2 = 4.71$	$\sigma^2 = 217.$

Data from 70 to 250 seconds were used in the following Correlations

$L_{21} = 3.83 \times 10^{-12}$	$L_{21} = 3.82 \times 10^{-12}$	$L_{21} = 3.93 \times 10^{-12}$
$L_{22} = -2.18 \times 10^{-10}$	$L_{22} = -5.89 \times 10^{-11}$	$L_{22} = -1.03 \times 10^{-11}$
$L_{211} = 0.0$	$L_{211} = 0.0$	$L_{211} = 0.0$
$L_{212} = 2.21 \times 10^{-14}$	$L_{212} = 0.0$	$L_{212} = 0.0$
$L_{222} = 0.0$	$L_{222} = -8.19 \times 10^{-13}$	$L_{222} = 0.0$
$\sigma^2 = 0.066$	$\sigma^2 = 0.064$	$\sigma^2 = 0.34$

RUN 12 (Continued)

L_{21} =	3.99×10^{-12}	L_{21} =	0.0
L_{22} =	0.0	L_{22} =	-4.42×10^{-10}
L_{211} =	0.0	L_{211} =	0.0
L_{212} =	0.0	L_{212} =	0.0
L_{222} =	0.0	L_{222} =	0.0
σ^2 =	0.46	σ^2 =	

Data from 120 to 250 seconds were used in the following Correlations

L_{21} =	3.84×10^{-12}	L_{21} =	3.86×10^{-12}	L_{21} =	3.99×10^{-12}
L_{22} =	-4.87×10^{-11}	L_{22} =	-2.92×10^{-11}	L_{22} =	0.0
L_{211} =	0.0	L_{211} =	0.0	L_{211} =	0.0
L_{212} =	0.0	L_{212} =	0.0	L_{212} =	0.0
L_{222} =	-5.28×10^{-13}	L_{222} =	0.0	L_{222} =	0.0
σ^2 =	0.081	σ^2 =	0.099	σ^2 =	0.58

L_{21} =	0.0
L_{22} =	-6.46×10^{-10}
L_{211} =	0.0
L_{212} =	0.0
L_{222} =	0.0
σ^2 =	3.09

RUN 12 (Continued)

Data from 170 to 250 seconds were used in the following Correlations

$L_{21} = 3.88 \times 10^{-12}$	$L_{21} = 3.89 \times 10^{-12}$	$L_{21} = 3.85 \times 10^{-12}$
$L_{22} = 8.15 \times 10^{-10}$	$L_{22} = 3.86 \times 10^{-11}$	$L_{22} = -3.48 \times 10^{-11}$
$L_{211} = 0.0$	$L_{211} = 0.0$	$L_{211} = 0.0$
$L_{212} = -1.06 \times 10^{-13}$	$L_{212} = 0.0$	$L_{212} = 0.0$
$L_{222} = 0.0$	$L_{222} = 3.70 \times 10^{-12}$	$L_{222} = 0.0$
$\sigma^2 = 0.020$	$\sigma^2 = 0.010$	$\sigma^2 = 0.086$

$L_{21} = 3.93 \times 10^{-12}$	$L_{21} = 0.0$
$L_{22} = 0.0$	$L_{22} = -1.02 \times 10^{-9}$
$L_{211} = 0.0$	$L_{211} = 0.0$
$L_{212} = 0.0$	$L_{212} = 0.0$
$L_{222} = 0.0$	$L_{222} = 0.0$
$\sigma^2 = 0.38$	$\sigma^2 = 1.51$

RUN 13

Data from 45 to 310 seconds were used in the following Correlations

$L_{21} = -2.11 \times 10^{-11}$	$L_{21} = 3.20 \times 10^{-13}$	$L_{21} = 5.23 \times 10^{-13}$
$L_{22} = 7.88 \times 10^{-11}$	$L_{22} = -9.39 \times 10^{-10}$	$L_{22} = 1.76 \times 10^{-10}$
$L_{211} = 6.22 \times 10^{-15}$	$L_{211} = 0.0$	$L_{211} = 0.0$
$L_{212} = 0.0$	$L_{212} = 1.63 \times 10^{-13}$	$L_{212} = 0.0$
$L_{222} = -1.91 \times 10^{-13}$	$L_{222} = -1.65 \times 10^{-12}$	$L_{222} = 0.0$
$\sigma^2 = 0.50$	$\sigma^2 = 0.54$	$\sigma^2 = 0.74$

$L_{21} = 4.03 \times 10^{-12}$	$L_{21} = 0.0$
$L_{22} = 0.0$	$L_{22} = 1.92 \times 10^{-10}$
$L_{211} = 0.0$	$L_{211} = 0.0$
$L_{212} = 0.0$	$L_{212} = 0.0$
$L_{222} = 0.0$	$L_{222} = 0.0$
$\sigma^2 = 19.4$	$\sigma^2 = 0.89$

Data from 95 to 310 seconds were used in the following Correlations

$L_{21} = -2.52 \times 10^{-11}$	$L_{21} = 7.38 \times 10^{-13}$	$L_{21} = 8.41 \times 10^{-13}$
$L_{22} = -4.79 \times 10^{-11}$	$L_{22} = -1.66 \times 10^{-9}$	$L_{22} = -7.86 \times 10^{-10}$
$L_{211} = 7.52 \times 10^{-15}$	$L_{211} = 0.0$	$L_{211} = 0.0$
$L_{212} = 0.0$	$L_{212} = 2.52 \times 10^{-13}$	$L_{212} = 1.21 \times 10^{-13}$
$L_{222} = 6.76 \times 10^{-13}$	$L_{222} = -1.68 \times 10^{-12}$	$L_{222} = 0.0$
$\sigma^2 = 0.046$	$\sigma^2 = 0.015$	$\sigma^2 = 0.21$

RUN 13 (Continued)

$L_{21} = 6.88 \times 10^{-13}$	$L_{21} = 3.32 \times 10^{-13}$	$L_{21} = 2.73 \times 10^{-12}$
$L_{22} = 9.60 \times 10^{-11}$	$L_{22} = 1.93 \times 10^{-10}$	$L_{22} = 0.0$
$L_{211} = 0.0$	$L_{211} = 0.0$	$L_{211} = 0.0$
$L_{212} = 0.0$	$L_{212} = 0.0$	$L_{212} = 0.0$
$L_{222} = 8.90 \times 10^{-13}$	$L_{222} = 0.0$	$L_{222} = 0.0$
$\sigma^2 = 0.48$	$\sigma^2 = 0.69$	$\sigma^2 = 8.30$

$L_{21} = 0.0$

$L_{22} = 2.10 \times 10^{-10}$

$L_{211} = 0.0$

$L_{212} = 0.0$

$L_{222} = 0.0$

$\sigma^2 = 0.71$

Data from 145 to 310 seconds were used in the following Correlations

$L_{21} = 7.21 \times 10^{-13}$	$L_{21} = 8.58 \times 10^{-13}$	$L_{21} = 6.60 \times 10^{-13}$
$L_{22} = -1.75 \times 10^{-9}$	$L_{22} = -1.22 \times 10^{-9}$	$L_{22} = 1.26 \times 10^{-10}$
$L_{211} = 0.0$	$L_{211} = 0.0$	$L_{211} = 0.0$
$L_{212} = 2.67 \times 10^{-13}$	$L_{212} = 1.79 \times 10^{-13}$	$L_{212} = 0.0$
$L_{222} = -1.95 \times 10^{-12}$	$L_{222} = 0.0$	$L_{222} = 0.0$
$\sigma^2 = 0.017$	$\sigma^2 = 0.066$	$\sigma^2 = 0.23$

RUN 13 (Continued)

L_{21} =	1.72×10^{-12}	L_{21} =	0.0
L_{22} =	0.0	L_{22} =	1.73×10^{-10}
L_{211} =	0.0	L_{211} =	0.0
L_{212} =	0.0	L_{212} =	0.0
L_{222} =	0.0	L_{222} =	0.0
σ^2 =	1.93	σ^2 =	0.50

Data from 195 to 310 seconds were used in the following Correlations

L_{21} =	7.90×10^{-13}	L_{21} =	7.25×10^{-13}	L_{21} =	1.15×10^{-12}
L_{22} =	-5.49×10^{-9}	L_{22} =	1.00×10^{-10}	L_{22} =	0.0
L_{211} =	0.0	L_{211} =	0.0	L_{211} =	0.0
L_{212} =	7.99×10^{-13}	L_{212} =	0.0	L_{212} =	0.0
L_{222} =	-4.79×10^{-12}	L_{222} =	0.0	L_{222} =	0.0
σ^2 =	0.009	σ^2 =	0.041	σ^2 =	0.45

L_{21} =	0.0
L_{22} =	1.82×10^{-10}
L_{211} =	0.0
L_{212} =	0.0
L_{222} =	0.0
σ^2 =	0.47

RUN 16

Data from 70 to 500 seconds were used in the following Correlations

$L_{21} = -9.15 \times 10^{-12}$	$L_{21} = 1.12 \times 10^{-12}$	$L_{21} = -1.22 \times 10^{-11}$
$L_{22} = 4.08 \times 10^{-11}$	$L_{22} = 2.04 \times 10^{-10}$	$L_{22} = 2.08 \times 10^{-11}$
$L_{211} = 3.18 \times 10^{-15}$	$L_{211} = 0.0$	$L_{211} = 4.00 \times 10^{-15}$
$L_{212} = 0.0$	$L_{212} = -3.20 \times 10^{-14}$	$L_{212} = 0.0$
$L_{222} = 1.01 \times 10^{-13}$	$L_{222} = -1.11 \times 10^{-13}$	$L_{222} = 0.0$
$\sigma^2 = 0.15$	$\sigma^2 = 0.14$	$\sigma^2 = 0.75$

$L_{21} = 1.32 \times 10^{-12}$	$L_{21} = 1.39 \times 10^{-12}$	$L_{21} = 2.53 \times 10^{-13}$
$L_{22} = 1.67 \times 10^{-10}$	$L_{22} = 2.08 \times 10^{-11}$	$L_{22} = -6.20 \times 10^{-11}$
$L_{211} = 0.0$	$L_{211} = 0.0$	$L_{211} = 0.0$
$L_{212} = -2.39 \times 10^{-14}$	$L_{212} = 0.0$	$L_{212} = 0.0$
$L_{222} = 0.0$	$L_{222} = 2.26 \times 10^{-13}$	$L_{222} = 0.0$
$\sigma^2 = 0.37$	$\sigma^2 = 2.15$	$\sigma^2 = 7.61$

$L_{21} = 3.02 \times 10^{-12}$	$L_{21} = 0.0$
$L_{22} = 0.0$	$L_{22} = -6.65 \times 10^{-11}$
$L_{211} = 0.0$	$L_{211} = 0.0$
$L_{212} = 0.0$	$L_{212} = 0.0$
$L_{222} = 0.0$	$L_{222} = 0.0$
$\sigma^2 = 43.1$	$\sigma^2 = 7.51$

RUN 16 (Continued)

Data from 170 to 500 seconds were used in the following Correlations

$L_{21} = 1.11 \times 10^{-12}$	$L_{21} = 1.10 \times 10^{-12}$	$L_{21} = 7.33 \times 10^{-13}$
$L_{22} = 9.85 \times 10^{-11}$	$L_{22} = -7.10 \times 10^{-12}$	$L_{22} = -3.88 \times 10^{-11}$
$L_{211} = 0.0$	$L_{211} = 0.0$	$L_{211} = 0.0$
$L_{212} = -1.60 \times 10^{-14}$	$L_{212} = 0.0$	$L_{212} = 0.0$
$L_{222} = 0.0$	$L_{222} = 1.13 \times 10^{-13}$	$L_{222} = 0.0$
$\sigma^2 = 0.092$	$\sigma^2 = 0.099$	$\sigma^2 = 0.56$

$L_{21} = 2.02 \times 10^{-12}$	$L_{21} = 0.0$
$L_{22} = 0.0$	$L_{22} = -5.49 \times 10^{-11}$
$L_{211} = 0.0$	$L_{211} = 0.0$
$L_{212} = 0.0$	$L_{212} = 0.0$
$L_{222} = 0.0$	$L_{222} = 0.0$
$\sigma^2 = 9.25$	$\sigma^2 = 0.0$

Data from 270 to 500 seconds were used in the following Correlations

$L_{21} = 9.78 \times 10^{-13}$	$L_{21} = 1.47 \times 10^{-12}$	$L_{21} = 0.0$
$L_{22} = -2.48 \times 10^{-11}$	$L_{22} = 0.0$	$L_{22} = -6.04 \times 10^{-11}$
$L_{211} = 0.0$	$L_{211} = 0.0$	$L_{211} = 0.0$
$L_{212} = 0.0$	$L_{212} = 0.0$	$L_{212} = 0.0$
$L_{222} = 0.0$	$L_{222} = 0.0$	$L_{222} = 0.0$
$\sigma^2 = 0.058$	$\sigma^2 = 1.22$	$\sigma^2 = 2.81$

RUN 16 (Continued)

Data from 370 to 500 seconds were used in the following Correlations

$L_{21} = 1.07 \times 10^{-12}$	$L_{21} = 9.39 \times 10^{-13}$	$L_{21} = 1.23 \times 10^{-12}$
$L_{22} = 3.82 \times 10^{-10}$	$L_{22} = -2.93 \times 10^{-11}$	$L_{22} = 0.0$
$L_{211} = 0.0$	$L_{211} = 0.0$	$L_{211} = 0.0$
$L_{212} = -5.81 \times 10^{-14}$	$L_{212} = 0.0$	$L_{212} = 0.0$
$L_{222} = 0.0$	$L_{222} = 0.0$	$L_{222} = 0.0$
$\sigma^2 = 0.018$	$\sigma^2 = 0.060$	$\sigma^2 = 0.41$

$L_{21} = 0.0$

$L_{22} = -9.89 \times 10^{-11}$

$L_{211} = 0.0$

$L_{212} = 0.0$

$L_{222} = 0.0$

$\sigma^2 = 1.77$

RUN 17

Data from 70 to 600 seconds were used in the following Correlations

$L_{21} = -7.68 \times 10^{-12}$	$L_{21} = 2.88 \times 10^{-13}$	$L_{21} = -8.79 \times 10^{-12}$
$L_{22} = 4.94 \times 10^{-11}$	$L_{22} = 6.22 \times 10^{-10}$	$L_{22} = -2.63 \times 10^{-11}$
$L_{211} = 2.48 \times 10^{-15}$	$L_{211} = 0.0$	$L_{211} = 2.70 \times 10^{-15}$
$L_{212} = 0.0$	$L_{212} = -1.05 \times 10^{-13}$	$L_{212} = 0.0$
$L_{222} = 9.82 \times 10^{-13}$	$L_{222} = -1.31 \times 10^{-12}$	$L_{222} = 0.0$
$\sigma^2 = 0.023$	$\sigma^2 = 0.026$	$\sigma^2 = 0.083$

$L_{21} = 5.77 \times 10^{-13}$	$L_{21} = 8.27 \times 10^{-13}$	$L_{21} = -5.08 \times 10^{-13}$
$L_{22} = 5.85 \times 10^{-10}$	$L_{22} = 1.22 \times 10^{-10}$	$L_{22} = -2.18 \times 10^{-10}$
$L_{211} = 0.0$	$L_{211} = 0.0$	$L_{211} = 0.0$
$L_{212} = -8.73 \times 10^{-14}$	$L_{212} = 0.0$	$L_{212} = 0.0$
$L_{222} = 0.0$	$L_{222} = 3.78 \times 10^{-12}$	$L_{222} = 0.0$
$\sigma^2 = 0.067$	$\sigma^2 = 0.62$	$\sigma^2 = 1.89$

$L_{21} = 2.34 \times 10^{-12}$	$L_{21} = 0.0$
$L_{22} = 0.0$	$L_{22} = -1.84 \times 10^{-10}$
$L_{211} = 0.0$	$L_{211} = 0.0$
$L_{212} = 0.0$	$L_{212} = 0.0$
$L_{222} = 0.0$	$L_{222} = 0.0$
$\sigma^2 = 7.71$	$\sigma^2 = 2.20$

RUN 17 (Continued)

Data from 170 to 600 seconds were used in the following Correlations

$L_{21} = -8.54 \times 10^{-12}$	$L_{21} = 4.43 \times 10^{-13}$	$L_{21} = 3.90 \times 10^{-13}$
$L_{22} = 4.05 \times 10^{-11}$	$L_{22} = 3.43 \times 10^{-10}$	$L_{22} = 4.51 \times 10^{-10}$
$L_{211} = 2.72 \times 10^{-15}$	$L_{211} = 0.0$	$L_{211} = 0.0$
$L_{212} = 0.0$	$L_{212} = -5.20 \times 10^{-14}$	$L_{212} = -7.19 \times 10^{-14}$
$L_{222} = 6.94 \times 10^{-13}$	$L_{222} = 7.40 \times 10^{-13}$	$L_{222} = 0.0$
$\sigma^2 = 0.009$	$\sigma^2 = 0.014$	$\sigma^2 = 0.016$

$L_{21} = 5.50 \times 10^{-13}$	$L_{21} = -3.53 \times 10^{-13}$	$L_{21} = 1.66 \times 10^{-12}$
$L_{22} = 5.13 \times 10^{-11}$	$L_{22} = -1.69 \times 10^{-10}$	$L_{22} = 0.0$
$L_{211} = 0.0$	$L_{211} = 0.0$	$L_{211} = 0.0$
$L_{212} = 0.0$	$L_{212} = 0.0$	$L_{212} = 0.0$
$L_{222} = 2.58 \times 10^{-12}$	$L_{222} = 0.0$	$L_{222} = 0.0$
$\sigma^2 = 0.015$	$\sigma^2 = 0.34$	$\sigma^2 = 3.21$

$L_{21} = 0.0$

$L_{22} = -1.44 \times 10^{-10}$

$L_{211} = 0.0$

$L_{212} = 0.0$

$L_{222} = 0.0$

$\sigma^2 = 0.42$

RUN 17 (Continued)

Data from 270 to 600 seconds were used in the following Correlations

$L_{21} = 4.44 \times 10^{-13}$	$L_{21} = 5.59 \times 10^{-13}$	$L_{21} = 8.79 \times 10^{-15}$
$L_{22} = 5.76 \times 10^{-10}$	$L_{22} = 5.62 \times 10^{-11}$	$L_{22} = -1.19 \times 10^{-10}$
$L_{211} = 0.0$	$L_{211} = 0.0$	$L_{211} = 0.0$
$L_{212} = -8.83 \times 10^{-14}$	$L_{212} = 0.0$	$L_{212} = 0.0$
$L_{222} = 0.0$	$L_{222} = 2.68 \times 10^{-12}$	$L_{222} = 0.0$
$\sigma^2 = 0.013$	$\sigma^2 = 0.012$	$\sigma^2 = 0.15$

$L_{21} = 1.15 \times 10^{-12}$	$L_{21} = 0.0$
$L_{22} = 0.0$	$L_{22} = -1.19 \times 10^{-10}$
$L_{211} = 0.0$	$L_{211} = 0.0$
$L_{212} = 0.0$	$L_{212} = 0.0$
$L_{222} = 0.0$	$L_{222} = 0.0$
$\sigma^2 = 1.12$	$\sigma^2 = 0.15$

Data from 370 to 600 seconds were used in the following Correlations

$L_{21} = 4.86 \times 10^{-13}$	$L_{21} = 5.19 \times 10^{-13}$	$L_{21} = 5.40 \times 10^{-13}$
$L_{22} = 1.32 \times 10^{-9}$	$L_{22} = 8.47 \times 10^{-10}$	$L_{22} = 4.34 \times 10^{-11}$
$L_{211} = 0.0$	$L_{211} = 0.0$	$L_{211} = 0.0$
$L_{212} = -1.99 \times 10^{-13}$	$L_{212} = -1.25 \times 10^{-13}$	$L_{212} = 0.0$
$L_{222} = -1.57 \times 10^{-12}$	$L_{222} = 0.0$	$L_{222} = 2.30 \times 10^{-12}$
$\sigma^2 = 0.0011$	$\sigma^2 = 0.0023$	$\sigma^2 = 0.0077$

RUN 17 (Continued)

$L_{21} = 2.70 \times 10^{-13}$	$L_{21} = 7.81 \times 10^{-13}$	$L_{21} = 0.0$
$L_{22} = -6.98 \times 10^{-11}$	$L_{22} = 0.0$	$L_{22} = -9.88 \times 10^{-11}$
$L_{211} = 0.0$	$L_{211} = 0.0$	$L_{211} = 0.0$
$L_{212} = 0.0$	$L_{212} = 0.0$	$L_{212} = 0.0$
$L_{222} = 0.0$	$L_{222} = 0.0$	$L_{222} = 0.0$
$\sigma^2 = 0.050$	$\sigma^2 = 0.27$	$\sigma^2 = 0.088$

Data from 470 to 600 seconds were used in the following Correlations

$L_{21} = 4.35 \times 10^{-13}$	$L_{21} = 5.58 \times 10^{-13}$	$L_{21} = 0.0$
$L_{22} = -2.81 \times 10^{-11}$	$L_{22} = 0.0$	$L_{22} = -1.04 \times 10^{-10}$
$L_{211} = 0.0$	$L_{211} = 0.0$	$L_{211} = 0.0$
$L_{212} = 0.0$	$L_{212} = 0.0$	$L_{212} = 0.0$
$L_{222} = 0.0$	$L_{222} = 0.0$	$L_{222} = 0.0$
$\sigma^2 = 0.0014$	$\sigma^2 = 0.015$	$\sigma^2 = 0.12$

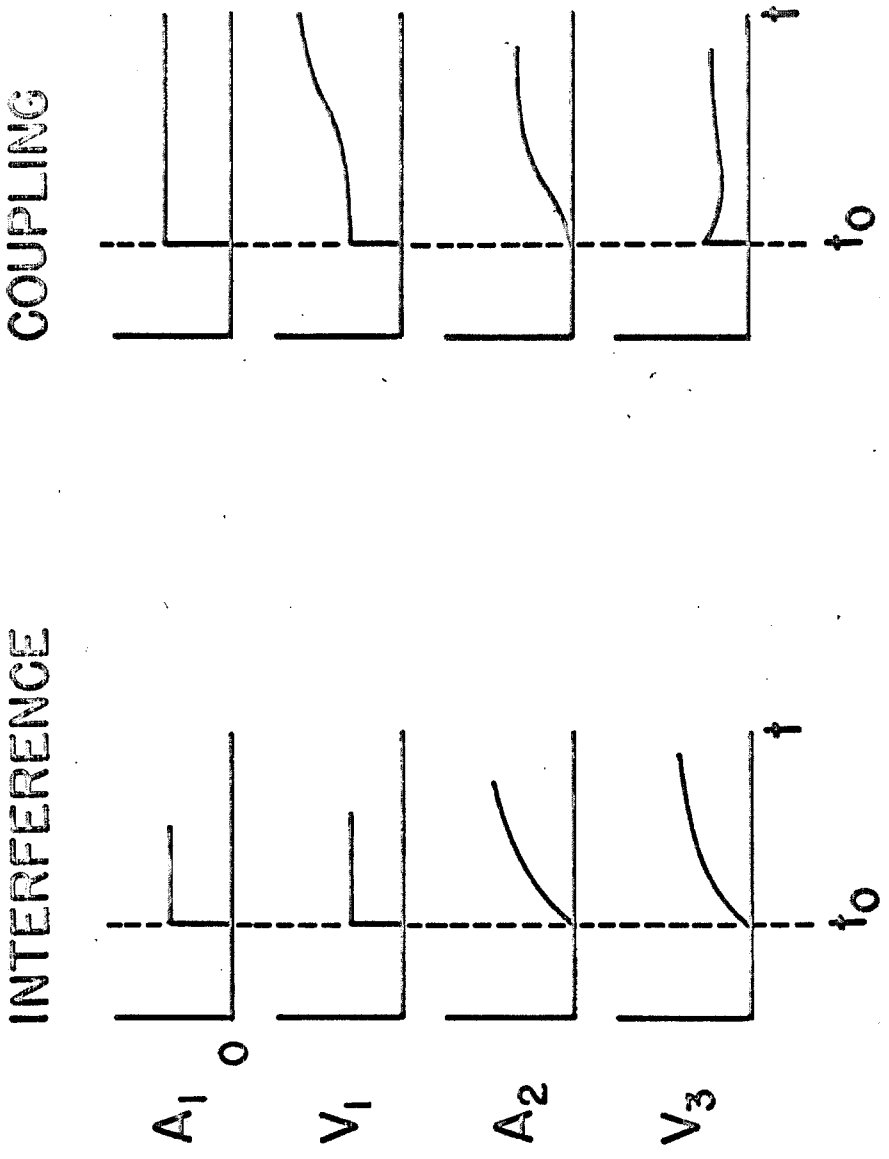

Figure 1. Comparison Between Interference and Coupling Phenomena.

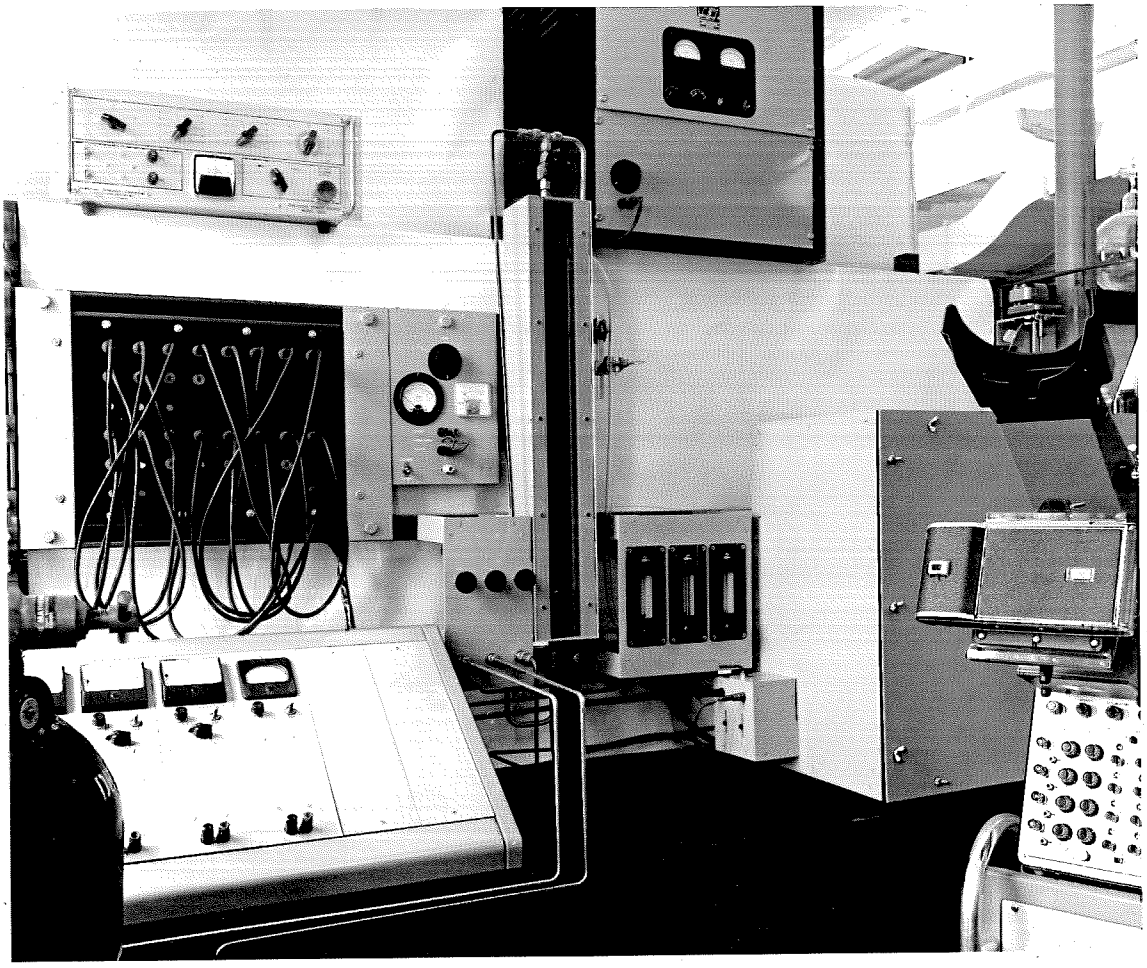

Figure 2. Primary Equipment.

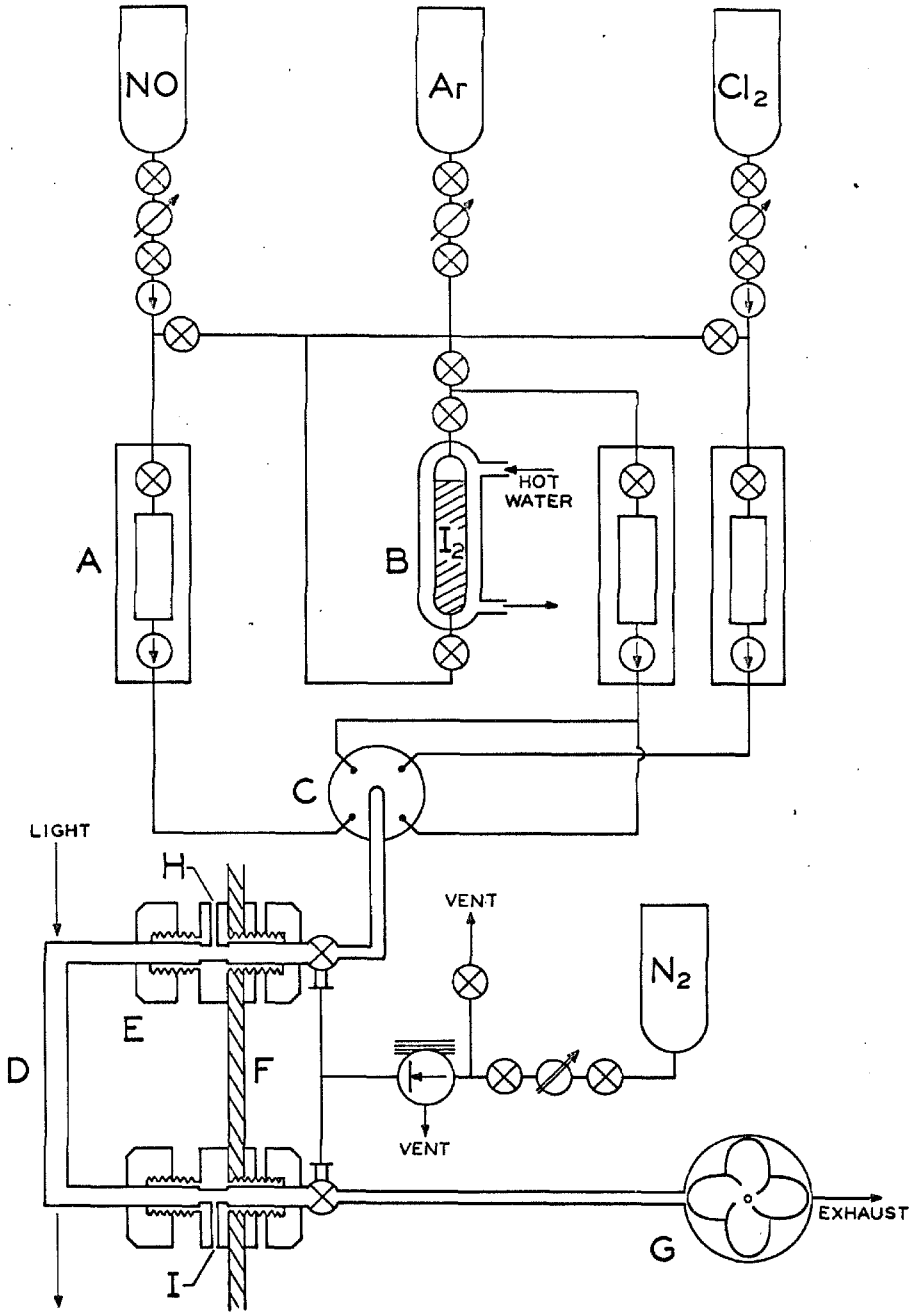

A ROTAMETER
B IODINE COLUMN
C MIXING CHAMBER
D REACTION CELL
E BULKHEAD FITTING
F ENCLOSURE WALL
G BLOWER
H TEMPERATURE PROBE
I PRESSURE PROBE
SOLENOID VALVE
VALVE
CHECK VALVE
LOW PRES. REGULATOR
HIGH PRES. REGULATOR
CONTROL VALVE

Figure 3. Flow System.

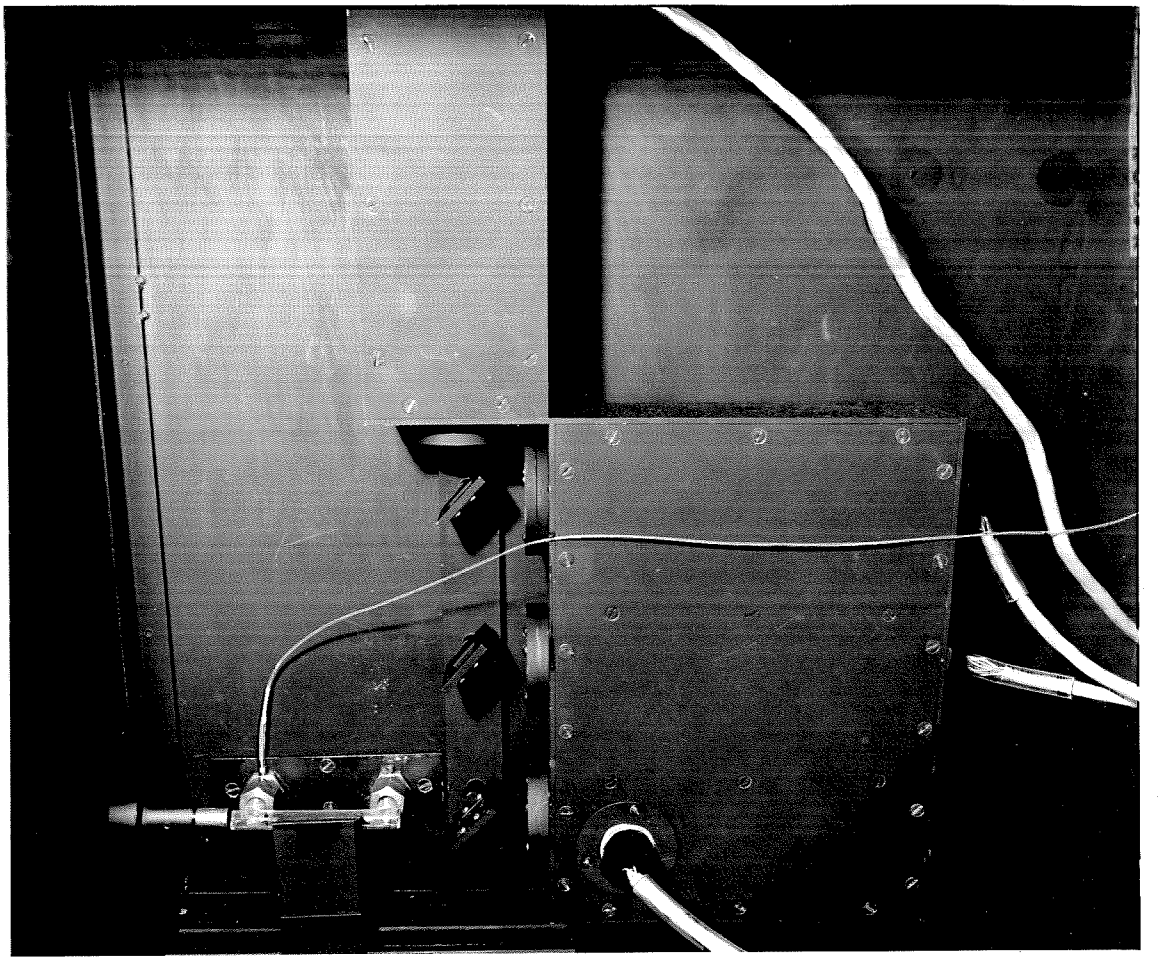

Figure 4. Interior of the Optical System Enclosure.

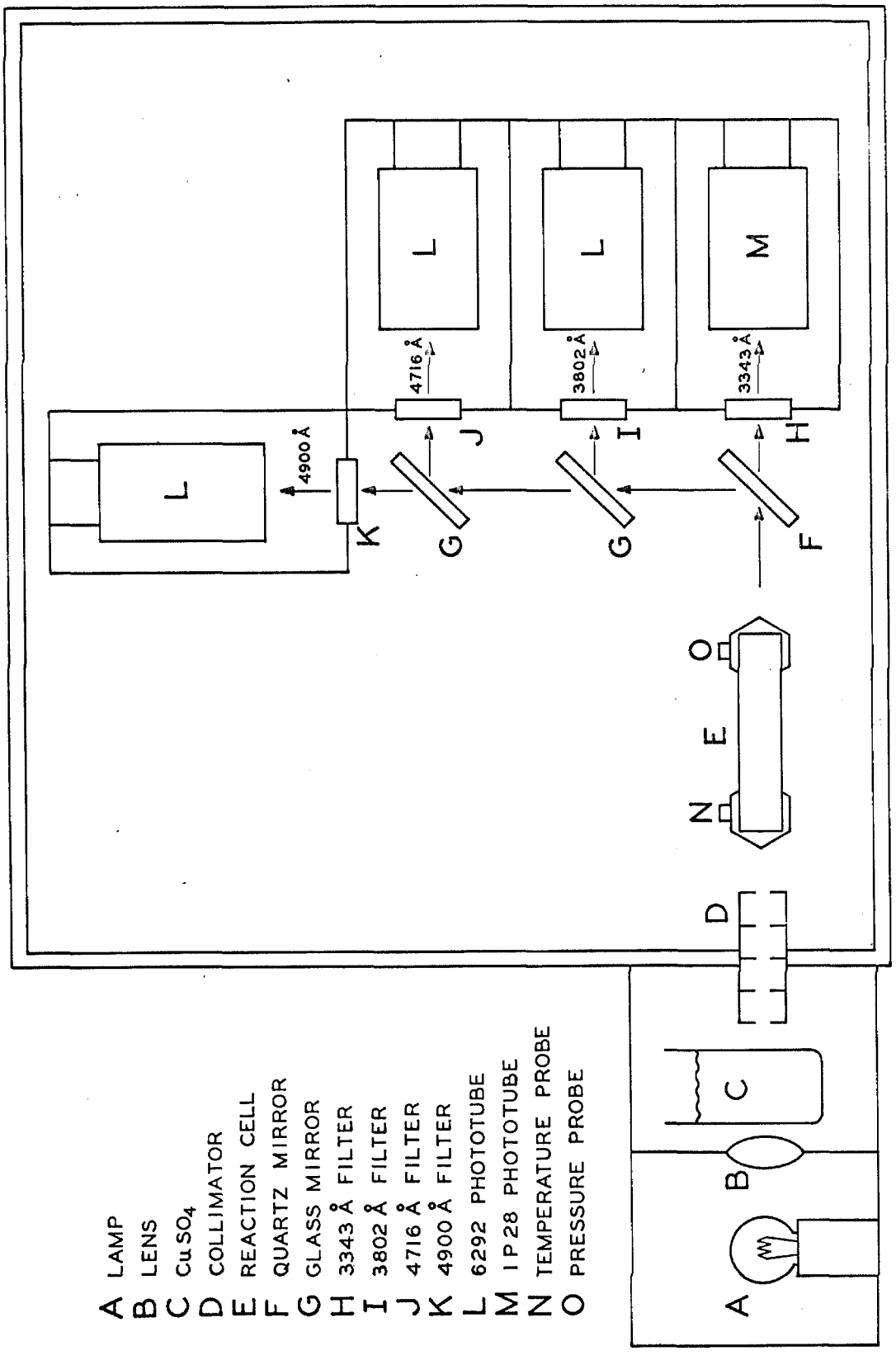

Figure 5. Optical System.

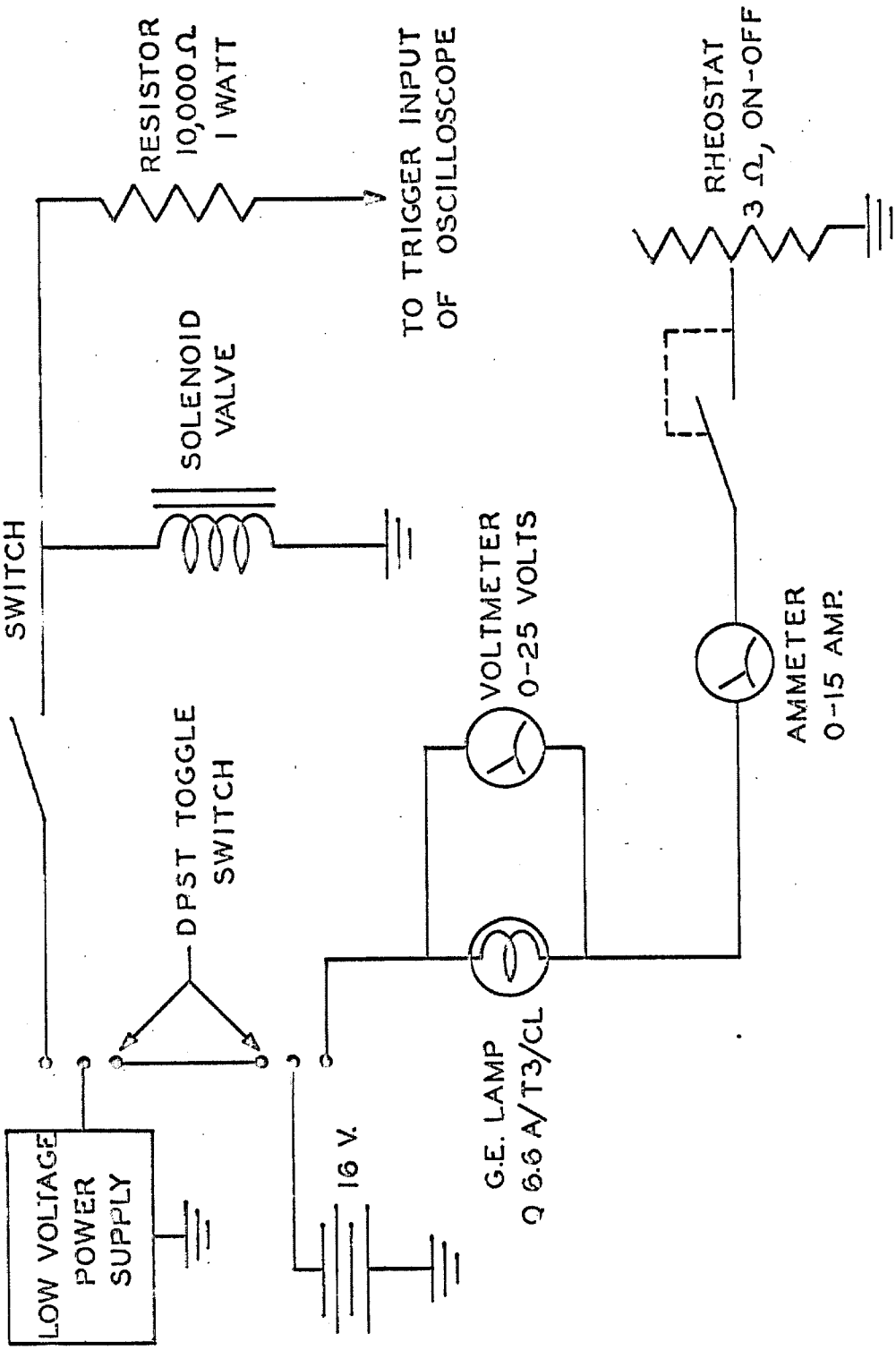

Figure 6. Light Source, Solenoid Valve, and Oscilloscope Trigger Circuits.

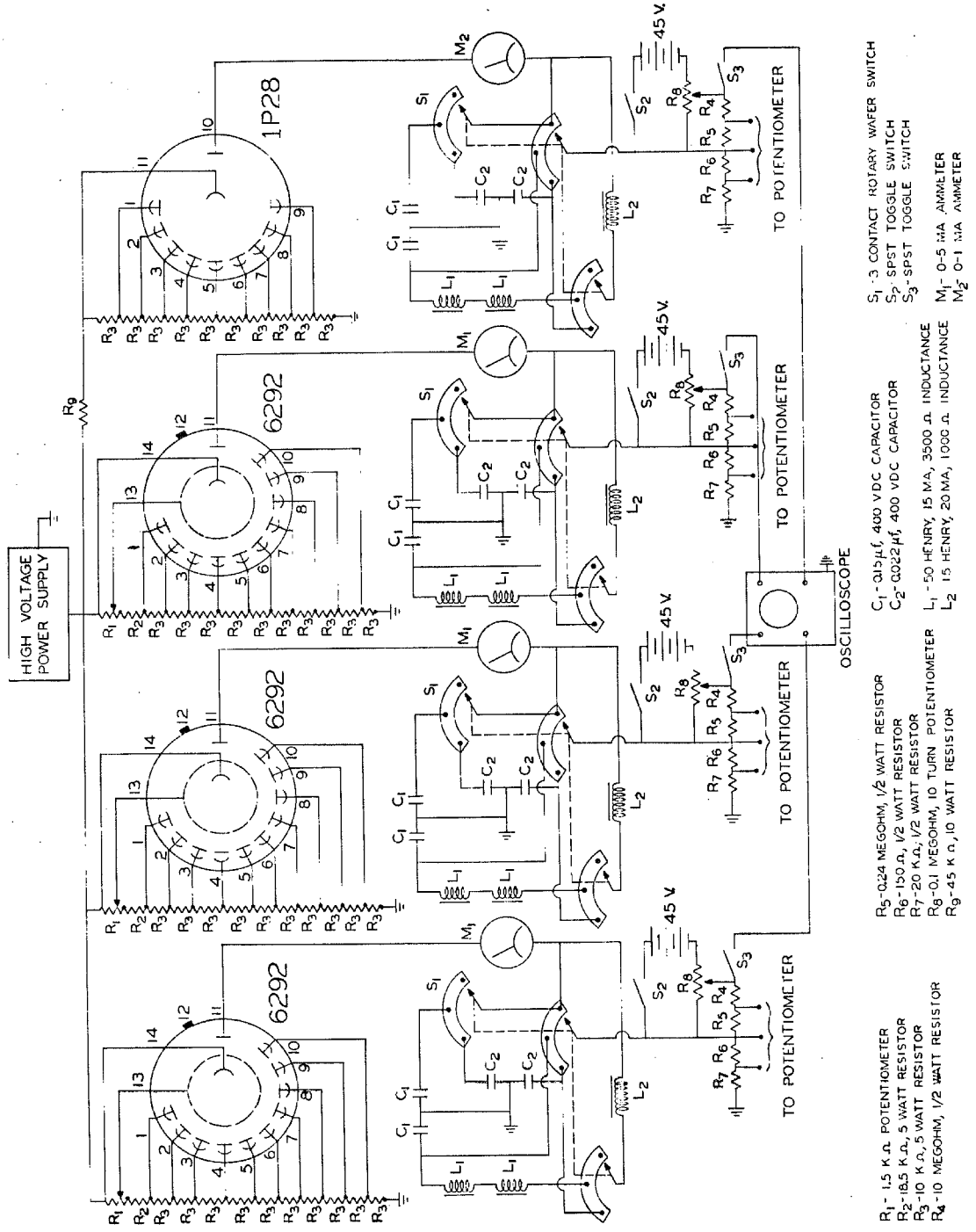

Figure 7. Main Electrical System.

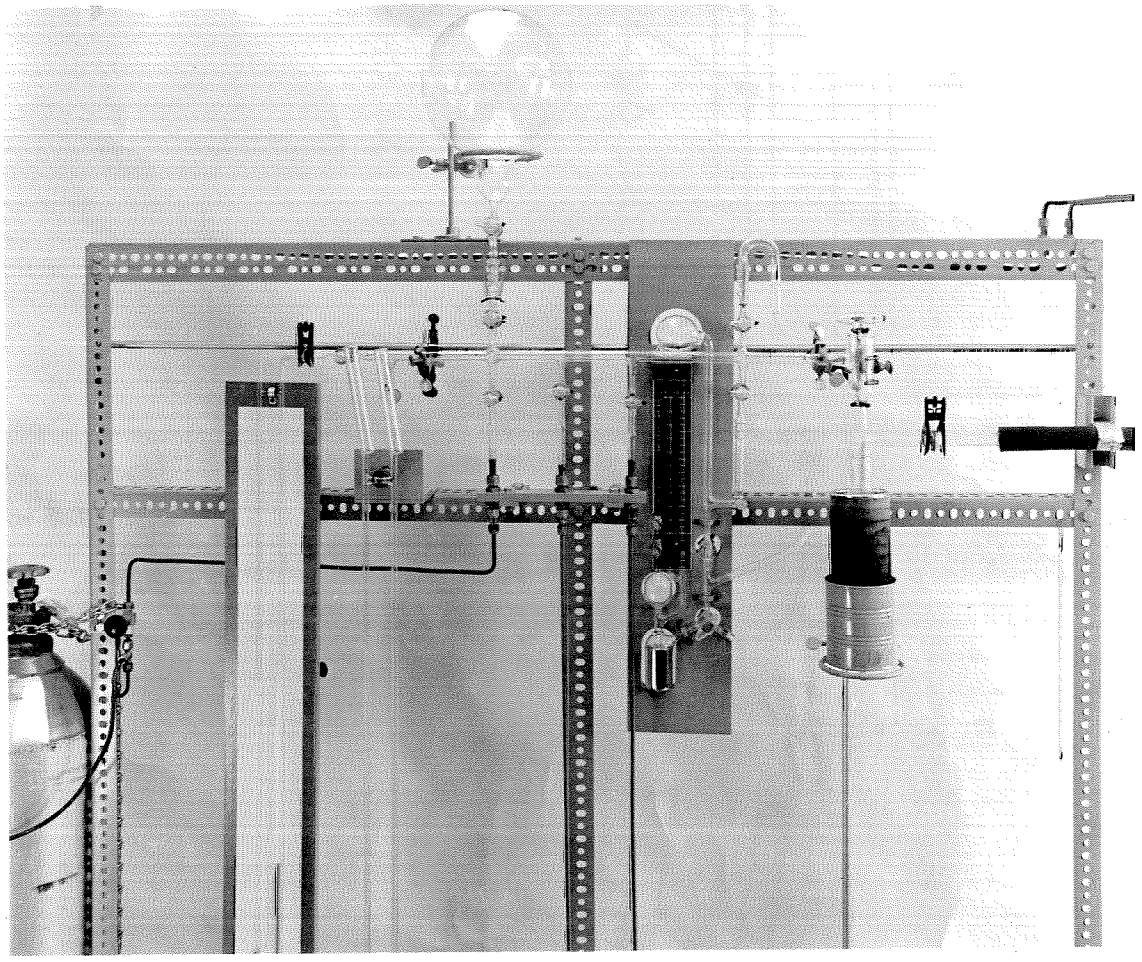

Figure 8. Vacuum System.

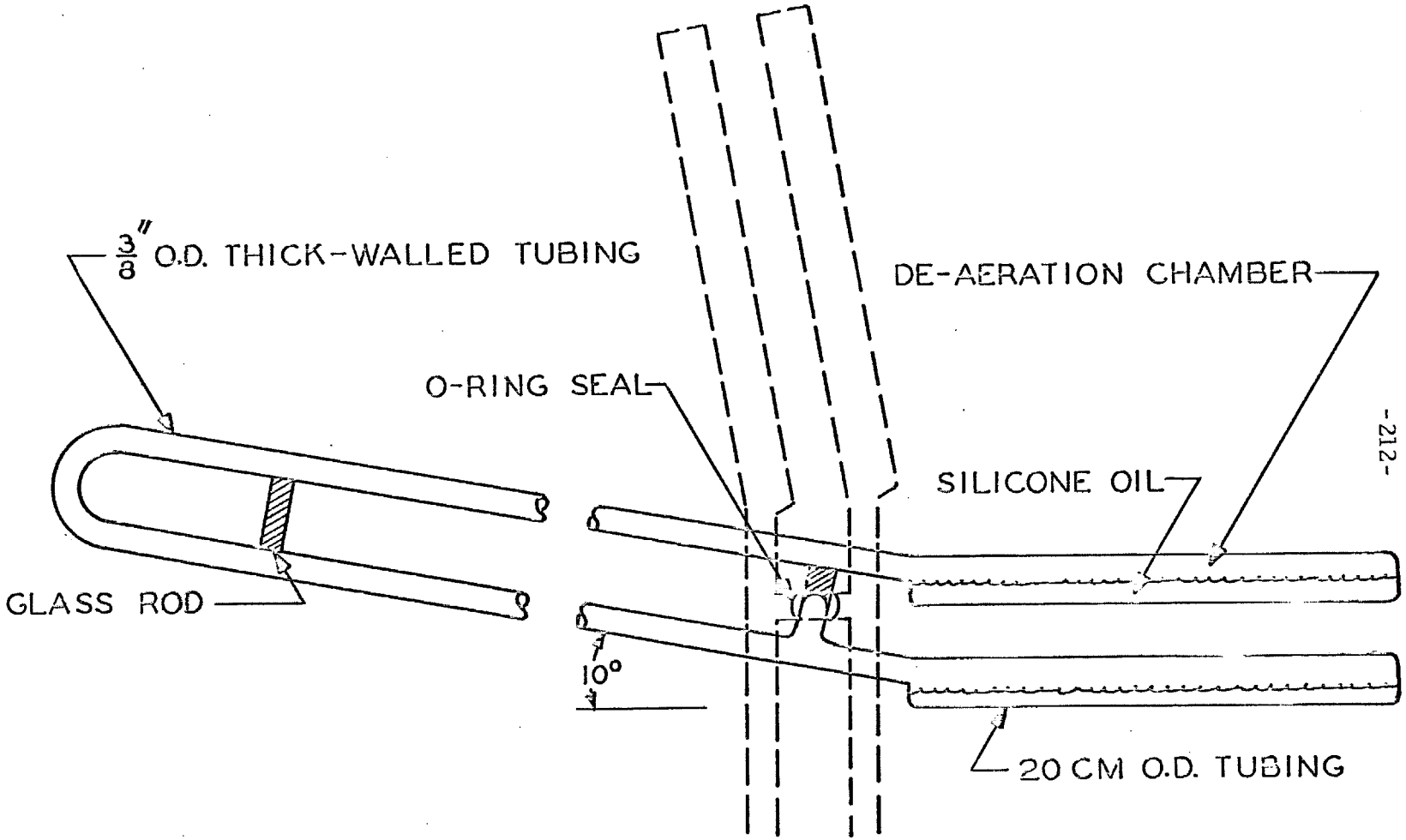

Figure 9. Silicone Oil Manometer. Dotted Lines Represent Manometer in its Measuring Position. Solid Lines Represent Manometer in "De-Aeration' Position.

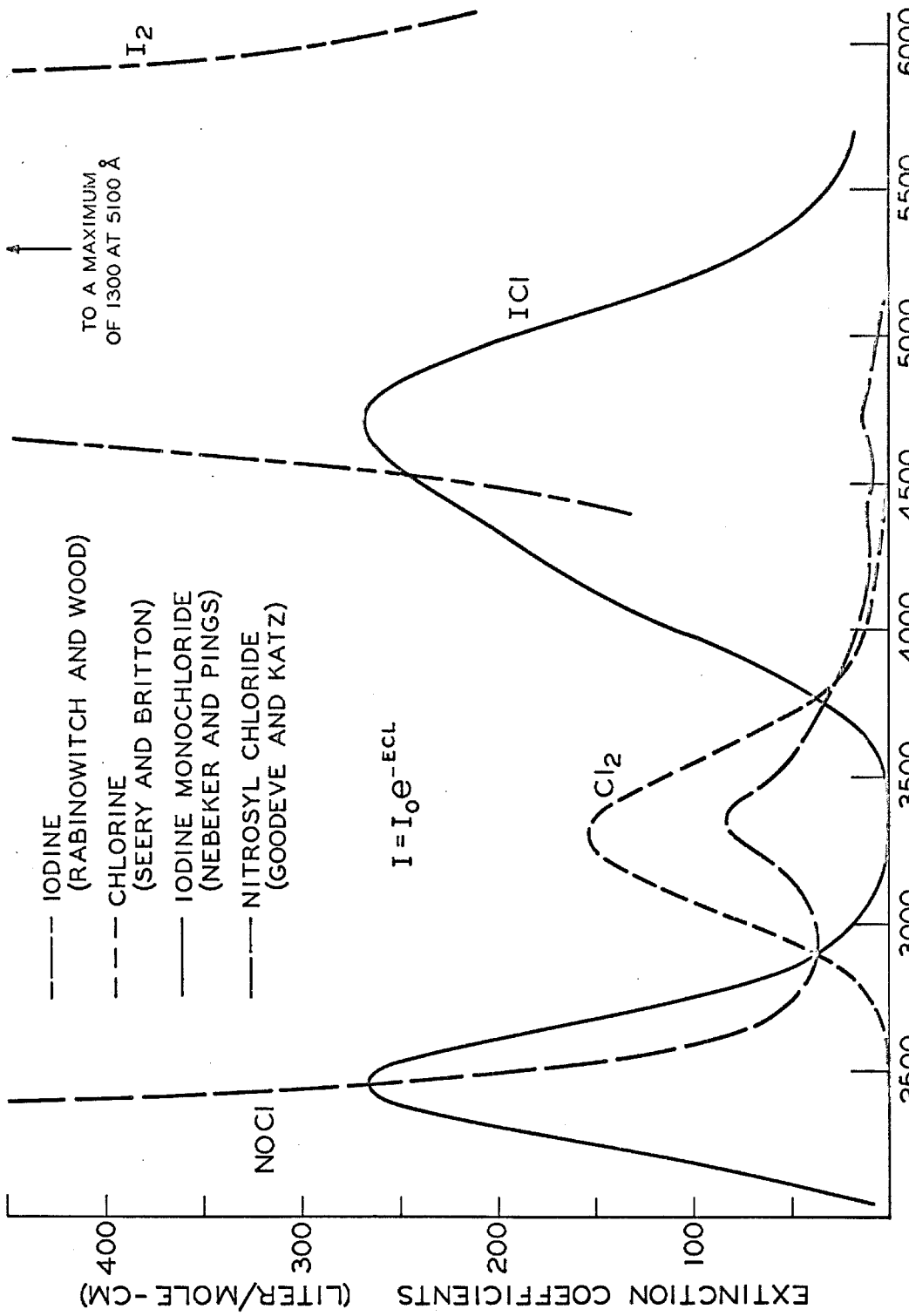

Figure 10. Wavelength Dependence of the Extinction Coefficients.

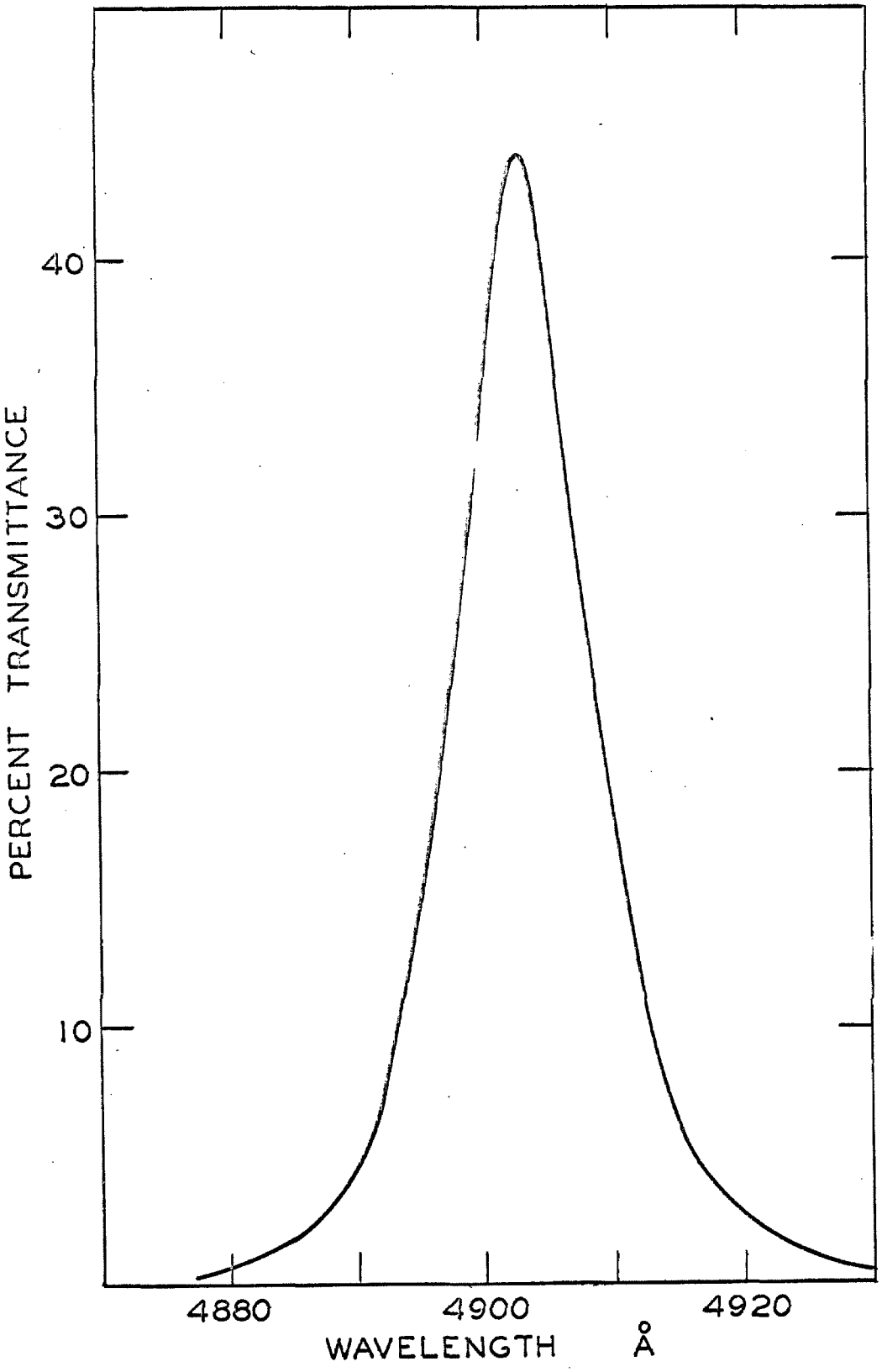

Figure 11. Transmittance of 4900 Å Interference Filter.

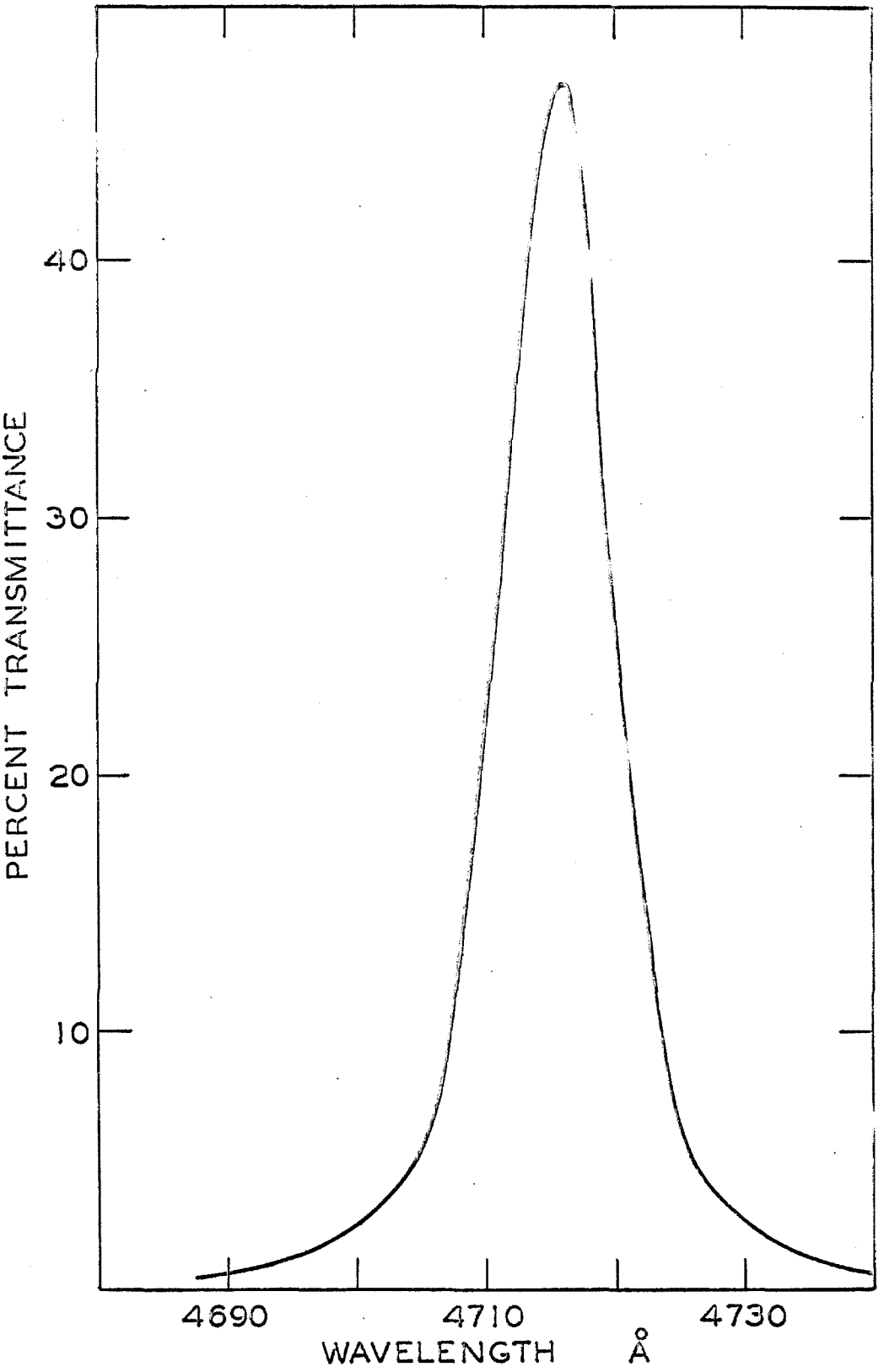

Figure 12. Transmittance of 4716 Å Interference Filter.

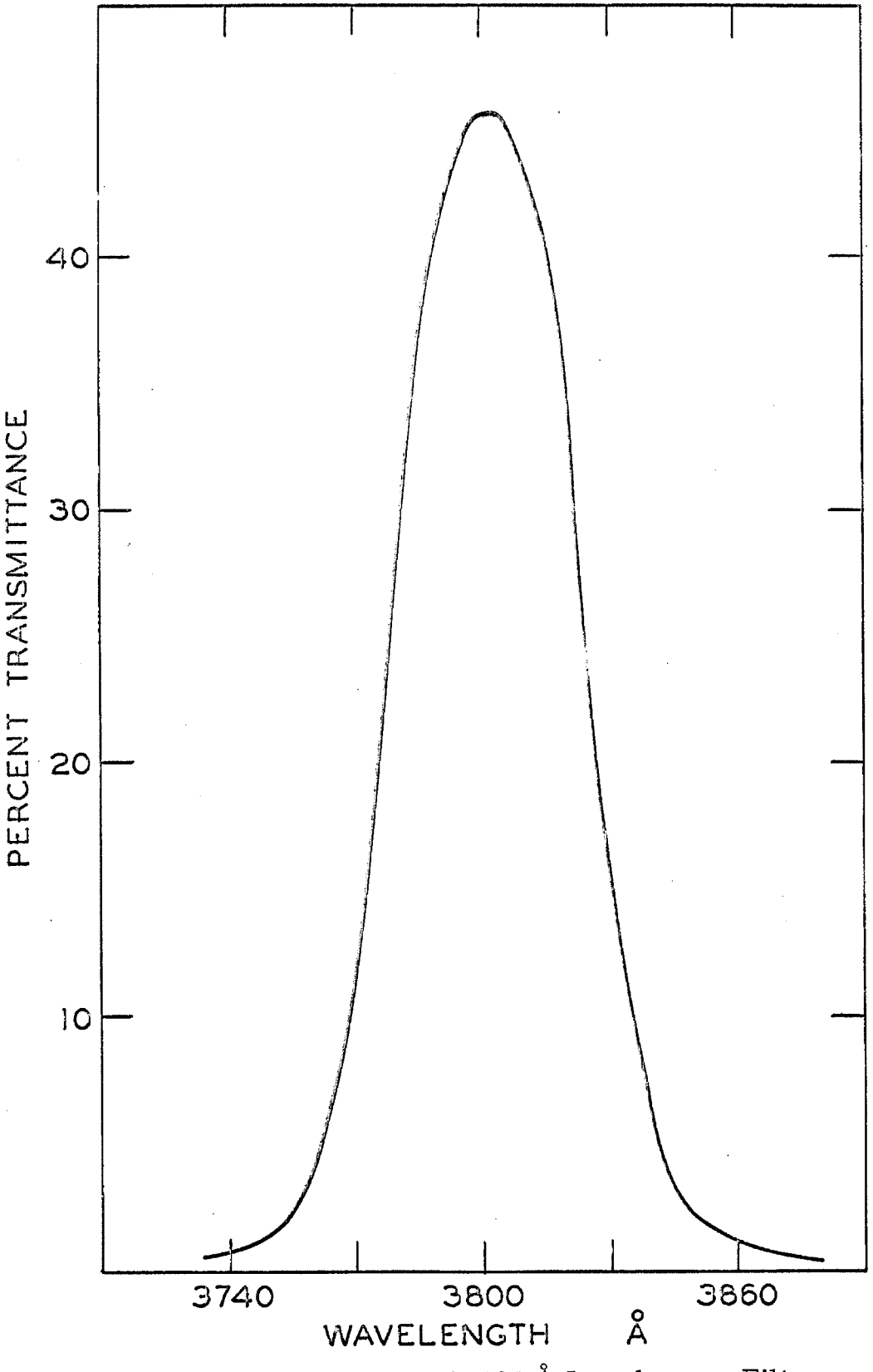

Figure 13. Transmittance of 3802 Å Interference Filter.

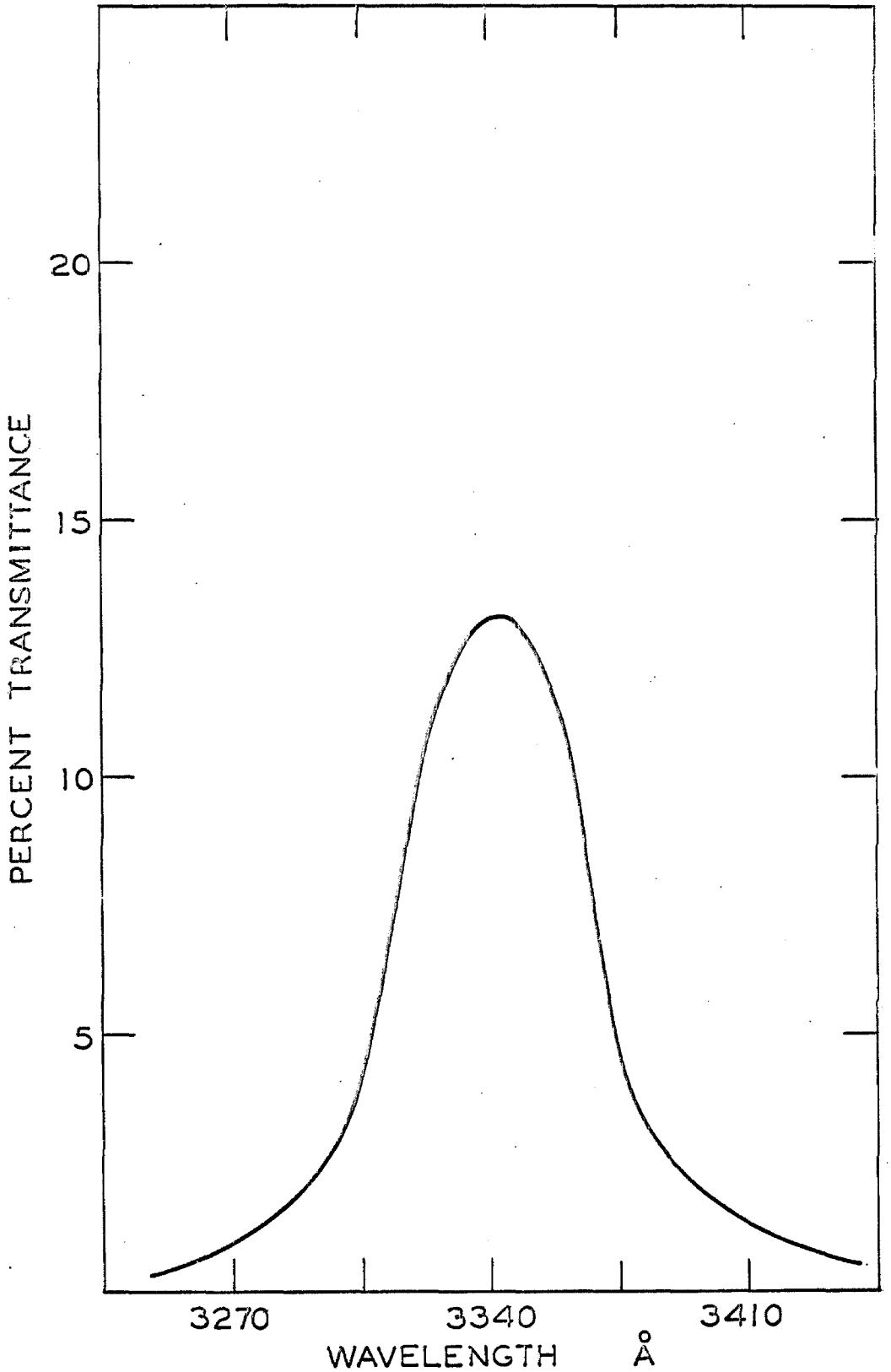

Figure 14. Transmittance of 3343 Å Interference Filter.

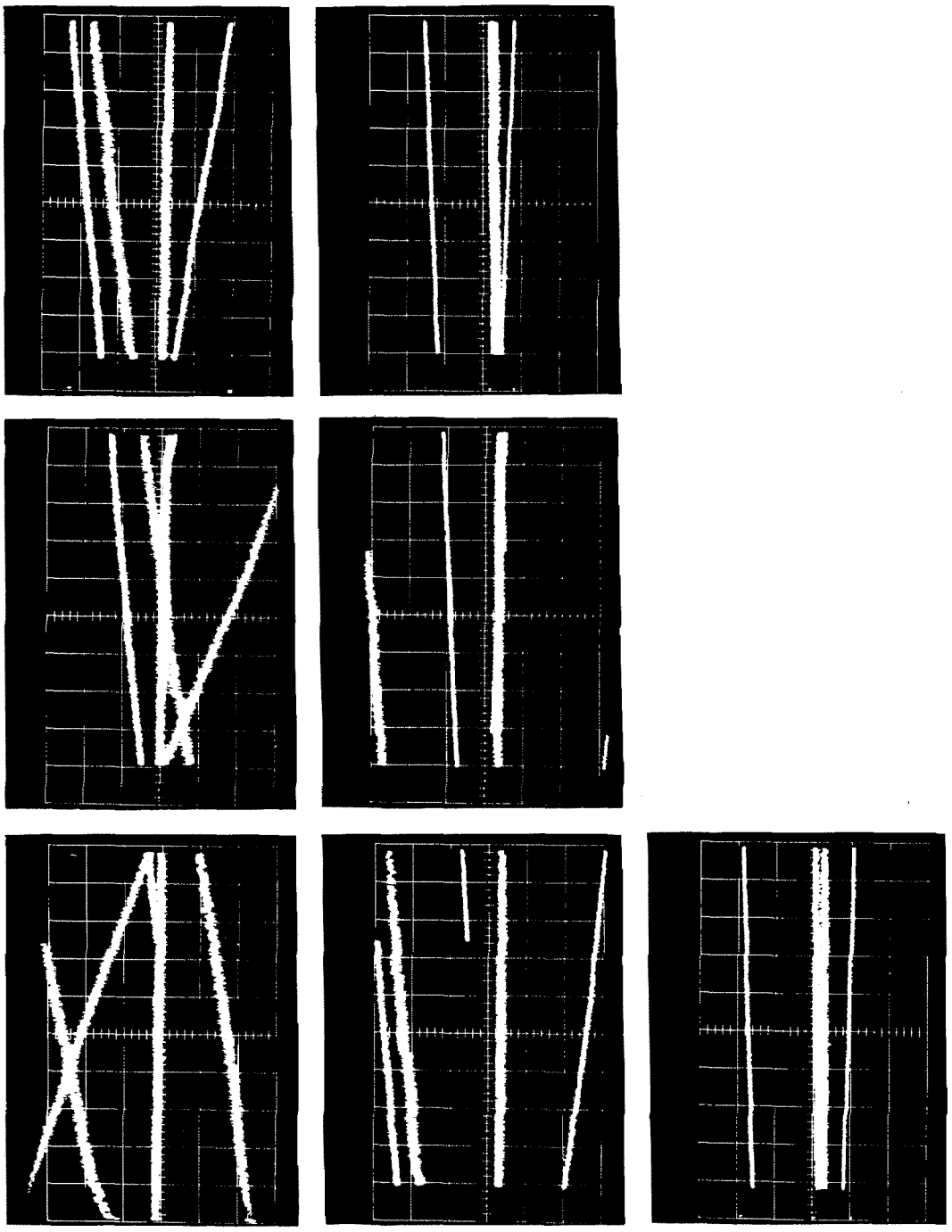

Figure 15. Photographs of Oscilloscope Traces. The Initial 350 Seconds of Run 17.

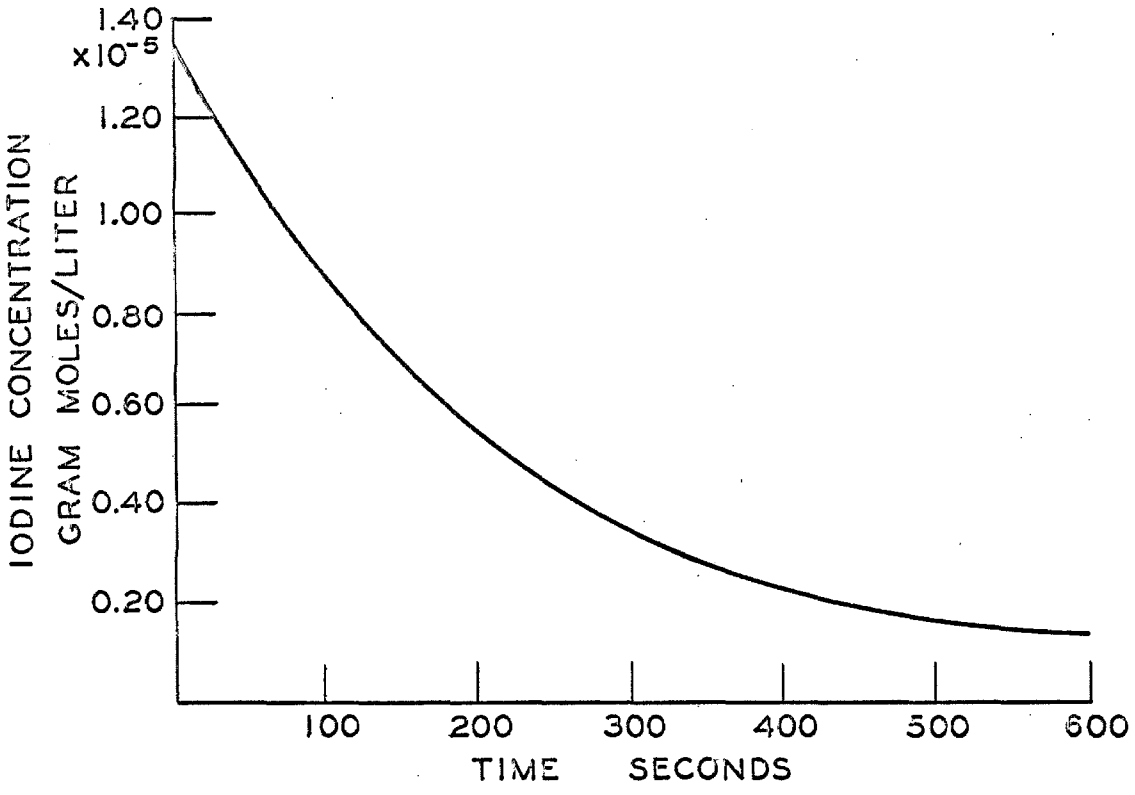

Figure 16. Iodine Concentration During Run 17.

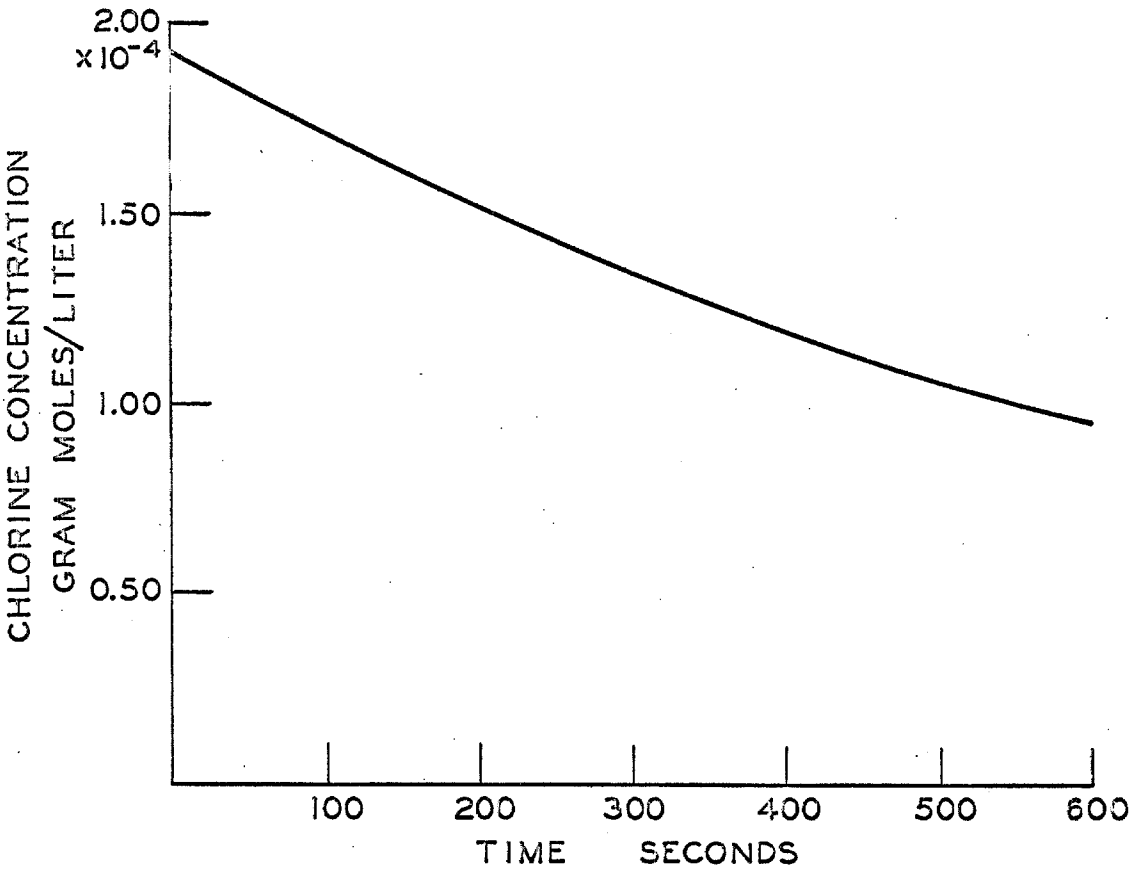

Figure 17. Chlorine Concentration During Run 17.

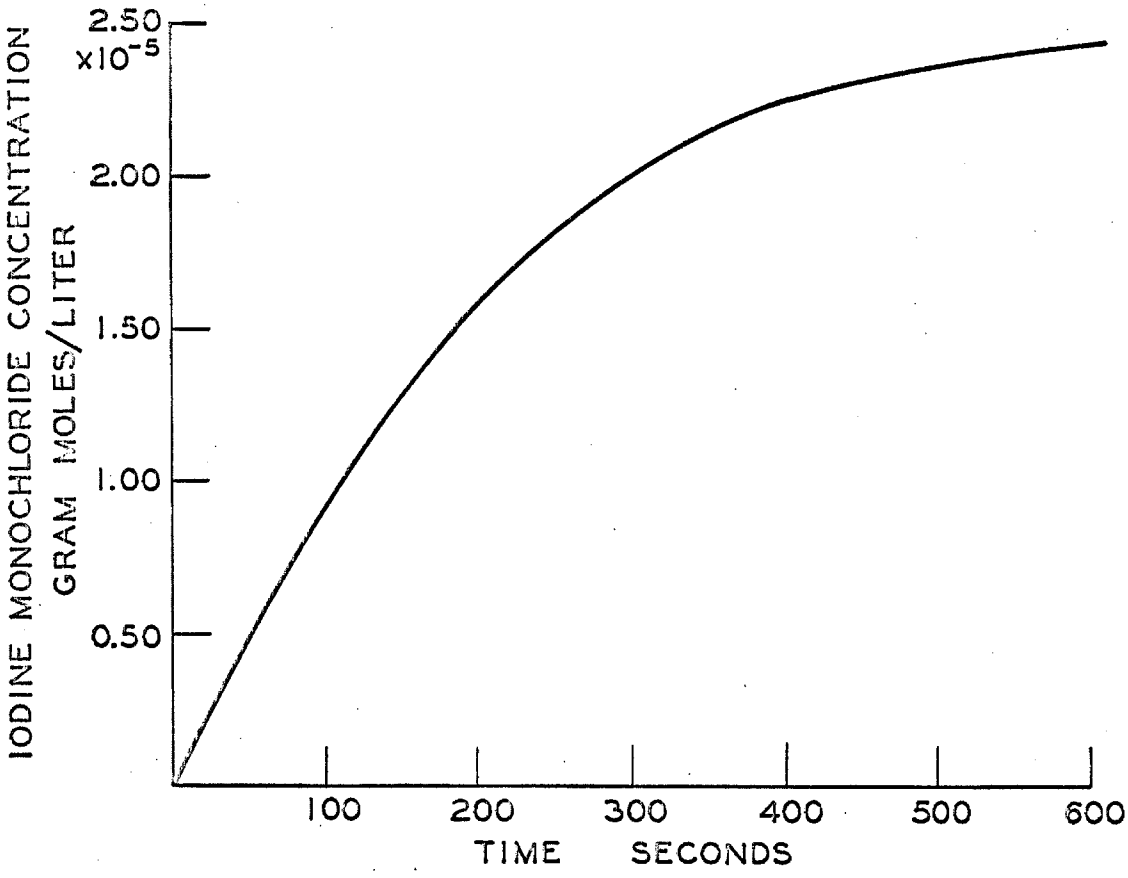

Figure 18. Iodine Monochloride Concentration During Run 17.

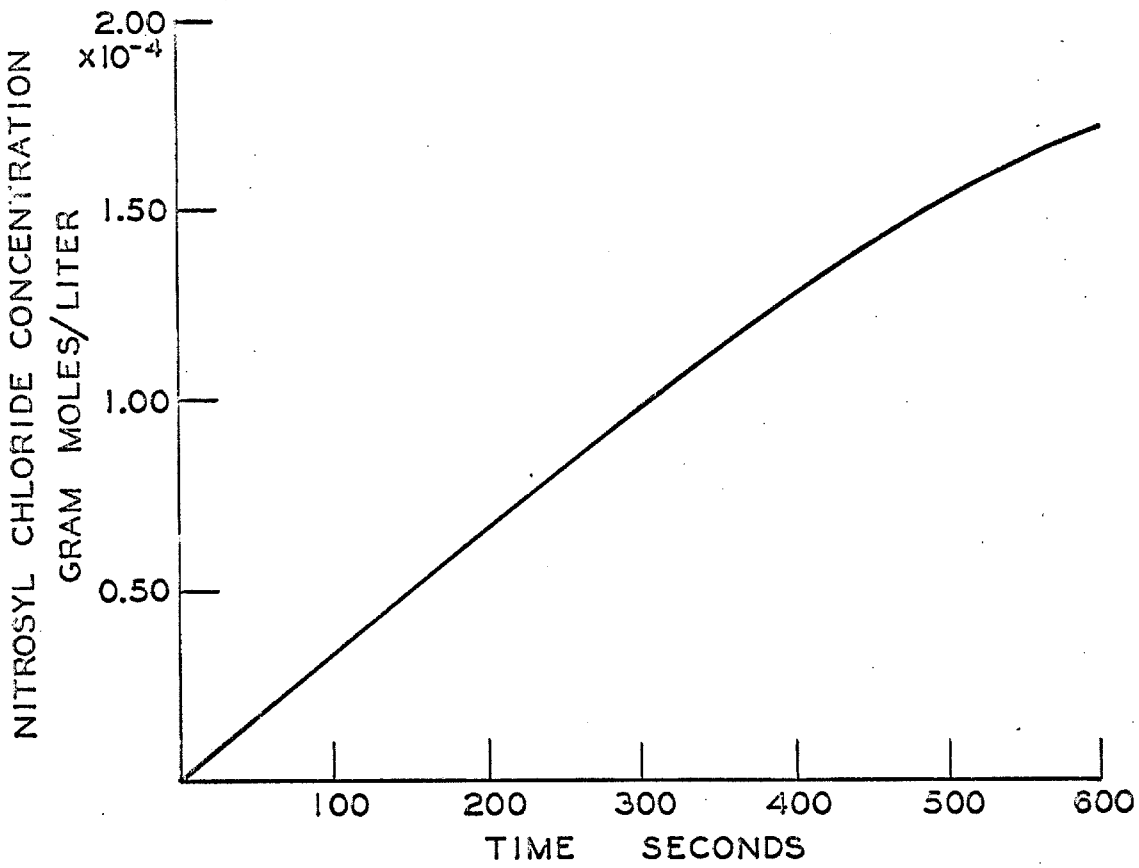

Figure 19. Nitrosyl Chloride Concentration During Run 17.

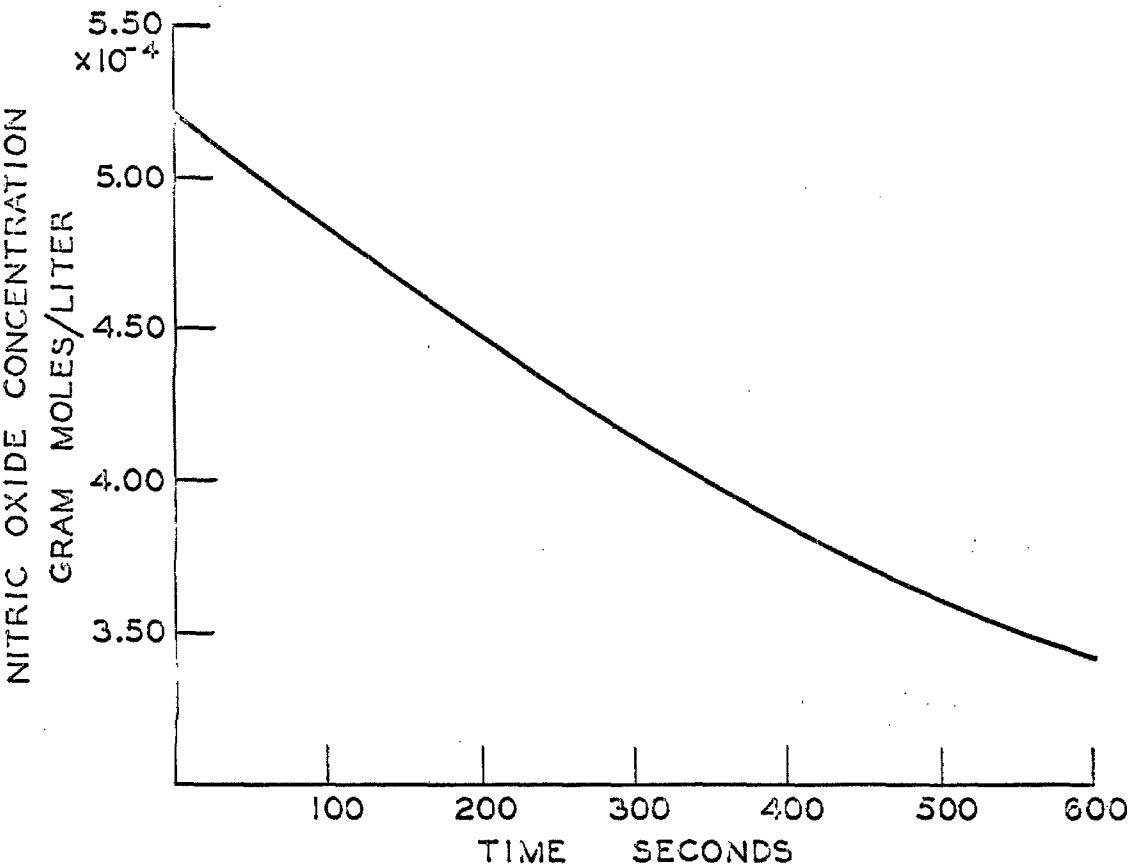

Figure 20. Nitric Oxide Concentration During Run 17.

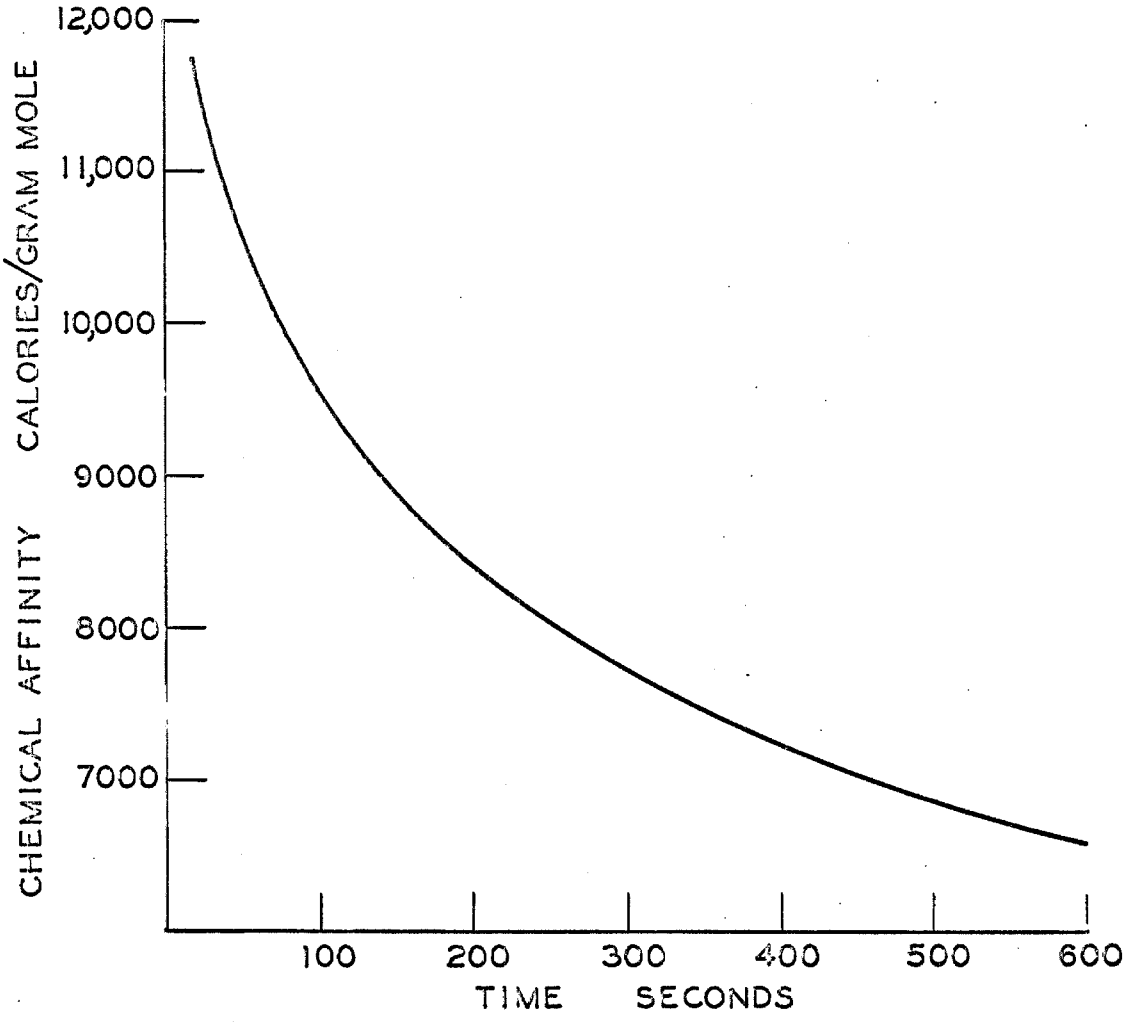

Figure 21. Chemical Affinity of Reaction 1 During Run 17.

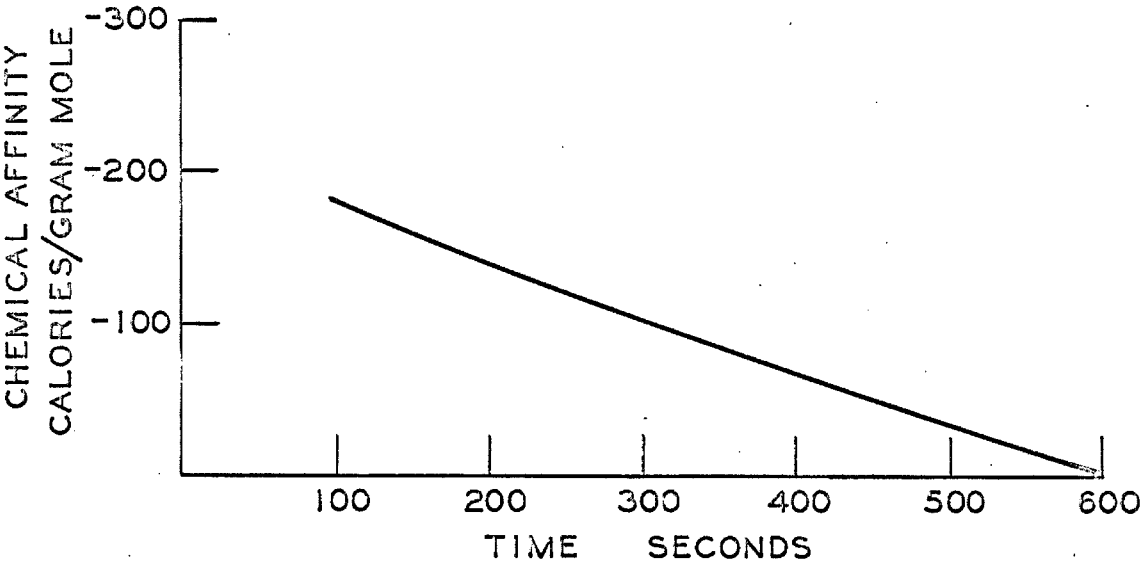

Figure 22. Chemical Affinity of Reaction 2 During Run 17.

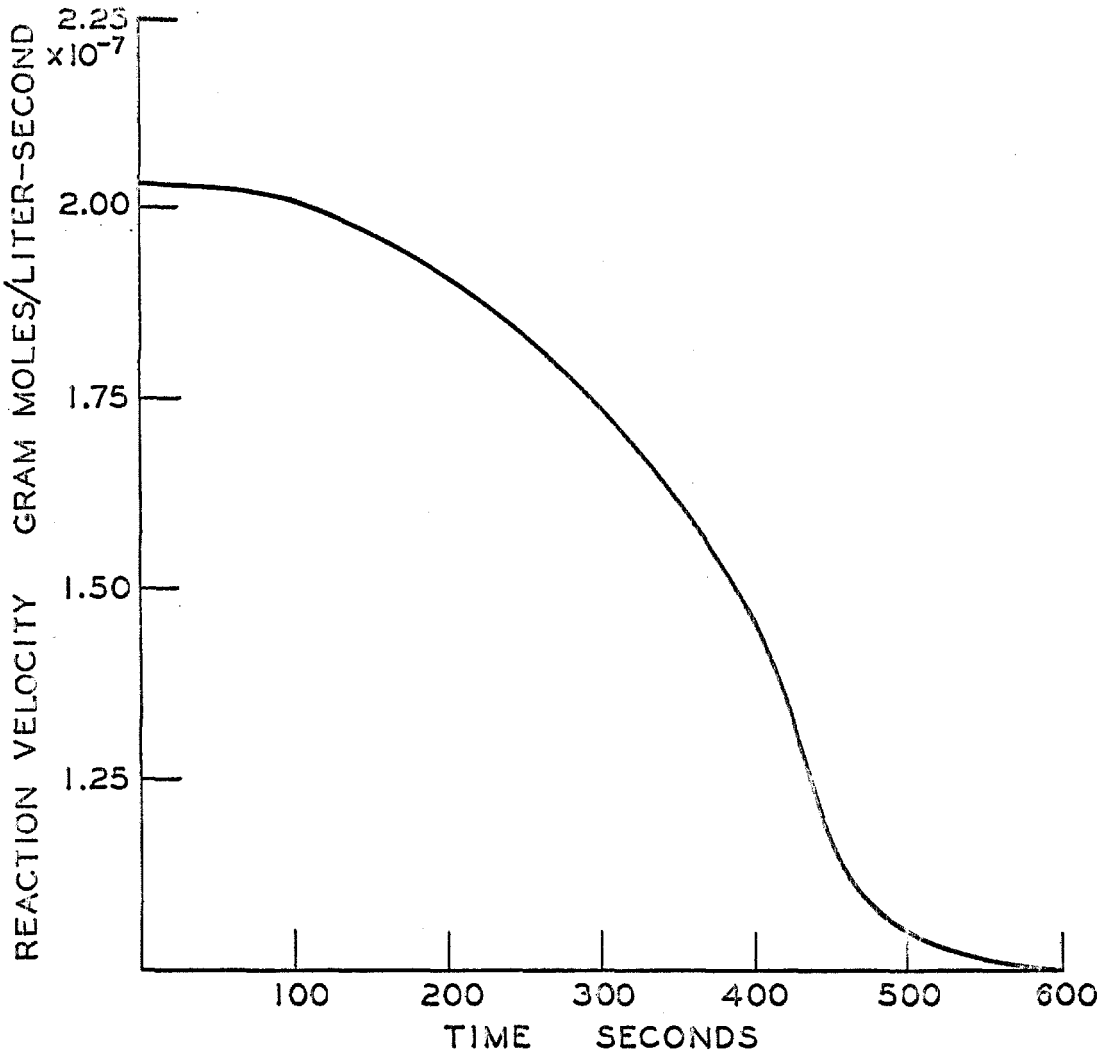

Figure 23. Velocity of Reaction 1 During Run 17.

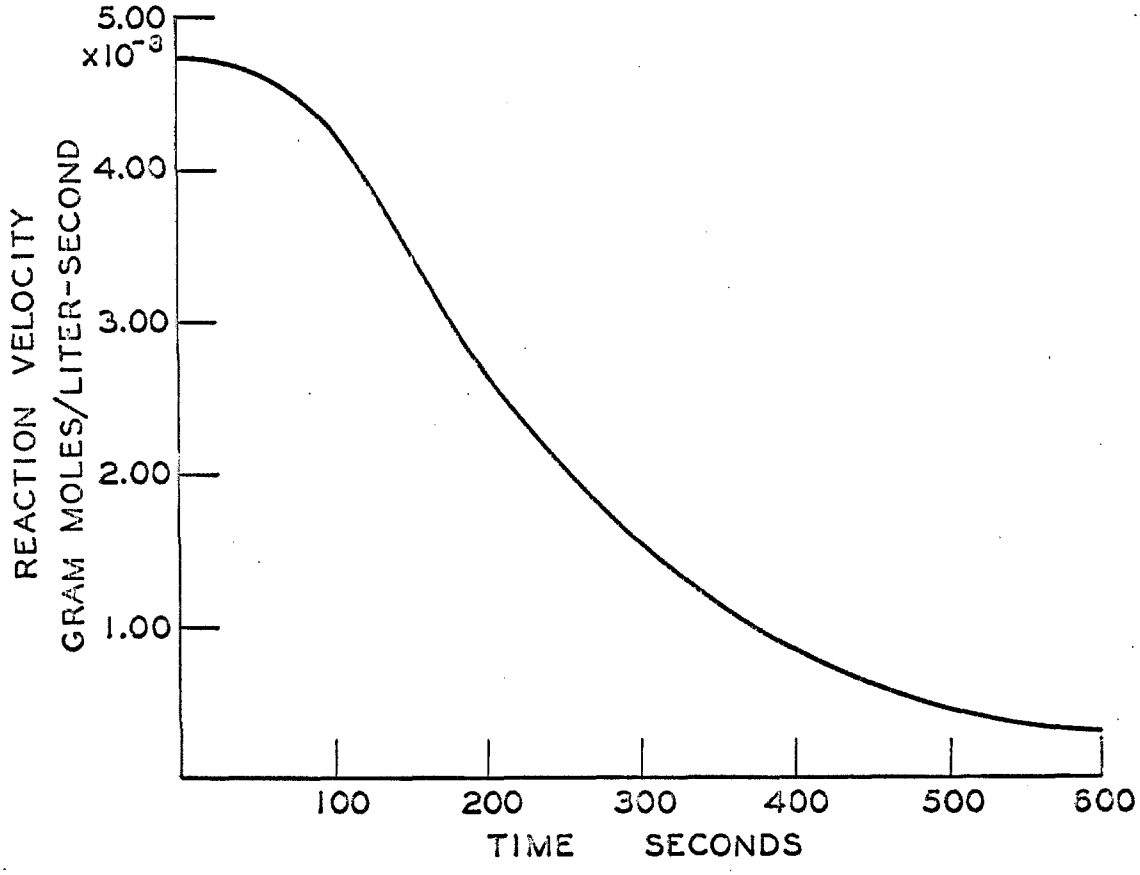

Figure 24. Velocity of Reaction 2 During Run 17.

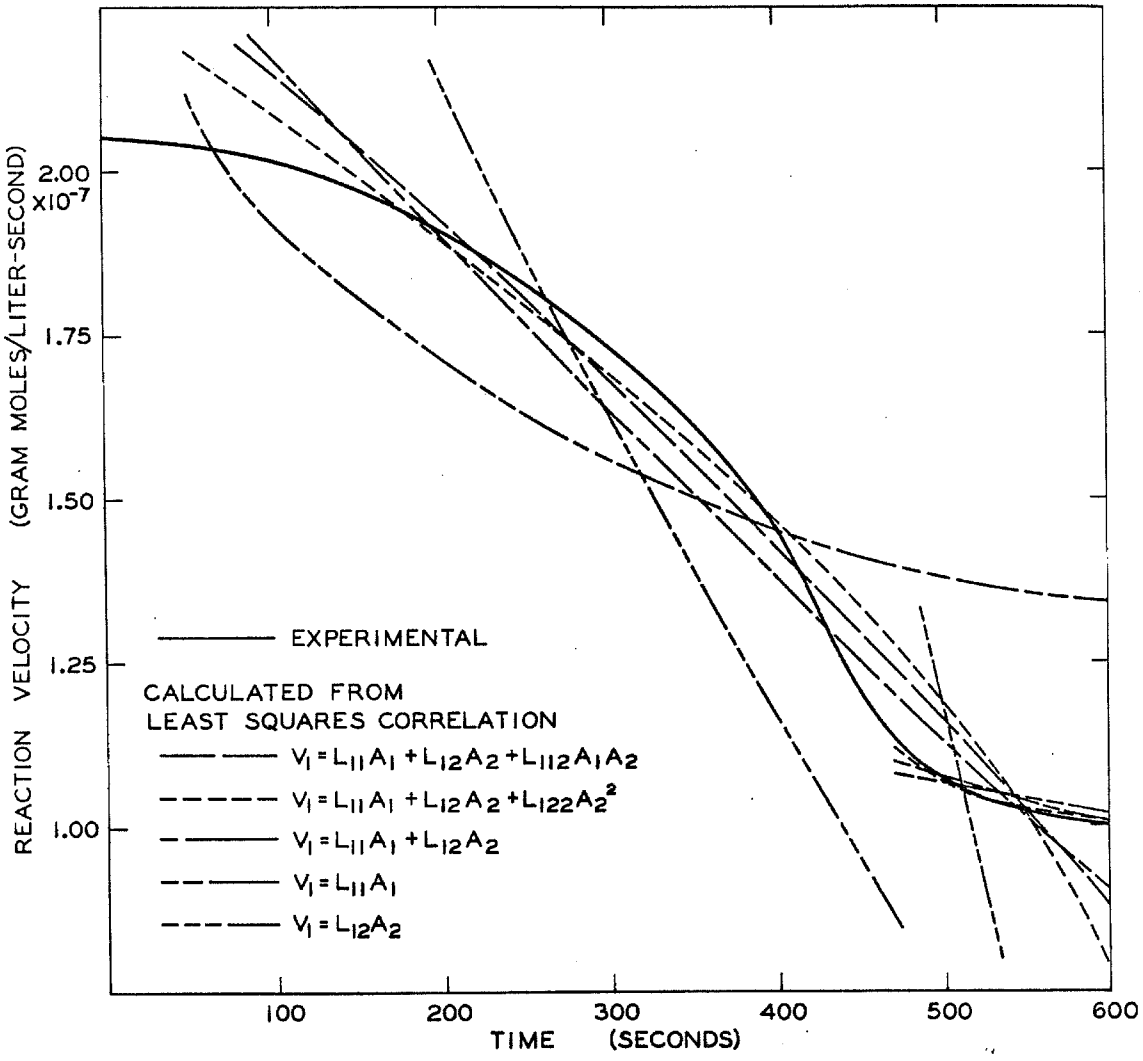

Figure 25. Comparison of Least Squares Correlations. Velocity of Reaction 1 During Run 17 Versus Time.

PROPOSITION 1

The existing data in the literature regarding extinction coefficients of iodine monochloride between 310 mμ and 370 mμ appear to be erroneous. A likely reason for this error is discussed, and improved data is presented[3].

A Cary Model 14 recording spectrophotometer with a quartz optical cell was used to examine the continuous absorption spectrum of iodine monochloride. Further details of the experimental work are given elsewhere[3].

In Figure 1, our results are compared to the data of Seery and Britton[4], Binder[1] at 18 °C, and Gibson and Ramsperger[2]. A line has been passed through our data and Binder's.

In the ultraviolet region, our measurements fall on the same curve as those of Binder, with Seery and Britton's results deviating slightly from this curve. However, in the region between 290 mμ and 370 mμ, the measurements of Binder and ourselves differ greatly from those of Seery and Britton.

Likely causes of these discrepancies can be given. Since chlorine has its maximum optical absorbency at 330 mμ, perhaps Seery and Britton failed to account for some residual chlorine in their optical cell. Also, because their data in the visible region is slightly displaced toward shorter wavelengths, we suspect that their instrument may not have been accurately calibrated. Seery and Britton also noticed that their data did not agree with that of Gibson

and Ramsperger[2]. However, Gibson and Ramsperger may not have reported extinction coefficients.

References

1. Binder, J. L., Physical Review, 54, 114 (1938).

2. Gibson, G. E. and Ramsperger, H. C., Physical Review, 30, 598 (1927).

3. Nebeker, E. B. and Pings, C. J., Journal of Physical Chemistry, 69, (1965).

4. Seery, D. J. and Britton, D., Journal of Physical Chemistry, 68, 2263 (1964).

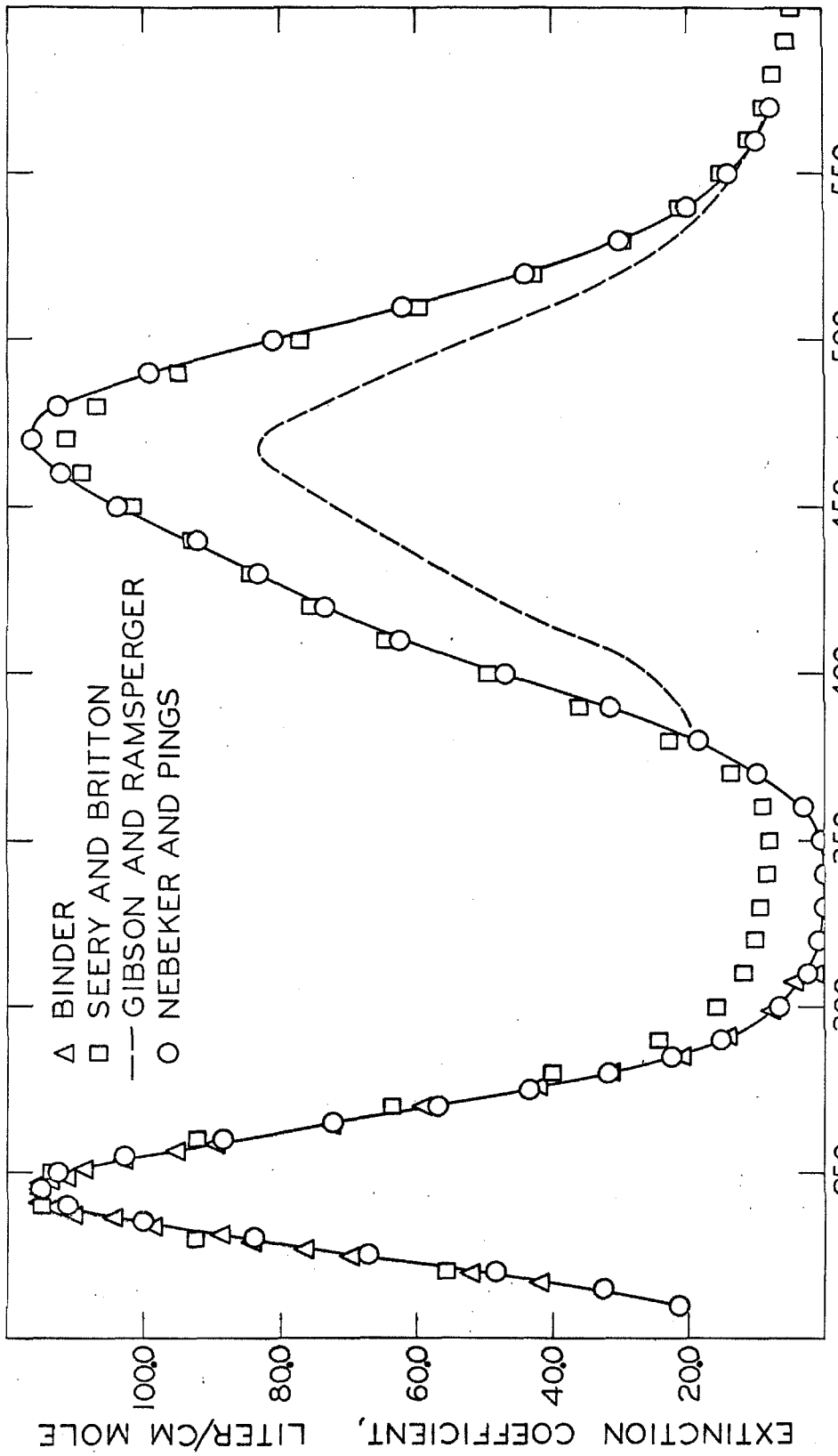

Figure 1. Extinction Coefficient of Iodine Monochlorine.

PROPOSITION 2

Momentum equations and equations of motion for variable mass systems are discussed. A suggestion for treating this type of system is given. The concepts are applied to a specific problem to show that, contrary to statements appearing in the literature, the rocket engine does not produce an external force on a rocket under conditions of optimum expansion in flight.

In 1961, Nebeker[7] noted that the momentum equations for variable mass systems were occasionally being misinterpreted in the literature[4, 11, 12, 13] and in practice[9]. Since that time, Bottaccini[1, 2], Meriam[6], and Thorpe[14] have called attention to the same problem and have discussed it in various ways.

Attention to this problem has resulted primarily from the recent interest in rockets and their behavior in flight. Therefore, the particular example of a rocket in flight will be examined.

Newton's Second Law of Motion essentially consists of two statements: 1) the time rate of change of momentum is equal to the force producing this change of momentum, and 2) this change takes place in the direction in which the force is acting[3, 5]. This first statement may be written

$$F = \frac{d}{dt}(m_r v_r) \tag{1}$$

where F is the sum of external forces acting on the rocket, m_r is the mass of the rocket with its unburned propellants, and v_r is

the velocity of the rocket with respect to an inertial coordinate system. Care must be used to employ consistent units in equation (1). Since equation (1) suggests differentiation of the mass with respect to time, an inference is made that this equation is applicable to variable mass systems. The difficulties which can be created in this way can be demonstrated.

If equation (1) is differentiated, the following expression is obtained

$$F = m_r \, dv_r/dt + v_r \, dm_r/dt \tag{2}$$

or,

$$F = m_r a_r + v_r \dot{m}_r \, . \tag{3}$$

For a system of constant mass, equation (3) reduces to the familiar form

$$F = m_r a_r \, . \tag{4}$$

Consider a rocket in flight under such conditions that aerodynamic, gravitational, centrifugal, and Coriolis forces can be neglected. Assume that the thrust of the rocket is acting along the line of motion, which is presumably along the axis of the rocket, and that the rocket engine is suitably designed so that optimum expansion occurs.

Under these conditions, in the field of rocketry the equation of motion for a rocket is usually written in the following form[9,13]

$$\text{Thrust} = m_r a_r \tag{5}$$

where the Thrust is defined by the equation[4, 8, 10, 13]

$$\text{Thrust} = - \dot{m}_g v_{gr} \tag{6}$$

where v_{gr} is the velocity of the gas relative to the rocket, and $\dot{m}_g$ is the mass flow rate of the gas. Equations (5) and (6) can be combined to give the equation of motion for the rocket[5, 13]

$$- \dot{m}_g v_{gr} = m_r a_r \, . \tag{7}$$

However, the above equation can be rearranged by noting that

$$v_{gr} = v_g - v_r \, , \tag{8}$$

where v_g is the velocity of the gas with respect to the inertial coordinate system, and

$$\dot{m}_g = - \dot{m}_r \tag{9}$$

to give

$$- \dot{m}_g v_g = m_r a_r + \dot{m}_r v_r \, . \tag{10}$$

Equation (10) is another form of the equation of motion for the rocket in flight under the conditions cited.

Because of the obvious similarity of equation (7) to the expression of Newton's Second Law of Motion for a system of constant mass, as given by equation (4), in the literature[4, 11, 12, 13] and in practice[9] the Thrust of a rocket engine, $- \dot{m}_g v_{gr}$, is erroneously called the external force on the rocket due to the engine. Since the rocket is an example of a system in which the <u>mass is not constant</u>, comparing

the equation of motion of the rocket to an expression of Newton's Second Law for a constant mass system certainly would not be expected to give the external force on the rocket.

On the other hand, if the equation of motion of a rocket in flight, equation (10), is compared to an expression of Newton's Second Law for a system in which the mass is not constant, equation (3), the external force on the rocket appears to be $-\dot{m}_g v_g$. However, by examining v_g, this so-called force, $-\dot{m}_g v_g$, is oriented in the direction of flight during the initial portion of the rocket's flight and diminishes gradually to zero as the magnitude of the velocity of the rocket with respect to the earth approaches the magnitude of the velocity of the gas with respect to the rocket. As the velocity of the rocket with respect to the earth is increased even further, this external force will become oriented in a direction opposite to the direction of flight. Since the behavior of this $-\dot{m}_g v_g$ term contradicts the second statement of Newton's Second Law of Motion, i.e. that change of momentum is in the direction in which the force is acting, $-\dot{m}_g v_g$ does not appear to be the external force on the rocket due to the engine.

A momentum balance equation can be written for the system consisting of the rocket with its unburned propellant and the expelled gas in order to verify the equation of motion for a rocket in flight as given by equation (10). For most purposes, conservation of momentum equations may be considered as supplementing Newton's Second Law with additional terms which describe the flux of momentum into and out of the system. Therefore, the conservation of momentum for

a variable mass system can be expressed by

rate of momentum into the system - rate of momentum out of the system + sum of external forces acting on the system = rate of momentum accumulation in the system (11)

This is a very useful method of generating momentum equations and equations of motion. The form of equation (11) is analogous to mass and energy conservation equations. However, in the case of momentum equations, the sum of external forces term takes the place of the "source-sink" term often used in the other equations.

If the system is chosen to include the rocket with its unburned propellant and also the expelled gas, under conditions which have been cited, no external forces or momentum fluxes into or out of the system will exist. Hence, equation (11) will reduce to

$$O = \text{rate of momentum accumulation in the system} \tag{12}$$

or

$$O = \frac{d(m_r v_r)}{dt} + \frac{d}{dt}\int_o^{m_g} v_g \, dm_g \tag{13}$$

where m_g is the mass of the gas. Equation (13) can be further simplified to the expression[1]

$$-\dot{m}_g v_g = m_r a_r + \dot{m}_r v_r \, . \tag{14}$$

Equation (14) is simply the equation of motion of a rocket in flight and is identical to equation (10).

---

[1] One method of reducing equation (13) to the form of equation (14) is

$$\frac{d(m_r v_r)}{dt} = -\frac{d}{dt}\int_o^{m_g} v_g dm_g = -\frac{d}{dt}\int_o^t v_g \dot{m}_g dt = -\dot{m}_g \frac{d}{dt}\int_o^t v_g dt$$

$$m_r a_r + \dot{m}_r v_r = -\dot{m}_g v_g$$

If the system is now chosen to be only the rocket itself with its unburned propellant, possibly some external force on the rocket can be found which can be attributed to the rocket engine. The momentum flux into the system will again be zero, but the momentum flux out of the system will be $\dot{m}_g v_g$. Equation (11) can then be written

$$- \dot{m}_g v_g + \text{external force acting on the rocket} = \frac{d(m_r v_r)}{dt} = m_r a_r + \dot{m}_r v_r . \tag{15}$$

As shown by a comparison of equation (15) with the equation of motion of a rocket, as given by either equation (10) or equation (14), the external force acting on the rocket will be zero and equation (15) reduces to

$$- \dot{m}_g v_g = m_r a_r + \dot{m}_r v_r \tag{16}$$

which is identical to equation (10) and (14). Therefore, the rocket engine exerts no external force on the system of the rocket with its unburned propellant under the conditions of optimum expansion.

Unfortunately, this matter is often treated incorrectly in the literature. As a result, in practice[9] some confusion and uncertainty is often introduced in the application of these ideas.

References

1. Bottaccini, M., American Institute of Aeronautics and Astronautics Journal, 1, 927 (1963).

2. Bottaccini, M., American Institute of Aeronautics and Astronautics Journal, 2, 1164 (1964).

3. Cajori, F., Newton's Principia, University of California Press, Berkeley, 1960.

4. Feodosiev, V. I. and Siniarev, G. B., Introduction to Rocket Technology, Academic Press, New York, 1959.

5. Housner, G. W. and Hudson, D. E., Applied Mechanics Dynamics, D. Van Nostrand Company, Inc., New York, 1950.

6. Meriam, J. L., Aerospace Engineering, 21, 52 (1962).

7. Nebeker, E. B., Research Report, California Institute of Technology, Pasadena, 1961.

8. Newell, H. E., Sounding Rockets, McGraw-Hill Book Company, Inc., New York, 1959.

9. Personal experience while employed at Rocketdyne (division of North American Aviation).

10. Rosser, J. B., Newton, R. B., and Gross, G. L., Mathematical Theory of Rocket Flight, McGraw-Hill Book Company, Inc., New York, 1947.

11. Sellers, J. P., American Rocket Society Journal, 75, 126 (1948).

12. Shepard, L. R., British Interplanatary Society Journal, 14, 37 (1955).

13. Sutton, G. P., Rocket Propulsion Elements, John Wiley & Sons, Inc., New York, 1958.

14. Thorpe, J. F., American Journal of Physics, 30, 637 (1962).

PROPOSITION 3

For a pseudoplastic fluid, the conventional Reynolds number employing an apparent viscosity of the pseudoplastic evaluated at the wall shear is useful in indicating the presence of laminar flow.

The Reynolds number is a familiar dimensionless grouping which is often used to determine whether laminar or turbulent flow exists in a pipe. For pseudoplastic fluids, a generalized Reynolds number, introduced by Metzner and Reed[3], is used

$$Re' = \frac{D_o^{n'} U^{2-n'} \rho}{8^{n'-1} K'} \qquad (1)$$

where D_o is the inside diameter of the pipe, U is the bulk velocity of the fluid, ρ is the specific weight of the fluid, n' is a flow behavior index, and K' is a fluid consistency index[2]. In employing this Reynolds number as a test for the presence of either laminar or turbulent flow, a correlation presented by Dodge and Metzner is often used.[1].

The application of this generalized Reynolds number is limited by the fact that some knowledge of n' and K' must be available. Also, the numerical computation of equation (1) is rather lengthy.

However, as shown below, the conventional Reynolds number employing an apparent viscosity of the pseudoplastic may often be very useful in indicating the existence of laminar flow. The apparent viscosity is evaluated at the particular value of wall shear encoun-

tered.

A Newtonian fluid is often defined by,

$$\tau = \eta(- du/dr) \tag{2}$$

where τ is the shear stress, η is the viscosity, and $(- du/dr)$ is the rate of shear. Upon introducing the apparent viscosity, η_a, which is equal to η for a Newtonian fluid, and writing the above equation at the wall of the pipe,

$$\tau_o = \eta_{ao}(- du/dr) . \tag{3}$$

For the laminar flow of a pseudoplastic fluid, with a bulk velocity U, the shear rate at the wall is given by[2]

$$(- du/dr)_o = \left[\frac{3n' + 1}{4n'}\right] (8U/D_o) . \tag{4}$$

For the same bulk velocity, the wall shear can be written

$$\tau_o = \eta_a' (8U/D_o) \tag{5}$$

where η_a' is an apparent viscosity obtained from a plot of τ_o versus $(8U/D_o)$. As shown by equation (6), η_a' will not, in general, be equal to η_{ao} unless only Newtonian fluids are considered. Upon combining equations (3), (4), and (5), the relationship between η_a' and η_{ao} is obtained

$$\eta_a' = \eta_{ao}\left[\frac{3n' + 1}{4n'}\right] . \tag{6}$$

Using the preceeding expression, equation (5) can be written

$$\tau_o = \eta_{ao} \left[\frac{3n' + 1}{4n'} \right] (8U/D_o) . \tag{7}$$

For a pseudoplastic fluid in laminar flow[2]

$$\tau_o = K'(8U/D_o)^{n'} . \tag{8}$$

Combine equations (7) and (8) to obtain

$$\eta_{ao} = K' \left[\frac{4n'}{3n' + 1} \right] (8U/D_o)^{n'-1} . \tag{9}$$

A conventional Reynolds number employing an apparent viscosity evaluated at the wall shear may be defined

$$Re = D_o U \rho / \eta_{ao} . \tag{10}$$

By combining equations (9) and (10), the following expression is obtained

$$Re = \left[\frac{3n' + 1}{4n'} \right] \left[\frac{D_o^{n'} U^{2-n'} \rho}{8^{n'-1} K'} \right] . \tag{11}$$

But the last factor in the above equation is merely Metzner and Reed's Reynolds number, and therefore, equation (11) can be written

$$Re' = \left[\frac{4n'}{3n' + 1} \right] Re . \tag{12}$$

Hence, in the laminar region, the Reynolds number, as defined by

equation (10), multiplied by the factor $4n'/(3n' + 1)$, is identical to the Reynolds number defined by Metzner and Reed.

For a pseudoplastic, $n' < 1.00$, and therefore,

$$\frac{4n'}{3n' + 1} < 1.00 . \qquad (13)$$

Hence, as shown by equation (12), Re' will always be less than Re for a pseudoplastic fluid. Therefore, if the experimental correlation of Dodge and Metzner is assumed to be valid and if the value of a Reynolds number calculated using equation (10) lies in the laminar region, laminar flow will certainly exist.

References

1. Dodge, D. W. and Metzner, A. B., A. I. Ch. E. Journal, 5, 189 (1959).

2. Longwell, P. A., Mechanics of Fluid Flow, Ms. 3017, Chemical Engineering Department, California Institute of Technology, Pasadena, 1958.

3. Metzner, A. B. and Reed, J. C., A. I. Ch. E. Journal, 1, 434 (1955).

PROPOSITION 4

For a chemical reacting system in which the independent stoichiometric equations can be identified, linear transformations of the fluxes and forces which destroy the symmetry of the phenomenological coefficient matrix are not applicable.

In the literature of non-equilibrium thermodynamics, a discussion[1, 2, 4, 5, 6, 7, 9] regarding the applicability of linear transformations of the fluxes and forces appearing in the phenomenological laws exists. A new set of fluxes, $\mathcal{J}'$, can be created by making a linear transformation on the original set of fluxes, $\mathcal{J}$, by the transformation matrix $\mathcal{P}$,

$$\mathcal{J}' = \mathcal{P} \cdot \mathcal{J} . \tag{1}$$

Similarly, using the transformation matrix $\mathcal{Q}$, a new set of forces, $\mathcal{X}'$, can be created from the original set, $\mathcal{X}$, by

$$\mathcal{X}' = \mathcal{Q} \cdot \mathcal{X} . \tag{2}$$

In any macroscopic theory, the rate of entropy production should be invariant, regardless which set of fluxes and forces are used to describe the reacting system. Imposing only this restriction, Davies[2] and de Groot and Mazur[5] show that the transformation matrices, $\mathcal{P}$ and $\mathcal{Q}$, are related by

$$\tilde{\mathcal{P}} \cdot \mathcal{Q} = \mathcal{I} + \mathcal{W} \mathcal{L} \tag{3}$$

where $\tilde{\mathcal{P}}$ is the transpose of $\mathcal{P}$, $\mathcal{I}$ is an identity matrix, $\mathcal{L}$ is the phenomenological coefficient matrix, and $\mathcal{W}$ is any skew symmetric matrix. Unfortunately, such transformations destroy the symmetry of the phenomenological coefficient matrix[2, 5], thereby destroying the Onsager reciprocity relations. Various arguments[2, 5, 6] have been proposed which set $\mathcal{W} = 0$, so that the transformation matrices are related simply by

$$\tilde{\mathcal{P}} \cdot \mathcal{D} = \mathcal{I} . \tag{4}$$

If $\mathcal{P}$ and $\mathcal{D}$ are related by the above expression, the symmetry of the phenomenological coefficient matrix is retained.

If the example of chemical reacting systems is considered, further insight into this problem may be obtained. Assume that the sufficient number, r, of independent stoichiometric equations can be identified to describe the reacting system

$$\sum_{\gamma=1}^{c} \nu_{\gamma\rho} M_{\gamma} = 0 \qquad \rho = 1, 2, \ldots, r , \tag{5}$$

where $\nu_{\gamma\rho}$ is the stoichiometric coefficient of the γth chemical species in the ρth equation, M_{γ} is the molecular weight of the γth species, and c is the total number of macroscopic chemical species present in the system. The stoichiometric equations can be subjected to a linear transformation, resulting in a new set of stoichiometric equations

$$\sum_{\gamma=1}^{c} \sum_{\rho=1}^{r} (a_{\rho'\rho})\nu_{\gamma\rho} M_{\gamma} = 0 \ , \qquad (6)$$

where $a_{\rho'\rho}$ is an element in the stoichiometric transformation matrix. De Donder[3] and Prigogine[8] show that this transformation of the stoichiometric equations is equivalent to the following velocity and affinity transformations

$$V_{\rho'} = \sum_{\rho=1}^{r} (a_{\rho'\rho})^{*} V_{\rho} \qquad \rho' = 1, 2, \ldots, r \quad (7)$$

$$A_{\rho'} = \sum_{\rho=1}^{r} (a_{\rho'\rho}) A_{\rho} \qquad \rho' = 1, 2, \ldots, r \quad (8)$$

where $(a_{\rho'\rho})^{*}$ is the cofactor divided by the determinant of the stoichiometric transformation matrix, V is the velocity, A is the chemical affinity, ρ refers to the number of the original stoichiometric equation, and ρ' refers to the number of the new stoichiometric equation created by the linear transformation. Alternatively, equations (7) and (8) can be written in matrix notation

$$\mathfrak{v}' = \mathfrak{P}^{o} \cdot \mathfrak{v} \qquad (9)$$

$$\mathfrak{A}' = \mathfrak{D}^{o} \cdot \mathfrak{A} \ . \qquad (10)$$

Referring to equations (7) and (8), the relationship between the velocity and affinity transformation matrices appears to be

$$\tilde{\mathfrak{P}}^{o} \cdot \mathfrak{D}^{o} = \mathfrak{I} \ . \qquad (11)$$

Hence, for a chemical reacting system in which the independent stoichiometric equations can be identified, linear transformation matrices of the fluxes and forces are related by equation (11). Therefore, as stated before, linear transformations using matrices related in this way do not destroy the symmetry of the phenomenological coefficient matrix thereby also destroying the Onsager reciprocity relations.

References

1. Coleman, B. D. and Truesdell, C., Journal of Chemical Physics, 33, 28 (1960).

2. Davies, R. O., Physica, 18, 182 (1952).

3. De Donder, Th., Bulletin de l'Academie Royale de Belgique (Classe des Sciences), 23, 770 (1937).

4. de Groot, S. R., Thermodynamics of Irreversible Processes, North-Holland Publishing Company, Amsterdam, 1962.

5. de Groot, S. R. and Mazur, P., Non-Equilibrium Thermodynamics, North-Holland Publishing Company, Amsterdam, 1962.

6. Hooyman, G. J., de Groot, S. R., and Mazur, P., Physica, 11, 360 (1955).

7. Meixner, J., Annalen der Physik, 43, 244 (1943).

8. Prigogine, I., Bulletin de l'Academie Royale de Belgique (Classe des Sciences), 32, 30 (1946).

9. Verschaffelt, J. E., Bulletin de l'Academie Royale de Belgique (Classe des Sciences), 37, 853 (1951).

PROPOSITION 5

Equating the activity of a radioactive nuclide with the experimentally observed count rate is an assumption which can easily lead to errors when the activity is a function of time. Examples of these errors are discussed for the particular example of the determination of the disintegration constant in simple radioactive decay. A parameter is given which is useful as a first approximation in determining the validity of this assumption.

The count rate is the following function of the activity of a sample

$$C = \frac{1}{\Delta t} \int_{t}^{t+\Delta t} A \, dt \qquad (1)$$

where Δt is the counting interval. A is the activity and C is the count rate, i.e. the number of counts observed in an interval of time Δt divided by Δt.

The disintegration behavior of a radioactive nuclide is often given by the expression[1]

$$N = N_o e^{-\lambda t} \qquad (2)$$

where N is the number of atoms present at time t, N_o is the number present at time $t = 0$, and λ is the disintegration constant. Often, N is difficult to measure directly. However, a quantity proportional to the disintegration rate, the activity, is easier to

measure,

$$A = k\left(\frac{-dN}{dt}\right) = k\lambda N = k\lambda N_o e^{-\lambda t} = A_o e^{-\lambda t} \qquad (3)$$

where k is the proportionality constant, and A_o is the activity at $t = 0$.

Experimentally, the count rate is measured. Often in practice, this count rate is equated to the activity. However, the activity is actually related to the count rate by equation (1). For the example of radioactive nuclides that disintegrate according to equation (2), the activity is given as a function of the count rate by

$$A = C\left(\frac{\lambda\Delta t}{1 - e^{-\lambda\Delta t}}\right). \qquad (4)$$

Frequently the disintegration constant, λ, must be measured. Examination of the methods which are used to experimentally measure the disintegration constant will indicate where the difficulties in equating the activity and count rate may lie.

Perhaps the most popular methods used to determine the disintegration constant are the specific activity and slope method[1]. The specific activity method is useful if the half-lives of the nuclides are long. Equation (3) can be written

$$\lambda = A_o/kN_o . \qquad (5)$$

Hence, the disintegration constant can be determined if k and N_o are known from other experimental measurements. Equation (5) can

be put in terms of the experimentally measured quantity, the count rate,

$$\lambda = \frac{C}{kN_o}\left(\frac{\lambda\Delta t}{1 - e^{-\lambda\Delta t}}\right) . \qquad (6)$$

Therefore, equating the count rate and activity could easily lead to errors if $\lambda\Delta t$ is large. Usually, the contribution of the $\lambda\Delta t/(1- e^{-\lambda\Delta t})$ factor is negligible for $\lambda\Delta t < 0.01$.

The application of the slope method is useful with nuclides of short half-lives. Combining equations (3) and (4) and taking the logarithm of the resulting expression gives

$$\ln\left[C\left(\frac{\lambda\Delta t}{1 - e^{-\lambda\Delta t}}\right)\right] = \ln A_o - \lambda t . \qquad (7)$$

As suggested by the form of this equation, the logarithm of the count rate is usually plotted against time, and the slope is measured to determine the disintegration constant. Of course, with $\lambda\Delta t < 0.01$, the count rate will very nearly approximate the activity, and no appreciable error will result. For $\lambda\Delta t > 0.01$, no error will result using this method if Δt is kept constant, that is, the counting intervals are kept constant.

Hence, $\lambda\Delta t$ appears from equations (4), (6), and (7) to be a useful parameter to establish the applicability of this assumption in simple radioactive decay. Note that λ is dictated by the radioactive nuclide, while Δt can be adjusted by the experimenter.

In most cases, the error introduced by equating the activity to the count rate is negligible. However, the experimenter cannot *a priori* neglect the possible errors that might be involved. Such errors are likely to become more pronounced when large time intervals are used. Large time intervals are necessitated when examining samples with low activities or when using a counting device which has a low counting efficiency.

Reference

1. Rowlands, S., Nucleonics, Vol. 3, No. 3, 2 (1948).